MONTANA STATE UNIVERSITY

The hydraulic transportation of solids in pipelines
by Robert Raymond Faddick

A thesis submitted to the Graduate Faculty in partial fulfillment of the requirements for the degree of DOCTOR OF PHILOSOPHY in Civil Engineering
Montana State University
© Copyright by Robert Raymond Faddick (1970)

Abstract:
The application of the Durand equation relating headlosses of mixtures of solids and water in pipelines to the hydraulic transport of woodchip mixtures and simulated woodchip mixtures was studied. The coefficients of the Durand equation were found to vary five-fold when correlating available headloss data for the hydraulic transport of woodchip mixtures in pipes of different diameters.

A dimensional analysis of a two-phase flow system produced five parameters: mixture friction factor, Reynolds number, particle concentration, specific gravity, and a parameter relating particle size and shape to pipe diameter. The parameters were applicable to mixtures of large plateshaped particles (such as woodchips) and water flowing in smooth pipes.

A limited experimental program provided four sets of headloss data using plastic chips to compliment four sets of available woodchip data. A plot of each of the eight tests on Stanton-type diagrams showed that the mixture friction factor increased with decreasing Reynolds number, increased with concentration, increased as the particle geometry - pipe diameter ratio decreased at a given Reynolds number, increased with particle specific gravity in the heterogeneous suspension regime and increased with increasing absolute values of particle-fluid specific gravity differential, in the sliding-bed regime. : The data were correlated by a curve fitting technique using a second order polynomial relating all the parameters except chip, specific gravity whose variation was considered too small to be included in the correlation equation. An error analysis indicated that 78 per cent of all the data were within 25 per cent of the values predicted by the correlation equation.

THE HYDRAULIC TRANSPORTATION OF SOLIDS IN PIPELINES

by

ROBERT RAYMOND FADDICK

A thesis submitted to the Graduate Faculty in partial fulfillment of the requirements for the degree

of

DOCTOR OF PHILOSOPHY

in

Civil Engineering

Approved:

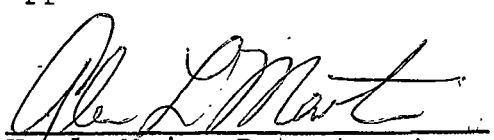

Head, Major Department

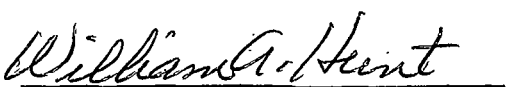

Chairman, Examining Committee

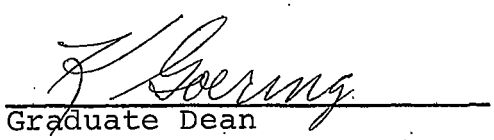

Graduate Dean

MONTANA STATE UNIVERSITY
Bozeman, Montana

March, 1970

ACKNOWLEDGEMENTS

This investigation was performed in Ryon Laboratory at Montana State University in Bozeman, Montana, under the supervision of Dr. William A. Hunt, Principal Investigator.

The project was sponsored by the Forest Engineering Research Branch of the Intermountain Forest Range Experiment Station, United States Forest Service, Department of Agriculture, as part of a cooperative aid agreement with the Department of Civil Engineering and Engineering Mechanics of Montana State University.

Because of the size and complexity of the program many people from several departments were involved. Their assistance was appreciated. In particular, the author would like to express his gratitude to his supervising professor, Dr. William A. Hunt, for his guidance and to Ronald E. Schmidt, Hydraulic Research Engineer of the Intermountain Station for his aid in operating the pipeline.

Finally, sincerest thanks to the author's wife, Mary, for her encouragement and assistance.

TABLE OF CONTENTS

LIST OF TABLES

LIST OF FIGURES

ABSTRACT

The application of the Durand equation relating head-losses of mixtures of solids and water in pipelines to the hydraulic transport of woodchip mixtures and simulated woodchip mixtures was studied. The coefficients of the Durand equation were found to vary five-fold when correlating available headloss data for the hydraulic transport of woodchip mixtures in pipes of different diameters.

A dimensional analysis of a two-phase flow system produced five parameters: mixture friction factor, Reynolds number, particle concentration, specific gravity, and a parameter relating particle size and shape to pipe diameter. The parameters were applicable to mixtures of large plate-shaped particles (such as woodchips) and water flowing in smooth pipes.

A limited experimental program provided four sets of headloss data using plastic chips to compliment four sets of available woodchip data. A plot of each of the eight tests on Stanton-type diagrams showed that the mixture friction factor increased with decreasing Reynolds number, increased with concentration, increased as the particle geometry - pipe diameter ratio decreased at a given Reynolds number, increased with particle specific gravity in the heterogeneous suspension regime and increased with increasing absolute values of particle-fluid specific gravity differential, in the sliding-bed regime.

The data were correlated by a curve fitting technique using a second order polynomial relating all the parameters except chip specific gravity whose variation was considered too small to be included in the correlation equation. An error analysis indicated that 78 per cent of all the data were within 25 per cent of the values predicted by the correlation equation.

CHAPTER I

INTRODUCTION

Although the pipeline transport of solids has been a commercial reality for a number of decades, there is still a dearth of design methods for predicting headlosses of mixtures of water and solids. The theory of hydraulic transport of solids in pipelines has not advanced sufficiently to the point where a commercial operation may be developed without pilot plant studies. This is particularly true for predicting the headlosses of mixtures of woodchips in water. Interest has been expressed in many countries in the hydraulic transport of woodchip mixtures as a means of realizing greater benefits to the pulp and paper industry. The chief advantage of this type of transportation is the more efficient utilization of small diameter timber for pulp and paper. The concept of pipelining pulpwood chips appears to have originated in 1957 with the Pulp and Paper Research Institute of Canada (PPRIC), but at present (1968), a commercial pipeline for transporting woodchips is not known to exist.

In 1961, Montana State University, in cooperation with the Intermountain Forest and Range Experiment Station of

the United States Forest Service in Ogden, Utah, began extensive investigations into the feasibility of pipelining mixtures of woodchips and water. Through a rather complete program of experimental and economic studies these institutions are establishing criteria to design, construct, and operate a woodchip pipeline system. This report deals with one of the phases of the overall study: headloss-concentration-velocity correlations for steady state flow of woodchips in a pipeline.

The first objective of this study is to critically examine the Durand-type correlation for predicting the headloss for mixtures of woodchips and water and also for mixtures of simulated woodchips and water transported in pipelines. A second objective is to define the variables necessary to describe the flow of mixtures of woodchips and water in pipelines. A third objective is to investigate a possible method for presenting the results of a limited experimental program in the form of Stanton-type diagrams to show the effects of volumetric concentration, specific gravity, and scale factor (particle size to pipe diameter) on the friction factor-Reynolds number correlations for flow in smooth pipes. A search was made for data evaluating the

loss due to friction for the transportation of pulpwood chips and water in various diameter pipes. Data from these sources were utilized along with the experimental data collected in this particular study to assist in the formulation of the headloss correlation.

CHAPTER II

REVIEW OF LIQUID-SOLID FLOW STUDIES

Some 110 years have elapsed since the first recorded attempt (6)[1] to transport solid particles of a macroscopic scale through a pipeline. Since that time much effort has been spent on the investigation of the flow of suspended solids in pipelines. If the flow of clear fluids in pipes is considered to be first generation research, then the pipeline transport of a particulate suspension in a fluid may be considered to be second generation research. The third generation of research, the pipeline transport of encapsulated solids in a fluid, is now under investigation by the Alberta Research Council (1).

Although considerable research has been done in the field of transportation of solids by pipelines, theory still lags practice. Much of the available headloss data (33), while showing systematic trends, display such wide variations and so many inconsistencies that they cannot be considered reliable guidelines for the design engineer.

---

[1]Numbers in parentheses refer to numbered references in the Literature Cited.

Due to the phenomenological complexities of fluid turbulence and distribution of solids in two-phase pipe flow, the attempts to develop a single correlation relating headloss to mixture velocity, volumetric concentration of solids and pipe diameter have not been entirely successful. Empirical equations have been established by researchers (11, 20, 32) to predict headlosses for given flow mixtures and concentrations of solids having certain physical properties, e.g. sands and gravels. It has been found (15, 33) that extension of these relationships to pipes with diameters different from those used in obtaining the particular correlations has proven unsatisfactory in predicting headlosses for mixtures of solids and water. Therefore, pipeline designers have been forced to resort to pilot plant studies for the design information necessary to establish full-scale pipeline operations. Much of the work has been done by commercial organizations and has not been released because of proprietary rights.

The work that is available and pertinent to this study is outlined below. Included are a discussion of the two-phase flow regimes in pipelines and some methods for

delineating the flow regimes followed by a review of the Durand headloss correlation. Past research on the transport of woodchip mixtures in pipelines is discussed with emphasis placed on the correlation equations and flow regimes. Finally, the Durand headloss correlation, as it applies to woodchip mixtures, is critically examined.

Flow Regimes

The classification of flow regimes of woodchips in pipelines is similar to that of sediment in open channels. In the latter, suspension flow, saltation flow and bedload flow may exist distinctly but all are usually present in some degree. Suspension flow implies that the sediment is maintained in suspension in the mainstream by the turbulence of the fluid, usually water. Saltation flow describes the regime in which heavier grains are transported by bouncing or jumping along the channel bed. Bedload flow is restricted to the case where the sediment is rolled or dragged along the channel bed by the channel flow but is not lifted into the mainstream of the moving water.

The flow regimes for conduit flow of solids are classified as follows:

1. Homogeneous flow
2. Heterogeneous suspension flow
3. Heterogeneous saltation flow
4. Bedload

Homogeneous flow regimes are those in which particles are small enough and in sufficient quantity to give the mixture an apparent viscosity different from that of the carrying fluid. The particles are held in uniform suspension by Brownian movement.

Heterogeneous flow regimes are those in which the fluid and solids comprise two distinct phases: the transporting medium and the discrete particles. The conveying liquid retains its own viscosity. Heterogeneous suspension flow occurs when the intensity of turbulence is sufficient to support all the solids in suspension although the concentration of solids or bulk density of the mixture may not be uniform throughout the cross-section of flow area.

Heterogeneous saltation flow occurs when the intensity of turbulence cannot support all the particles and the gravitational forces causes the heavier particles to settle out of suspension. The particles are then bounced or rolled

along the pipe invert by the motion of the flow.

A bedload forms when some of the particles are deposited either in a moving or stationary bed on the bottom of the pipe. The stationary bed is not completely immobile but its rate of movement is noticeably slower than the mainstream flow above the bed. The remainder of the particles are usually in heterogeneous saltation flow along the surface of the bed and in heterogeneous suspension flow above the bed.

Methods for Delineating Flow Regimes

The delineations of the flow regimes are more qualitative than quantitative because of the difficulty in separating the regimes. The characteristics of the mixture flow are a function of the particle properties (size, shape, and specific gravity), the fluid properties (density, viscosity), the intensity of turbulence, and the concentration of particles. As the interrelationship of these variables is not understood, the mechanisms of the transport process have not been formulated in an explicit equation.

Other investigators have delineated the flow classifications in various ways which differ from the manner presented above. For example, Durand (11) chose the particle size to differentiate between the regimes, that is, the nominal particle diameter d_n, which is the diameter of a sphere having the same volume as the particle. Later Durand's co-workers, Condolios, Chapus, and Constans (7), apparently realizing the limitations of d_n in delineating the flow regimes, noted that their more recent investigations indicated that both the particle size and concentration were implicit factors in the delineation of the heterogeneous suspension flow regime but they did not elaborate on this point.

Govier and Charles (15) attempted to simplify the flow regimes as those comprising settling or non-settling slurries. A settling slurry was defined as equivalent to the bedload flow described previously. The non-settling slurry was defined as equivalent to either heterogeneous suspension flow or homogeneous flow depending upon the fineness of the solids being transported. Generally, the finer the particle size for a given particle specific gravity, the lower is its

settling velocity, and the greater is its chance to form a non-settling slurry. A slurry which was in the transition zone between the settling and non-settling state corresponded to the heterogeneous saltation flow described previously. Govier and Charles were aware of the importance of the concentration of solids and the intensity of the fluid turbulence in distinguishing between settling and non-settling slurries. They did not incorporate these parameters directly in the categorization of the slurries. However, Govier and Charles realized that the particle settling velocity embodied more of the particle properties than just the particle size so it was chosen to distinguish between the two types of slurries. They also observed that increasing particle concentration permitted larger particles to form non-settling slurries.

Condolios et al. (8) and Wasp et al. (29) have cited cases where the addition of fine particles to a mixture of water and coarse particles has changed the flow regime sufficiently to decrease the energy requirements for transport below that for transporting the coarse mixture alone.

Methods for determining the particular flow regime for a given combination of particle properties and

concentrations and flow properties have not been satisfactorily established. Methods for making these determinations would enable designers to avoid certain undesirable flow regimes. For example, although the minimum headlosses for a given concentration generally occur where the bedload regime begins to form (11), it is the regime in which plugging is imminent due to excessive deposition. Heterogeneous suspension flow may be undesirable also due to high velocities consequently causing high power requirements.

Although flow regimes cannot be determined analytically, they can be observed during tests designed to measure the energy requirements for transporting a given mixture.

Durand Headloss Correlation

The most popular headloss correlation for solids-transport in a pipeline using water as the fluid is that of Durand (11) who performed an extensive series of tests transporting sands and gravels (grain size of 0.14 to 5.1 mm) in water through pipes ranging from 1.5 to 28 in. in diameter. Durand proposed the empirical equation:

$$\phi = K\psi^m \qquad \text{..... (2.1)}$$

where $\phi = (i_m - i)/C_v.i$;

i_m = hydraulic gradient of the mixture expressed as ft of water/ft of pipe length;

i = hydraulic gradient of clear-water flow, ft/ft;

C_v = volumetric concentration of solids (fraction),

K = constant, 180 from Gibert (14);

$$\psi = V_m^2 \sqrt{gd_n/V_s^2}\ /gD$$

V_m = mean velocity of mixture flow, fps;

g = gravitational acceleration, ft/sec^2;

d_n = weighted mean nominal particle diameter, ft, which is the diameter of a sphere of the same volume as the particle;

V_s = particle settling velocity, fps;

D = internal pipe diameter, ft; and

m = exponent, -1.5 from Gibert (14).

Eq. (2.1) is valid for sands and gravels with a specific gravity, s, of 2.65. To include the effect of specific gravity of other solids Durand and Condolios (10) modified the relationship as follows:

$$\phi = 124 \left[\frac{gD(s-1)}{V_m^2} \cdot \frac{V_s}{\sqrt{gd_n(s-1)}} \right]^{1.5} \quad \text{..... (2.2)}$$

or $$\phi = 85 \left[\frac{gD(s-1)}{V_m^2} \cdot \frac{V_s}{\sqrt{gd_n}} \right]^{1.5} \quad \text{..... (2.3)}$$

Eq. (2.1) is usually seen in an expanded form in the literature either as Eq. (2.2) or Eq. (2.3). The differences between the two forms are the value of the coefficient K and the term (s-1), the apparent specific gravity of the solids submerged in water. The latter term is retained in the denominator of Eq. (2.2) and increases the value of K. In Eq. (2.3) the coefficient K = 180 has been divided by $(s-1)^{1.5}$ with s = 2.65.

Other correlations have been proposed by Newitt et al. (20), Worster (32), and Spells (27), but they have not been readily accepted, generally because very small diameter pipes were used in the laboratory tests to substantiate the formulations of the correlations.

Woodchip Pipeline Research

For the past decade various researchers have investigated

the transportation of pulpwood chips in pipelines. McColl (19) of PPRIC undertook a study to determine the feasibility of transporting 1/2-in. laboratory-cut chips in a 2-in. diameter copper pipe. From his study he concluded that pulpwood chips were amenable to transportation by pipeline. Because McColl did not consider the headloss data to be reliable, for unspecified reasons, he did not present any correlations between headlosses and flow.

In a broader study by this Institute, Elliott and de Montmorency (12) investigated the chemical, mechanical, hydraulic and economic aspects of the transportation of field-cut chips in an 8-in. diameter aluminum pipe. The chemical pulping tests indicated that no appreciable loss of pulp strength was likely to be caused by the amount of residence time expected in a commercial pipeline. While Elliott and de Montmorency did not present an equation for the correlation of the headloss to flow characteristics, they did provide a logarithmic plot of $\emptyset$ versus $V_m/\sqrt{D}$. Later Stepanoff (28) claimed that the PPRIC data fitted the form:

$$\phi = 4gD/V_m^2 \quad \ldots\ldots\ldots\ldots\ldots\ldots \quad (2.4)$$

Elliott and de Montmorency's data gave:

$$\phi = 1.25\ (4gD/V_m^2)^{1.03} \quad \ldots\ldots\ldots\ldots\ldots\ldots \quad (2.5)$$

for 41 measurements taken in the 8-in. pipe. Adding McColl's 18 measurements taken in the 2-in. pipe to the data from Elliott and de Montmorency, the combined data gave the expression:

$$\phi = 1.29\ (4gD/V_m^2)^{0.935} \quad \ldots\ldots\ldots\ldots\ldots\ldots \quad (2.6)$$

Both Eq. (2.5) and Eq. (2.6) yield values of ϕ from 10 to 24 per cent higher than Eq. (2.4) as given by Stepanoff.

Faddick (13) measured the headlosses of pulpwood chips in a 4-in diameter aluminum pipe for maximum volumetric concentrations of only 17 per cent compared to Elliott and de Montmorency's 30 per cent. A line of best fit through the 59 data points produced the relation:

$$\phi = 2.51\ (4gD/V_m^2)^{1.42} \quad \ldots\ldots\ldots\ldots\ldots\ldots \quad (2.7)$$

Wasp et al. (30) in an economic study utilizing both Elliott and de Montmorency's and Faddick's data noted that the latter's headlosses, when projected to an 8-in. diameter pipe produced values generally 25 per cent higher than Elliott and de Montmorency's.

As this investigation neared completion the author received headloss data for woodchip mixtures in a 6-in. diameter pyrex pipe from a woodchip study in progress under the direction of A. Soucy at Laval University (26). The data were in tabulated form and no immediate comparison with a Durand-type equation was made. Instead, a comparison of the woodchip data was postponed to Chapter V in which the individual studies of McColl, Faddick, Soucy, and Elliott and de Montmorency in 2-, 4-, 6-, and 8-in. diameter pipes, respectively, were compared by means of a simplified version of the Durand equation. All the available woodchip data are listed in Appendix G.

Flow Regimes for Woodchip Transport

Because no data are available for delineating the various woodchip flow regimes the following description is stated in general terms based on visual observations by Faddick (13). The homogeneous flow regime is not applicable to woodchip transport. Heterogeneous suspension flow may occur for low volumetric concentrations (about 10 per cent) and high mixture velocities, (about 10 fps in a 4-in. pipe)

but this combination is not the most economical according to Hunt's (16) economic analysis of a woodchip pipeline. Therefore, this flow regime will not be considered. Heterogeneous saltation flow without a bedload, but which may include moving dune formations, is also not economical due to the small volumetric concentrations (less than 15 per cent) which characterize this regime.

Assuming a minimum volumetric concentration of 20 per cent and mixture velocities ranging from 3 to 8 fps in pipe sizes from 4 to 10 in. in diameter (16, 13) as the probable range for commercial operations, the mode of transport in an economical system would be a sliding bedload flow. The regime would be heterogeneous saltation flow at the upper surface of the bed and heterogeneous suspension flow above the bed. The lower portion of the bed would slide not quite as a continuous phase because the upper portion of the bed, as previously mentioned, would be in saltation and the velocity of the upper portion of the bed during this type of flow would exceed the velocity of the lower portion of the bed. A bedload of saturated woodchips always slides along the pipe invert. Granular solids differ in that a

bedload of sand or gravel can slide but it also can be relatively stationary with only the upper portion of the bedload showing noticeable forward motion.

Discussion of the Correlations

The correlations reviewed display certain weaknesses which may explain some of the discrepancies encountered when applied to systems other than those for which they were developed.

Condolios, Chapus, and Constans (8) noted that the strength of Durand's equation lies in its ability to predict satisfactorily the headlosses for uniform sands and gravels, mixtures of sands and gravels with two different grain sizes in varying proportions, mixtures of sands and gravels with a wide grain distribution, and for natural sands. A weakness of the correlation is that it cannot be applied to solids of neutral buoyancy. When the specific gravity of solids is equal to that of water, Eqs. (2.2) and (2.3) yield a mixture hydraulic gradient equal to the clear-water hydraulic gradient. But this may not always be the case. Woodchips have a specific gravity which depends upon moisture content

and may range from 0.7 to 1.125. Yet the headloss produced by a mixture of woodchips and water is significantly greater than that for water (13).

Zandi and Govatos (33) have demonstrated that while Eq. (2.1), is the best available correlation it appears to be overextended when applied to an accumulation of data which they collected from many published and unpublished studies on slurry flow in pipes.

Babcock (3) in a series of carefully-controlled tests, experimented extensively with the Durand equation, Eq. (2.1), and found that the mixture hydraulic gradient i_m, was not linearly dependent on the volumetric concentration C_v, at low concentrations and high velocities. He also observed that the term gd_n/Vs^2, which is a form of drag coefficient C_d, had a vague role in that a logarithmic plot of $\emptyset$ versus $V_m^2/gD(s-1)$ for several sands showed all the points to fall on a straight line whereas a graph of $\emptyset$ versus $V_m^2\sqrt{C_d}/gD(s-1)$ for the same data showed the points to fall on several parallel lines. Babcock concluded that the dimensionless groupings of $\emptyset$ and ψ of Eq. (2.1) were the cause of excessive scatter in his data, and that Eq. (2.1) may not describe

a two-phase flow system properly.

Questions concerning the validity of applying Eq. (2.1) to all solids transported in pipelines have not been confined only to experimental verification. Barr (4) has contended that the equation does not provide a valid correlation of experimental data because it violates similarity criteria based on ratios of forces. He claims that Eq. (2.1) is incomplete in that it lacks a d/D ratio (some particle dimension to pipe diameter), and a viscosity term, but it retains V_s, the particle settling velocity, and i, the clear-water hydraulic gradient, both of which he considers to be extraneous. Rearrangement of the expression for ψ in Eq. (2.1) will yield the ratio d_n/D along with the ratios V_m/V_s and $V_m/\sqrt{gD}$. Barr apparently discounts this rearrangement because none of the more common combinations of pressure, gravity, friction, or inertial forces will give the accompanying ratio of mixture velocity to particle settling velocity. He suggests that the particle settling velocity is certainly a valid property for describing the free-fall characteristic of a single particle; the question is whether the particle settling velocity is a valid property for describing the

pipeline flow of a mixture of particles.

A simplified version of the Durand equation, Eq. (2.1) formulated in an attempt to correlate the headloss for the pipeline transport of woodchips can be expressed in the form of Eq. (2.4) as suggested by Stepanoff (28), that is

$$\phi = K\ (4gD/V_m^2)^m = K\ (\Psi_1)^m \quad \ldots\ldots\ldots\ldots\ldots \quad (2.8)$$

The validity of the form is questioned when the data observed by McColl, Faddick and Elliott in 2-, 4-, and 8-in. diameter pipes are used to determine the coefficient K and the exponent m (Eqs. 2.6, 7, and 5). Table I shows the variation of K and m using the data from the 2-in., 4-, and 8-in. diameter pipes.

TABLE I.

K, m for $\phi = K\ (\Psi_1)^m$ based on headloss data of woodchip mixtures in 2-, 4-, 8-in. diameter pipes.

Investigator	Pipe Diameter, in inches	Coefficient, K	Exponent, m
(1)	(2)	(3)	(4)
All PPRIC tests	2,8	1.29	0.935
Faddick	4	2.51	1.42
Elliott, de Montmorency	8	1.25	1.03

As the woodchips used in these investigations were basically the same size for all the tests, the variation in K and m may have two explanations: (1) differences in the technique used in obtaining the data and differences in the precision with which the data were taken, provided variations of the magnitude indicated; and (2) a correlating equation of this form is not suitable for extrapolating the headloss data for a mixture of woodchips and water to pipes of a diameter different from that used for obtaining the specific values of K and m.

In other words, on the basis of the data presented, it appears that the ratio of the size of the chips to the diameter of the pipe may have a significant effect on the mixture headloss.

If Durand's equation is apparently not an adequate headloss correlation for a woodchip mixture, then the fact that this equation works for sands and gravels of different sizes, requires additional comment. The ratios of nominal particle diameter to pipe diameter (d_n/D) ranged from about 0.0003 to 0.02. Durand's upper value of d_n/D just approaches the lower value of the chip size to pipe diameter ratio used

in the woodchip tests. The ratios for the woodchip tests are given in Chapter III. Although the sand and gravel shapes were not specified in Durand's study, they were undoubtedly not as flat and rectangular as woodchips. Other factors may also have been involved. For example, Durand's study never utilized volumetric concentrations greater than 20 per cent whereas concentrations as high as 40 per cent were attained in the woodchip tests. In addition, all the tests by Durand were performed in steel pipes whose roughnesses were not specified. The major differences between Durand's tests and the woodchip tests appear to have been the relatively larger size and flatter shape of the woodchips over the sands and gravels. It is possible then, that there is a critical size and/or shape of particle in a given pipe diameter beyond which the mixture headloss as given by Eq. (2.1) changes significantly.

Because the Durand equation is not in a form applicable to neutrally-buoyant particles and because a simplified version of the Durand equation does not appear to account for the ratio of chip size to pipe diameter,

this investigation was initiated to study another approach to the correlation of headloss and pipeline flow of a mixture of simulated woodchips in water. The approach described in the following chapter considers the use of the Stanton diagram with modifications to account for the properties of the solid phase.

CHAPTER III

METHOD OF INVESTIGATION

A determination of a headloss correlation for transporting solids in pipelines requires an understanding of two-phase flow characteristics.

Soo (25) has outlined two methods for the study of the dynamics of multiphase systems.

1. "Treating the dynamics of single particles and then trying to extend to a multiple particle system in an analogous manner as in molecular (kinetic) theory."

2. "Modifying the continuum mechanics of a single fluid in such a way as to account for the presence of particles."

He further states, "extension to multiple particle systems from dynamics of single particles has not been particularly successful except in isolated cases."

Flow Characteristics of Woodchip Mixtures

Two-phase flows of woodchips and water do not comprise a continuum because the discrete particles in a given volume of flowing mixture are spaced such that it is possible to isolate a differential volume which may contain all liquid, all solid, or part of both. However, because

of the difficulties in experimentally determining the internal shear mechanisms of such a flow, the system is most expediently analyzed by the continuum concept when applying the equation of momentum to elemental volumes large enough to contain the average properties of the entire mixture.

The flow regime of woodchips and water can be either heterogeneous suspension flow (Fig. 3-1a), heterogeneous saltation flow, sliding bed flow, or a combination of all three. These regimes have been described in the previous chapter. In the general case (Fig. 3-1b), the concentration profile is nonuniform and unsteady, i.e.,

$$C_v = C_v\ (r,\ \theta,\ z,\ t) \quad \ldots\ldots\ldots\ldots\ldots\ldots \quad (3.1)$$

Individual particles migrate depending on the intensity of the turbulent velocity fluctuations u, v, w in the z, r, θ directions, respectively. However, for steady flow of the mixture, the time-averaged concentration profile, (Fig. 3-1b) undergoes no net change over the length of test section.

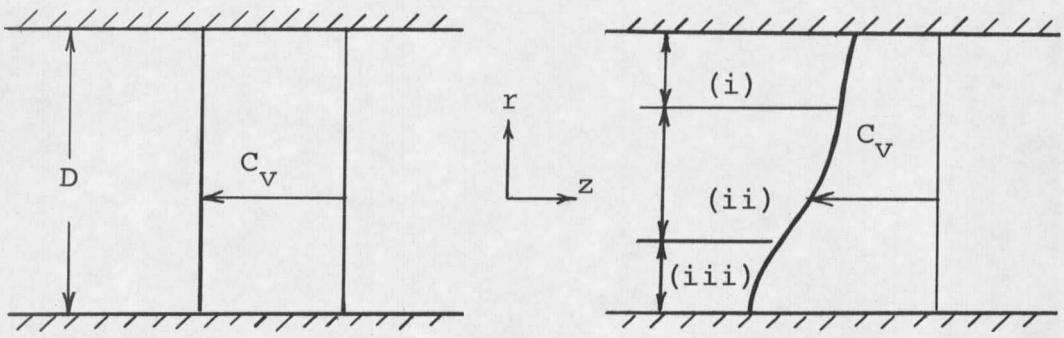

a. Heterogeneous suspension flow, uniform concentration profile, ($\partial C_v/\partial\theta = \partial C_v/\partial r = 0$). Turbulent velocity fluctuations predominate.

b. (i)-Heterogeneous suspension flow
(ii)-Heterogeneous saltation flow
(iii)-Sliding bed flow
Non-uniform concentration profile, ($\partial C_v/\partial\theta \neq 0$; $\partial C_v/\partial r \neq 0$). Gravity effects predominate.

Fig. 3-1. Concentration Profiles

The mixture flow is assumed to be steady, incompressible and turbulent throughout a test section of constant diameter giving

$$\frac{\partial C_v}{\partial z} = 0 \qquad \ldots\ldots\ldots\ldots\ldots\ldots\ldots \quad (3.2)$$

and

$$\frac{\partial C_v}{\partial t} = 0 \qquad \ldots\ldots\ldots\ldots\ldots\ldots\ldots \quad (3.3)$$

The mixture density is by definition:

$$\rho_m = \rho(1+C_v(s-1)), \qquad \ldots\ldots\ldots\ldots\ldots\ldots (3.4)$$

giving the following relations for the mixture density:

$$\frac{\partial \rho_m}{\partial r} \neq 0; \quad \frac{\partial \rho_m}{\partial \theta} \neq 0 \qquad \ldots\ldots\ldots\ldots\ldots\ldots (3.5)$$

The mixture density thus varies across the cross section of the pipe. The mixture density and particle concentrations are interrelated as shown by Eq. (3.4). Their distribution is affected by the interrelationship between the gravity force acting on the submerged particles and the level of turbulent fluctuations inherent in the mixture flow. The interrelationship between gravity and turbulence is only qualitative but suffices to demonstrate the complexities of two-phase flow.

When the specific gravity of the particles is near that of the carrying medium, the mixture density for normal transport concentrations will not vary greatly over the cross section of the pipe. For example, a volumetric concentration of 30 per cent of saturated woodchips ($s \simeq 1.13$) in water gives a bulk mixture density ρ_m, equal

to 1.039ρ, an increase of less than 4 per cent over the density of water. For a sand slurry of the same concentration the mixture density is $1.5\ \rho$. Relative to a sand mixture then, the mixture density of a slurry of woodchips or any near neutrally-buoyant particles will not differ greatly from the density of water regardless of the magnitude of the local concentration, that is,

$$\frac{\partial \rho_m}{\partial r} \simeq 0; \quad \frac{\partial \rho_m}{\partial \theta} \simeq 0 \qquad \text{..... (3.6)}$$

However, the absolute value of ρ_m will still be important insofar as denser mixtures require more energy for transport than less dense mixtures at the same flow conditions.

Momentum Equation

Before analyzing two-phase flows it is useful to briefly discuss single-phase flow. The flow is assumed to be steady, incompressible, and turbulent throughout a horizontal pipe of constant diameter. A macroscopic element comprising the length L is considered. See Fig. 3-2.

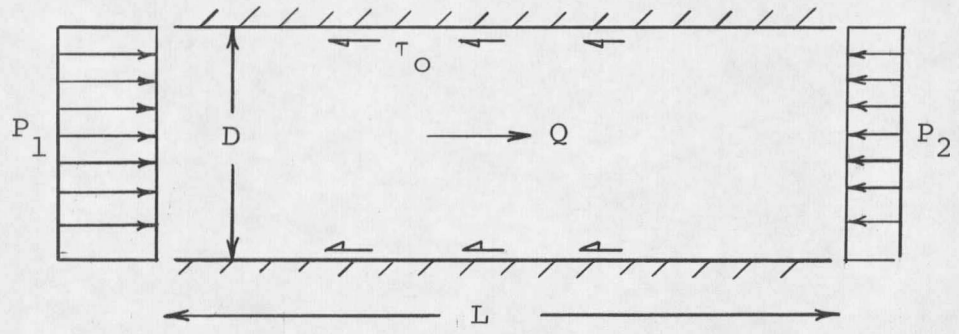

Fig. 3-2. Single-Phase Flow System

The time-averaged equation of motion reduces to a force balance between the pressure gradient and wall shear:

$$(P_1-P_2)\ \pi\ D^2/4 = \tau_o \pi DL \qquad \text{..... (3.7)}$$

from which

$$\tau_o = \Delta P \cdot D/4L \qquad \text{..... (3.8)}$$

When Eq. (3.8) is nondimensionalized with the inertia term $\rho V^2/2$, the friction factor f, is obtained:

$$2\tau_o/\rho V^2 = \Delta P \cdot D/2\rho V^2 L = f \qquad \text{..... (3.9)}$$

To be consistent with the majority of the literature in fluid mechanics, the Darcy-Weisbach form of friction factor is used rather than Fanning friction factor, i.e.,

$$f = 2gDi/V^2 \qquad \ldots\ldots\ldots\ldots\ldots\ldots\ldots \quad (3.10)$$

where i is the slope of the hydraulic grade line. The friction factor is a function of the Reynolds number, Re, where

$$Re = VD/\nu \qquad \ldots\ldots\ldots\ldots\ldots\ldots\ldots \quad (3.11)$$

and the relative roughness of the pipe, which for purposes of this study can be expressed by the parameter k/D. The three parameters f, Re, and k/D constitute the well-known Stanton diagram for pipe flow.

For two-phase flows in pipes, the parameters f and Re are modified to f_m and Re_m, respectively, to denote mixture flows. The mixture friction factor is given by

$$f_m = 2gD\ i_m/V_m^2 \qquad \ldots\ldots\ldots\ldots\ldots\ldots\ldots \quad (3.12)$$

where i_m is the slope of the mixture hydraulic gradeline in feet of water per foot length of pipe and the mixture Reynolds number is given by

$$Re_m = V_m D/\nu \qquad \ldots\ldots\ldots\ldots\ldots\ldots\ldots \quad (3.13)$$

The fluid kinematic viscosity is used because the apparent viscosities of a woodchip and water mixture cannot be measured conveniently.

Fig. 3-3 shows a macroscopic element of a two-phase flow system.

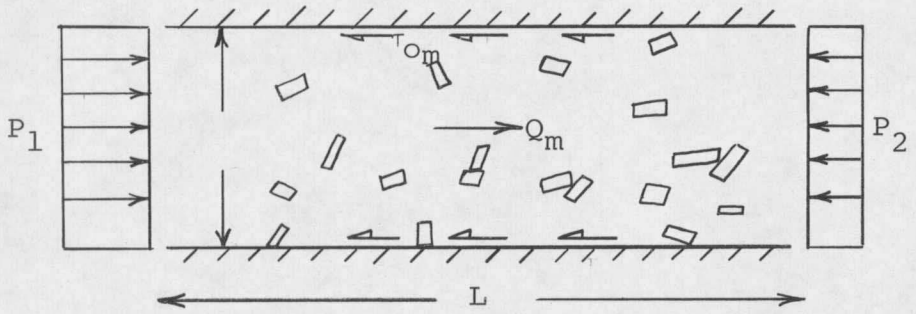

Fig. 3-3. Two-Phase Flow System

The wall shear stress τ_{o_m} must reflect the effects of the solids as well as the viscous and turbulent effects of the fluid. The shear stress at the wall includes the effects of mechanical friction of the particles and the fluid friction.

Particle mechanical friction includes the effect of the particles rubbing on the pipe wall. See Fig. 3-3. The greater the number of particles (concentration) of a given size, the greater is the probability of interference.

The pipe diameter also influences the degree of particle interference. Other factors involved are the particle geometry and material (surface texture). For example, heavy spheres will roll along the pipe invert whereas heavy plate shapes will slide along the pipe invert. Also, as the difference between the specific gravities of the particle and fluid increases, the normal force exerted by the particles on the pipe wall increases thereby increasing the particle resistance to movement.

The shear stress at the wall reflects the fluid friction through the action of the fluid viscosity and the effect of pipewall roughness on the velocity gradient of the mixture. The mean mixture velocity is considered to be a measure of the interaction between the solid and liquid phases because for a given power input the mean velocity of flow varies with the properties of the solids being transported.

The effects of particle surface texture on two-phase flow systems will not be considered in this study. Other effects which are not well understood or cannot easily be measured should be noted. The sliding-bed regime and the

heterogeneous saltation flow regime destroy the axial symmetry of flow and produce a mixture density gradient over the cross section of flow. Also, the interrelationship between particles and turbulence is poorly understood. For example, Daily and Hardison (9) reported an increase in the axial turbulent velocity fluctuation u, and the mixture friction factor, with the addition of solids.

Collectively, the shear stress at the wall appears to be dependent upon the following variables; particle concentration, density, size and shape, pipe diameter and wall roughness, fluid viscosity and density, gravity and velocity of flow. The premise adopted herein, is that if the particle size and shape are adequately defined (to be discussed later), the particle settling velocity need not be defined when the mixture velocity is also defined. The foregoing description provides a set of variables which can be expected to affect the headloss and hydraulic gradient of a mixture of woodchips and water flowing in a pipe. The mixture hydraulic gradient may be written in the following functional form:

$$i_m = i_m\ (C_v,\ d,\ D,\ \rho_s,\ \rho,\ k,\ V_m,\ g,\ \mu) \quad \ldots\ldots (3.14)$$

where C_v = particle concentration;

d = particle size and shape factor (to be discussed later);

D = pipe diameter;

ρ_s = particle density;

ρ = fluid density;

k = Nikuradse equivalent sand-grain roughness;

V_m = mean mixture velocity;

g = gravitational acceleration; and

μ = dynamic viscosity of the fluid.

The mixture hydraulic gradient i_m, is replaced by h_{f_m}/L, where h_{f_m} is the mixture headloss measured in feet of water over the test section length L, also in feet. From dimensional analysis (Appendix B), eight parameters are obtained which give the following functional relationship:

$$\phi\ (h_{f_m}/D,\ C_v,\ d/D,\ \rho_s/\rho,\ k/D,\ gD/V_m^2,\ \nu/V_mD,\ L/D) = C_1 \quad \ldots\ldots (B.2)$$

Inspection of the definition of the mixture friction factor, Eq. (3.12) reveals that it is a combination of the first,

sixth, and eighth parameters given in Eq. (B.2):

$$f_m = 2(h_{f_m}/D)\ (gD/V_m^2)\ (D/L) \quad \ldots\ldots\ldots\ldots\ldots\ldots \quad (B.3)$$

and the functional relationship reduces to:

$$f_m = f_m\ (Re_m,\ C_v,\ k/D,\ d/D,\ s) \quad \ldots\ldots\ldots\ldots\ldots\ldots (3.15)$$

For two-phase flows the mixture friction factor f_m, is considered to be not only a function of the mixture Reynolds number Re_m, and relative roughness k/D, but also, of three other parameters: C_v, d/D, and s. The mixture Reynolds number is the ratio of inertial forces to viscous forces acting on the mixture flow, that is, it characterizes the turbulence or lack of turbulence in the flow, at least for a given type and concentration of particles. The number of particles is characterized by C_v; the scale factor d/D characterizes particle size and shape relative to the pipe diameter. The density of the particles relative to water ρ_s/ρ, is given by s.

The effect of gravity on a two-phase flow system requires additional explanation. It is constant as long as the difference in specific gravities between the solid

phase and liquid phase is constant. The interaction between the constant gravity term and variable mixture shear term helps to explain qualitatively the flow regimes in two-phase flow. At low mixture Reynolds number and high concentrations the turbulent velocity fluctuations are apparently too small to support the solids in a uniform suspension. The gravity force causes the heavy solids to settle out of the flow to form a distorted concentration profile such as that given by the sliding-bed regime (Fig. 3-1b). At high flows and low concentrations the turbulent velocity fluctuations predominate thus producing a uniform concentration profile typical of heterogeneous suspension flow.

The parameters given by Eq. (3.15) are not the only forms that the variables can take (4,5); however, these forms provide a workable set of parameters for the particular system in this investigation and are used to form the basis of a headloss correlation.

The number of parameters suggests that a universal correlation of the form

$$f_m = f_m(V_m D/\nu,\ C_v,\ k/D,\ s,\ d/D) \quad \ldots\ldots\ldots\ldots\ldots \quad (3.15)$$

could be formulated only through an extensive testing program resulting in a library of Stanton diagrams. However, one simplification of Eq. (3.15) is immediately possible. For flow in smooth pipes the relative roughness parameter k/D, approaches zero. This precludes a headloss correlation for flow in rough pipes but all the woodchip data compiled to date (1968) have been obtained with smooth pipes. Another possible simplification is to combine the particle size and shape into one variable. This is discussed below.

Particle Size-Pipe Diameter Ratio

It was postulated from the comparison of coefficients and exponents tabulated in Table I that a measure of the ratio d/D (representative particle size to pipe diameter), may be required to correlate the straight pipe headlosses for the transport of particles in different pipe sizes. Both the particle size and shape must be considered. This is evident from the classical relationship between the drag coefficient and Reynolds numbers for particles dropped in a quiescent fluid. The particle shape is the third parameter. For example, if a piece of putty is dropped into still fluid, it falls with a velocity depending on the shape of the putty.

In all cases, the volume of the putty is constant but its shape and surface area vary.

The size and shape of spheres are not difficult to measure but those for irregular shaped particles are. Alger and Simons (2) have proposed a shape factor SF, from a study of particle fall velocities for irregular-shaped particles. This factor includes the surface area of the particles and has a value of 1.0 for spheres. The shape factor is given by

$$SF = \frac{c}{\sqrt{ab}} \cdot \frac{d_a}{d_n} \qquad \text{..... (3.19)}$$

where c = particle thickness;

a = longest dimension of particle;

b = shortest width dimension of particle;

d_a = diameter of a sphere having the same surface area as the particle; and

d_n = nominal diameter or diameter of a sphere having the same volume as the particle.

For a sphere, c, a, and b are all equal to the diameter. The surface area of irregular-shaped particles is difficult to determine but the flat rectangular-shaped particles considered in this study are easily measured, however.

For ungraded particles a weighted mean shape factor $\overline{SF}$ is obtained by sieving the particles into an arbitrary number (n) of size ranges and measuring average values of the particle dimensions for each size range. The first range contains the fraction p_1 of the total number of particles, the second range contains the fraction p_2 and so on. For example, $\overline{c}$, the weighted mean particle thickness, is given by

$$\overline{c} = p_1 c_1 + p_2 c_2 + \cdots + p_n c_n \quad \ldots\ldots\ldots\ldots\ldots\ldots \quad (3.20)$$

The weighted mean value of the shape factor becomes

$$\overline{SF} = \frac{\overline{c}}{\sqrt{\overline{a}\,\overline{b}}} \cdot \frac{\overline{d}_a}{\overline{d}_n} \quad \ldots\ldots\ldots\ldots\ldots\ldots\ldots\ldots \quad (3.21)$$

The weighted mean value of Alger and Simon's shape factor is dimensionless but it can be modified to form a value of d for an irregular-shaped particle when multiplied by $\sqrt{\overline{a}\,\overline{b}}$. Hence the ratio d/D becomes

$$\frac{d}{D} = \frac{\overline{SF}}{D} \cdot \sqrt{\overline{ab}} = \frac{\overline{c}}{D} \cdot \frac{\overline{d}_a}{\overline{d}_n} \quad \ldots\ldots\ldots\ldots\ldots\ldots\ldots \quad (3.22)$$

where the characteristic particle dimension d comprises the weighted mean values of c, d_a and d_n. Whether the particles are of regular or irregular shape, the dimensions a, b and c must be measured physically. The value of d_a for irregular-shaped particles can be determined by measuring the amount of dye or paraffin required to coat the particles. The value d_n can be measured by fluid displacement. For very small particles these methods would not be practical, but then particle shape would not be as critical. For regular-shaped particles without excessively rough surfaces it is easier to obtain d_a and d_n from physical measurements of the particles. Woodchips are sufficiently smooth and uniform in shape to be measured directly. Unless the particles are of both uniform size and shape, a sieve analysis is still required to obtain the weighted mean values of the shape factor.

All the woodchip experimenters used ungraded woodchips. McColl (19) used specially made chips of nominal length 1-1/2 in. Because of their cross-sectional area all chips passed a 9/16-in. screen despite their nominal length and 80 per cent were retained on a 3/8-in. screen. The remaining 20 per cent were retained on a 1/4-in. screen. Elliott

and de Montmorency (12) used large chips of which 64 per cent passed a 1-1/8-in. screen but were retained on a 1/2-in. screen. Faddick (13) used slightly smaller chips all of which were under 1 in. and 50 per cent were retained on a 1/2-in. screen. The chips used at Laval University (26) were all under 2 in. and 33 per cent were retained on a 1/2-in. screen.

Table II gives the shape factor and d/D ratios for some previous woodchip tests and the plastic chip studies described in the following chapter. The nominal woodchip sizes given in column 2 are estimated averages from which the values a, b, c, d_a, and d_n were calculated directly. Size analyses of the woodchips were never made for the purpose of obtaining weighted mean dimensions. Consequently, the woodchip shape factor and d/D ratio are approximate.

Experimental Program

A limited experimental program was established to study the effect of the parameters Re_m, C_v, s_g and d/D on the friction factor for mixtures of simulated woodchips and water in smooth circular horizontal pipes. Because this was

TABLE II.- ESTIMATED VALUES OF SF AND d/D FROM CHIP STUDIES

Pipe internal diameter, inches D	Nominal chip sizes, inches	Approx. shape factor SF	Approx. chip dimension, inches d	Approx. scale factor d/D
(1)	(2)	(3)	(4)	(5)
1.837 (19)[a]	1-1/2x1/2x1/8	0.204	0.177	0.0966
8.412 (12)	1x3/4x1/8	0.202	0.174	0.0208
4.026 (13)	1x3/4x1/8	0.202	0.174	0.0433
6.000 (26)	1x3/4x1/8	0.202	0.174	0.0291
3.938[b]	1/2x3/8x1/10	0.293	0.1272	0.0324
3.000[b]	1/2x3/8x1/10	0.293	0.1272	0.0424

[a]denotes reference

[b]MSU study

a preliminary study, the variables s and D, were limited to two values each. The data used for the analysis of the effects of these parameters were obtained by measuring the headlosses versus Reynolds numbers for a mixture of plastic chips and water flowing in smooth circular horizontal pipes of two different diameters. Two types of chips were used,

each having a different specific gravity although all the chips had the same uniform size and shape. The experimental test facilities are described more fully in the next chapter.

CHAPTER IV

EXPERIMENTAL TEST FACILITIES AND DATA COLLECTION

Tests to measure the friction losses for transporting mixtures of simulated woodchips and water in a pipeline were conducted in a test loop designed for a complete woodchip pipeline transport studies project. This section describes the particles used, the experimental test facilities, data collection and processing, and the test procedures.

Plastic Chips

Plastic chips of uniform size, shape and specific gravity were used to simplify the problem of determining the weighted mean values of the chip properties. The plastic chips also overcame the problems associated with maintaining a fresh supply of wood chips and of coping with the putrid odor of deteriorating wood chips. The dimensions of the plastic chips were approximately half of those considered to be an optimum size by wood pulp manufacturers. The chip size was selected to preserve the ratio of maximum chip dimension to pipe diameter expected to be encountered in an operating prototype installation. This ratio was approximately that of a 1 x 3/4 x 1/4-in. woodchip to an 8-in.

diameter pipe modelled by a 1/2 x 3/8 x 1/10-in. plastic chip in a 4-in. diameter pipe. The 8-in. diameter pipe was determined to be an optimum size for a wide range of transport rates in Hunt's (16) economic analysis. Three types of plastic chips were utilized: red cycolac chips with a specific gravity s, of 1.04; blue ethocell chips, s = 1.05 yellow polyethylene chips, s = 0.92. The manufacturer, Commercial Plastics Company of Chicago, stated that variations in the specific gravities of any one chip type were caused by variations in the coloring pigments. The variations measured $\pm$ 0.4 per cent. Tolerances on the chip sizes were $\pm$ 0.004 in. on thickness and $\pm$ 1/32 in. on length and width. The effect of the tolerances on the d/D parameter was less than 5 per cent.

The settling velocities of individual chips averaged 0.13 fps for the ethocell chips and 0.12 fps for the cycolac chips. The rise velocity of the polyethylene chips averaged 0.15 fps. The chip settling velocities were of the same order of magnitude as the turbulent velocity fluctuations for the range of Reynolds numbers covered in the tests. From Laufer's study (18) it can be shown that at

mid-radius of a 4-in. smooth pipe carrying clear water with a Reynolds number range of 50,000 to 500,000, the values of v and w, the radial and tangential turbulent velocity fluctuations, are 0.12 and 0.15 fps, respectively.

Because of similar properties the red and blue chips were combined in one batch for the test program. The red and blue chip batch (s=1.045) shall hereafter be called the heavy chips and the yellow chips (s=0.92) shall hereafter be called the light chips.

Experimental Test Facilities

The study initially utilized a 700-ft pipe loop which was "on line" with an IBM 1620 II digital computer and which permitted the use of a rapid data collection system. A shorter test loop (200 ft) was also being used for valve testing while headloss data were collected in the longer test loop. When the valve tests in the short loop and the headloss tests in the long loop were completed, the shorter test loop was used to obtain additional headloss data by manual reading of manometer deflections.

General Equipment

A comprehensive report by Schmidt (24) describes the apparatus, its design, construction, calibration and operational procedures. Herein, only the equipment pertinent to this study is briefly described.

The experimental pipeline facilities consisted of a 700-ft (long) test loop and a 200-ft (short) test loop, of 4-in. diameter pipe, separation drum, combination chip-hopper and water storage tank, conveyer belt, water-chip mix tank, pump and motor set, various control valves, two magnetic flow meters, pressure transducers and a central operation console which provided access to most of the control devices necessary to operate the pipeline. See Fig. 4-1.

Pipeline

The pipeline consisted of 20-ft sections of aluminum and 6-ft sections of transparent acrylic pipe connected either by Victaulic or Dresser couplings for quick dismantling in the event of plugging. A straight horizontal

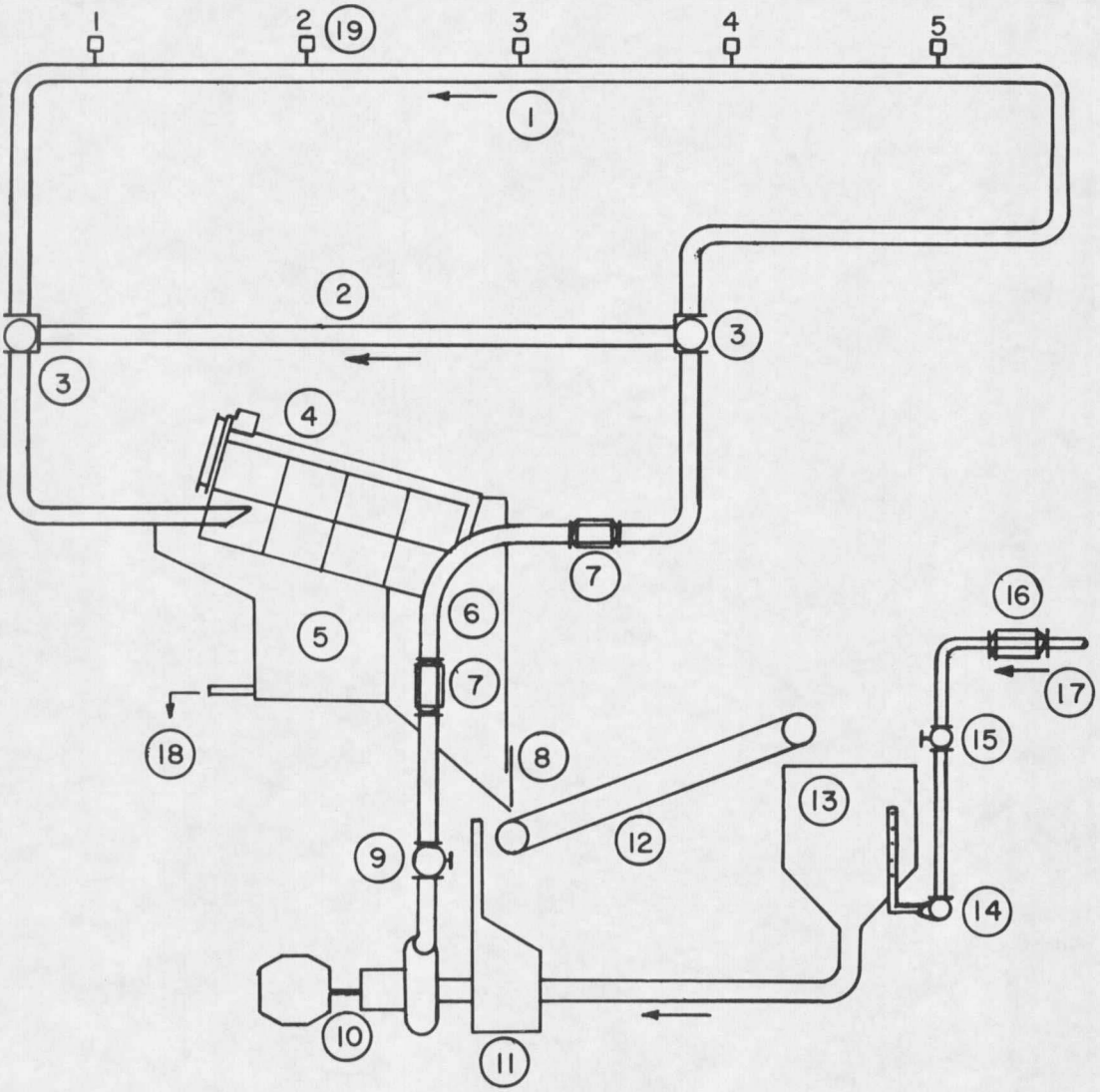

1. Long Test Section
2. Short Test Section
3. 3-Way Valve
4. Rotating Drum
5. Water Collection
6. Chip Storage-Hopper
7. Mix Flow Meter
8. Supply Gate
9. Control Valve
10. Pump and Motor
11. Console
12. Conveyer
13. Mix Tank
14. Overflow Valve
15. Control Valve
16. Water Flow Meter
17. From Elevated Tank
18. To Sump
19. Pressure Transducers

Fig. 4-1. Schematic of Pipe Line System

section 250 ft in length consisting entirely of 20-ft acrylic pipe lengths provided a location for measuring head-loss and for observing the modes of chip transport. A 221-ft test section established in this 250-ft run contained five equally-spaced pressure transducers. This number of measuring stations enabled the detection of any clump formations of chips or other transient flow conditions in the test section by indicating variations in the hydraulic gradient with time. Each pressure transducer was connected to a piezeometer ring which tapped into the acrylic pipe at four equally spaced locations on the periphery of the pipe. The taps were 1/8-in. diameter holes made flush with the pipe interior. Although the plastic chips could not enter the tapped holes it was mandatory to install sediment pots to prevent foreign particles from entering the pressure transducers.

Injection and Separation Equipment

The chip storage hopper and water storage tank were constructed as a single unit. Above them was an inclined rotating drum for separating the chips and water. Its

cylindrical framework was enclosed by 1/4-in wire mesh. An 18-in wide conveyer belt, 10 ft long and inclined upwards at 20 degrees delivered the chips from the chip hopper to the mix tank. The conveyer was necessary because headroom was not sufficient in the laboratory to permit the chip storage-hopper to be installed directly above the mix tank. A vertical gate with a ratchet control was used to regulate the flow of chips through the chip hopper onto the conveyer.

The mix tank was 3 ft in diameter and 3.5 ft high with a conical bottom and a 5-in. suction line (reduced to 4 in. at the pump's suction flange). Clear water was pumped from a sump in the laboratory to an elevated tank with an over-flow. A Foxboro magnetic flowmeter, gate valve, and auto-matic Clayton float valve were installed in a 3-in. diameter pipe which connected the elevated tank to the mix tank. The 3-in. water supply pipe entered the mix tank from the bottom next to the tank's discharge pipe. It terminated as a stand-pipe 20 in. in length and 1.55 ft from the top of the mix tank. The standpipe was capped but 1-in. circular perfor-ations along its surface produced a vortex-free flow of water with a minimum of air entrainment. No external devices

were required to agitate the plastic chip mixture in the mix tank. The tank was designed to have little "dead" storage, i.e., a short retention period for the mixture. This type of design is applicable when the mix tank does not have to serve as a reservoir for the pipeline.

The float valve was used simply as a safety device to prevent the mix tank from overflowing. It also secured a minimum fluid level in the mix tank that prohibited vortices from forming which could carry air into the solids-handling pump.

For the lighter than-water plastic chips, difficulty was encountered in making the chips sink into the pump suction piping. A sheet metal 45-degree funnel was placed in the mix tank with its stem inserted tightly into the suction piping to overcome this. The top of the funnel was 18 in. below the top of the mix tank. A 1/4-in wire mesh was attached to the perimeter of the funnel and the perimeter of the mix tank to contain the chips but allow water into the funnel. The volume of the mix tank was reduced substantially so that the weight of the chips falling off the conveyer into the funnel virtually pushed chips into the

stem of the funnel and into the pump suction piping. This arrangement required surveillance to ensure that the head of water in the mix tank exceeded the height of the sheet metal cone.

Fluctuations of less than 1 in. per min in the mix tank for a nominal mix flow of 400 gpm and 1/4 in. per min for a nominal flow of 100 gpm were tolerated. This produced a variation in the mix flow of less than 1 per cent.

Flow Control

An Allis-Chalmers 4 x 4-in. centrifugal solids-handling pump was used with a 9-1/2-in. NSX impeller. The pump's flow capacity and head requirements were based on a maximum anticipated velocity of 10 fps in the 700-ft line. This was satisfied by a design discharge of 400 gpm with an 80-ft head of which 13 ft was the static lift between the mix tank surface level and the discharge point.

The pump was driven by a General Electric 15-hp, 220-volt DC shunt-wound motor, rated at 2600 rpm. A rheostat control on the motor was used to regulate the pump speed and hence the discharge.

A 4-in. Grinnel diaphragm valve downstream from the pump was also used for flow control when the pipeline contained clear water; it remained open for mixture flows.

Magnetic Flowmeters

Foxboro magnetic flowmeters were used to measure the flow rates; a 4-in. meter for the mixture discharge and a 3-in. meter for the water supply. The difference between the mixture discharge and clear-water discharge gave the discharge of solids which, when divided by the mixture discharge, produced the volumetric concentration. Both meters were placed in horizontal sections of pipe with the mixture meter located approximately 275 ft upstream of the test section entrance. The output signals of the meters were recorded permanently on 0-400-gpm flow-charts located at the central operation console.

Pressure Transducers

Pipeline pressures in the test section were measured by five potentiometer-type gauge pressure transducers (type 4000) manufactured by Computer Instruments Corporation of

Hempstead, New York. Item 19 on Fig. 4-1 shows their locations (#1, 2, 3, 4, 5) on the 221-ft test section. The upstream pressure transducer was situated 42 pipe diameters downstream of a 4-ft radius U-turn. Visual observations of the test runs did not detect any noticeable swirling of the mixture at transducer #5 due to the U-turn.

The transducers were protected from excess pressures by a solenoid valve controlled by a valve-actuating circuit. The circuitry monitored the transducer output voltage such that at 95 per cent of the full capacity output, a relay closed, activating the solenoid valve. Valve closure isolated the transducer and dropped the transducer pressure to zero. The manufacturer claimed an error less than 1 per cent for independent linearity, repeatability, temperature sensitivity, and static-error band. This was confirmed for all but temperature sensitivity when the transducers were calibrated.

Short Test Loop System

As the tests in the long test loop system neared completion it was noticed that the heavier plastic chips

readily formed plugs at flows of about 150 gpm. The head-discharge characteristic curve of the pump was quite flat at this flow and was suspected of producing unstable cond-tions leading to complete flow stoppages.

The Allis-Chalmers pump was then replaced by a Fairbanks-Morse 3-x3-in. centrifugal solids-handling pump which had a steeper head-discharge characteristic curve at flowrates of 100 to 200 gpm. The 5-in. suction piping to the mix tank was also replaced by 3-in. piping. The smaller pump necessitated a reduction in headlosses in the test system. This was achieved by reducing the length of the test section. A 56-ft length of acrylic 4-in. pipe was inserted to short circuit the 221-ft test section. See item 2 on Fig. 4-1.

Because of the phase-out of the "on line" digital computer processing caused by relocation of the computing facilities, pressure transducers were not installed on the short loop system. Instead, a simple water-air differential manometer was connected to the 31.48-ft test section through a four-tap piezometer ring as previously described.

The greatly reduced testing time and effort prompted a further extension of testing to check the effect of the

parameter d/D. Budget restrictions limited the pipe size to 3-in. acrylic pipe in the short loop system. A test section of 41.28 ft was connected by a pair of three-tap piezometer rings to water-air and mercury-water differential manometers.

The test procedure for the short loop was essentially the same as for the long test loop. The chief difference was that the pipeline was not "on line" with a computer. Therefore, when the flow was steadied the flowcharts were marked and the manometer deflections were recorded manually and averaged over several minutes. Raw data comprising manometer deflections, mixture temperature, clear-water and mixture discharges were evaluated to give friction factors, concentrations, and mixture Reynolds numbers. The computations were made and the graphs were plotted using a Hewlett Packard 2116A digital computer.

Data Collection and Processing

The experimental pipeline system was essentially "on line" with an analog computer and digital computer. The system could be instantaneously monitored and data selected, stored or processed.

Some twenty channels of pipeline data were always monitored as part of the data collection system for the overall pipeline project, but for this study only six channels were utilized; these were the five channels for the pressure transducers and one channel to measure the input excitation voltage to drive the transducer sensors. The output voltages of the electronic sensors in the five pressure transducers were received by an analog-to-digital converter which was interfaced to a digital computer. This allowed the line pressure at the five points of the test section to be monitored as digital data on an IBM 1620 II digital computer. More details on the analog-to-digital data recording system are given in Appendix C.

Details of the equipment calibration are given in Appendix D.

Test Procedure

The water was changed for each major test run. All test procedures were started by pumping clear water from the laboratory supply into the mix tank until it was filled. Then the solids-handling pump was started against the closed

diaphragm valve. The valve was opened so as to fill the pipeline gradually. As the mix tank volume decreased, more water was admitted by opening the gate valve on the clear-water supply line. Through valve manipulation and regulation of the pump speed the mix tank volume was steadied for any desired pipeline flow.

The system was allowed to warm up for a minimum of 30 minutes while pumping at about maximum capacity of 400 gpm of clear water. During this time the multiplexer and power supplies were turned on and adjusted to a standard 15 volts.

For the tests using clear water only, the flow was regulated by the gate valve on the clear-water supply line, the diaphragm valve at the pump discharge, and by the rheostat that controlled the pump speed. Both flowmeters showed identical flowchart readings when the mix tank volume was constant.

When chips were to be pumped, the rotary drum and belt conveyer were started after some arbitrary clear-water flow had been established. The gate on the chip hopper was raised to allow the chips to fall onto the conveyer belt which lifted them into the mix tank where the agitation

produced by incoming clear water thoroughly mixed with the chips. Mixture flow and concentration were controlled by the chip-hopper gate, the pump speed and the clear-water valve. The diaphragm valve downstream from the pump remained wide open whenever chips were being pumped. Generally, it was easier to hold the mixture velocity steady while varying the concentration although for some tests the opposite procedure was adopted.

The chip mixture was drawn into the pump and transported through the pipeline into the rotary screen drum where the water was returned to the laboratory sump for recirculation. The chips tumbled out of the drum into the chip hopper and onto the conveyer belt to repeat the cycle.

When the flowchart readings were steady and the mix tank level was constant the console-operator signalled the computer attendant by telephone to start the computer print-out. At the same time the operator marked the flowcharts to correspond with the computer print-out. The computer printed and punched the twenty channels of data, of which only the output voltages of the five pressure transducers and the excitation voltage to drive them pertained to this study.

Also printed and punched was the number of times (as pre-selected by the computer attendant) each data channel was read and averaged before being recorded. The mixture temperature was recorded for each test.

To shut down the system, the gate on the chip hopper was closed to cut off the chip supply to the mix tank. The clear-water supply and pump speed were adjusted to maintain a sufficient volume of water in the mix tank. When all the chips had been discharged from the pipeline into the chip-hopper, the drum and conveyer belt were turned off. Then the clear-water valve and the diaphragm valve were closed to cease the pipeline flow.

Data Processing

The mixture flow was given directly by flowcharts. The volumetric concentration was obtained from the mixture flow Q_m and the water flow Q_w, as follows:

$$C_v = \frac{Q_m - Q_w}{Q_m} \quad \ldots\ldots\ldots\ldots\ldots\ldots\ldots\ldots \quad (4.1)$$

The hydraulic gradients for the mixture flow (i_m) and clear-water flow (i) were computed as follows. Each transducer voltage was divided by the excitation voltage supplying

the sensors. The ratio was inserted into the calibration curve for the particular transducer to give the piezometer head in feet for that transducer station. The hydraulic gradient was computed as the differnce in any two piezometer heads (ft) divided by the distance between them (ft).

The five computed piezometer heads gave a possible combination of ten hydraulic gradelines. The mean hydraulic gradient and its standard deviation were computed for each combination of transducer stations. Also, the number of observations was recorded.

Preliminary observations of both clear-water and mixture flow showed the standard deviation of the hydraulic gradient for each of the ten test sections to be a minimum for the longest test section length. The standard deviations of the hydraulic gradient in the shortest test sections (55 ft) were as much as double those in the longest test section length. Therefore, to avoid the compiling and reducing of an excess of data the full 221-ft test section was used for computing the headloss.

Upon completion of the testing program all computations for the long loop system were made on an SDS-Sigma 7 computer.

The data measurements included the volumetric concentration, mixture flow and temperature, hydraulic gradient of the mixture and mixture temperature.

The heavy chip tests included 75 runs in the long test loop with 4-in. diameter pipe, 51 runs in the short test loop with 4-in. diameter pipe, and 40 runs in the short test loop with 3-in. diameter pipe. The velocity range was 2.5 to 10 fps in the 4-in. pipe and 5 to 18 fps in the 3-in. pipe. Volumetric concentrations of 10, 15, 20, 25 and 30 per cent were studied.

The light chip tests included 71 runs in the long test loop with 4-in. diameter pipe and 60 runs in the short test loop with 3-in. diameter pipe. The velocity range was 2.5 to 10 fps in the 4-in. pipe and 4 to 17 fps in the 3-in. pipe. Volumetric concentrations of 10, 15, 20 and 25 per cent were used. The temperature range for all the tests was 60 to 75°F.

Clear-water tests were run in each pipe size to establish the clear-water hydraulic gradient.

CHAPTER V

PRESENTATION OF RESULTS

Previously, researchers (11, 12, 32), have presented their data as a series of curves with three parameters: i_m as ordinate versus abscissa $V_m/\sqrt{gD}$ for varying C_v. The resulting graph applied only to the solids used in the study. Additional studies with solids of different sizes required separate graphs. A set of studies for various solid sizes was correlated by multiplying the parameter V_m^2/gD, by the reciprocal of a type of particle Froude number gd_n/V_s^2, where d_n is the nominal particle diameter and V_s is the particle settling velocity. The product of the two parameters gave a form of the term Ψ. The mixture hydraulic gradient was modified to $(i_m-i)/C_v.i$, or φ, to complete the correlation. The parameter (s-1) was incorporated as shown in Eqs. (2.2) and (2.3) for solids other than those with a specific gravity of 2.65. The parameters k/D, Re_m and d/D were not included.

In this study, the parameters i_m and $V_m/\sqrt{gD}$ are replaced by f_m so that a diagram of the Stanton type can be used, plotting f_m versus Re_m for various values of C_v with the other three parameters either held constant or

varying over a known range. The parameter s, is used rather than (s-1), there being no apparent advantage in using the latter. The parameter k/D was not required in this study because smooth pipes were used.

The headloss measurements obtained for mixtures of water and plastic chips are presented in a form similar to Stanton diagrams but modified by the properties of the mixture. The Nikuradse smooth-pipe resistance equation (21)

$$1/\sqrt{f} = 2 \log (Re\sqrt{f}) - 0.8 \quad \ldots\ldots\ldots\ldots\ldots \quad (5.1)$$

is also shown on each Stanton diagram as the reference for flows with zero concentration. The range of Reynolds numbers covered in the study was 55,000 to 400,000. The clear-water headloss data are listed in Tables E-II, IV, V, and VI of Appendix E.

Plastic Chip Tests

Figs. 5-1 and 5-2 are Stanton-type diagrams for the combined batch of red and blue chips (s=1.045) for varying concentrations and fixed values of the parameters d/D and s. The headloss data used in these graphs are listed in Tables E-I, II and IV of Appendix E. Fig. 5-1 also includes

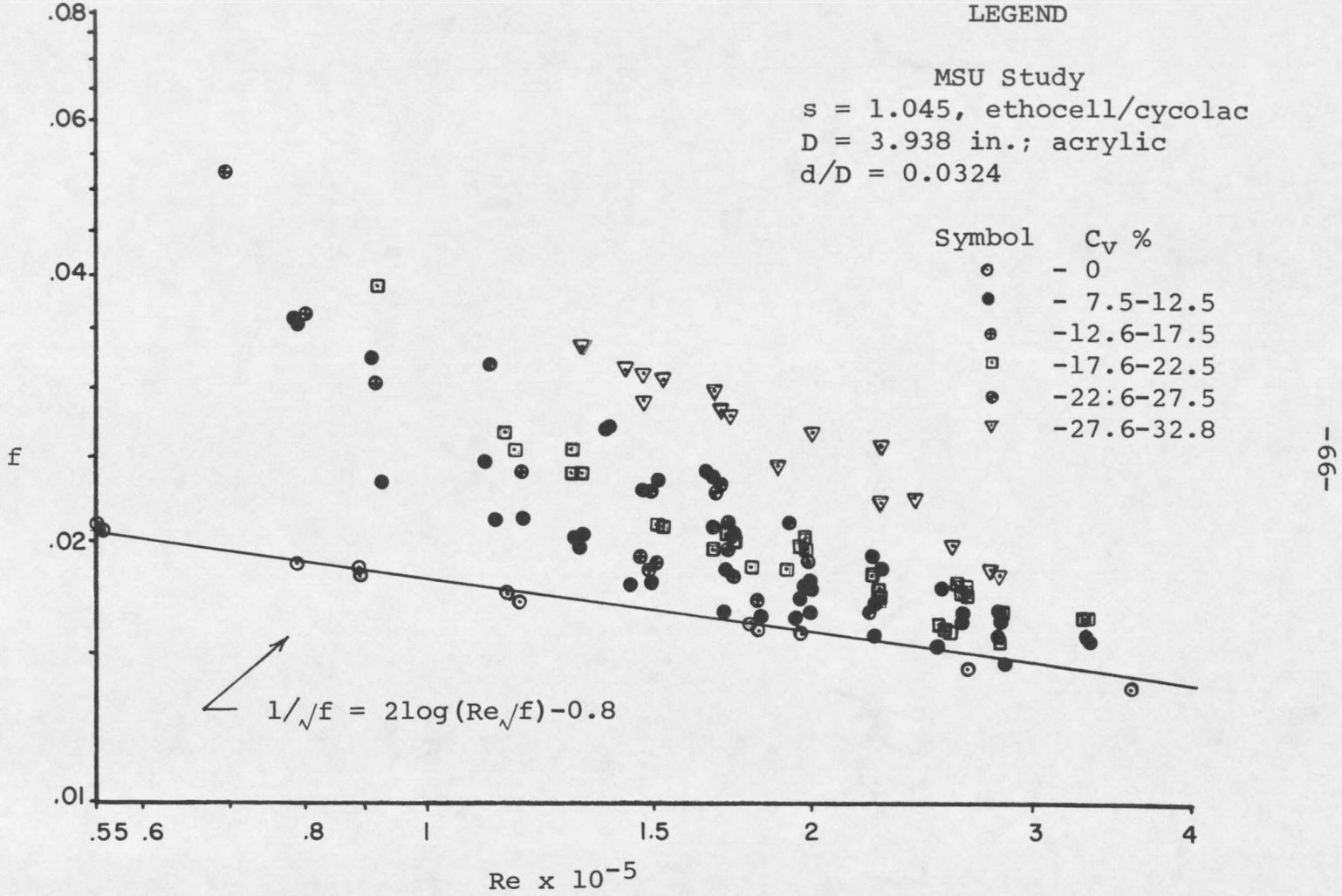

Fig. 5-1. Stanton Diagram for Plastic Chips.

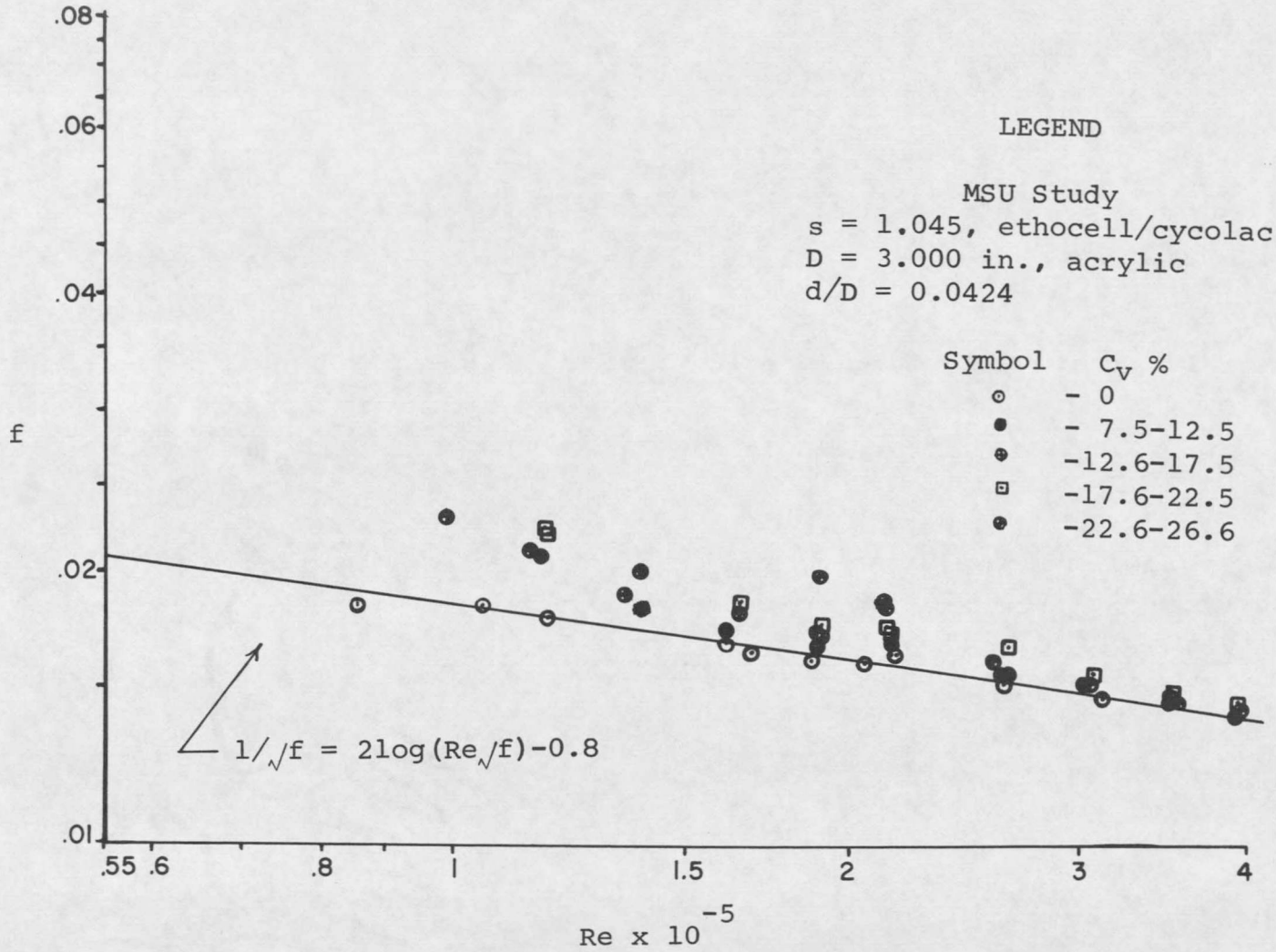

Fig. 5-2. Stanton Diagram for Plastic Chips.

headlosses measured in the series of valve tests by Johnson (17) using 4-in. diameter pipe in the 200-ft. loop when no valve was in the test section. As mentioned earlier, both the valve tests and headloss tests were conducted using the same basic apparatus during a six-month period. Data taken from Johnson's tests are listed separately in Table E-III of Appendix E.

Figs. 5-3a, b are photographs of a low and high concentration of heavy chips at a low velocity.

Stanton-type diagrams for the yellow chips (s=0.92) are given in Figs. 5-4 and 5-5 with the pertinent data listed in Appendix E as Tables E-V and VI. Figs. 5-6a, b are photographs of a low and high concentration of light chips at a low velocity.

Flow Regime Delineations

A visual distinction between heterogeneous suspension flow and heterogeneous saltation flow was difficult to make because of the high velocities involved, particularly in the 3-in. diameter pipe. The transition from heterogeneous saltation flow to a sliding-bed regime was somewhat easier

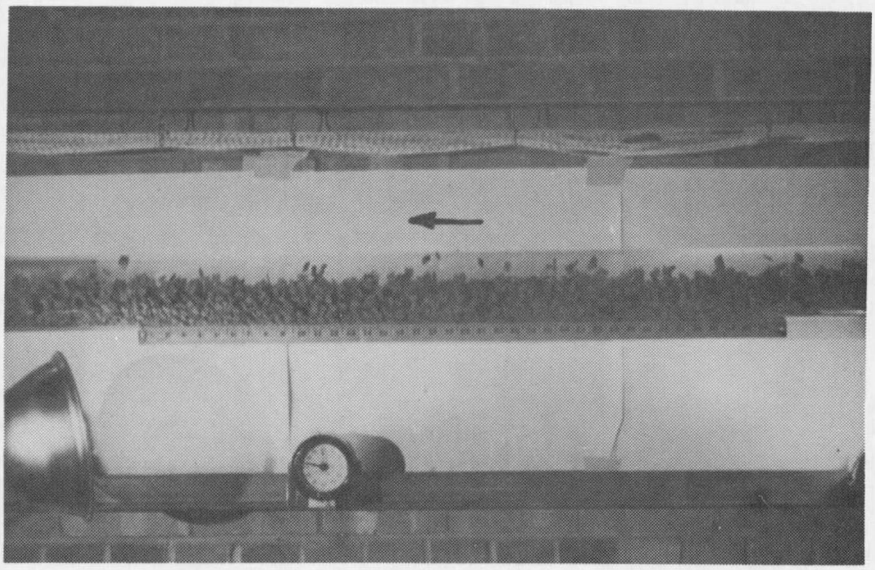

a. V_m = 3.93 fps; C_v = 10.1 per cent

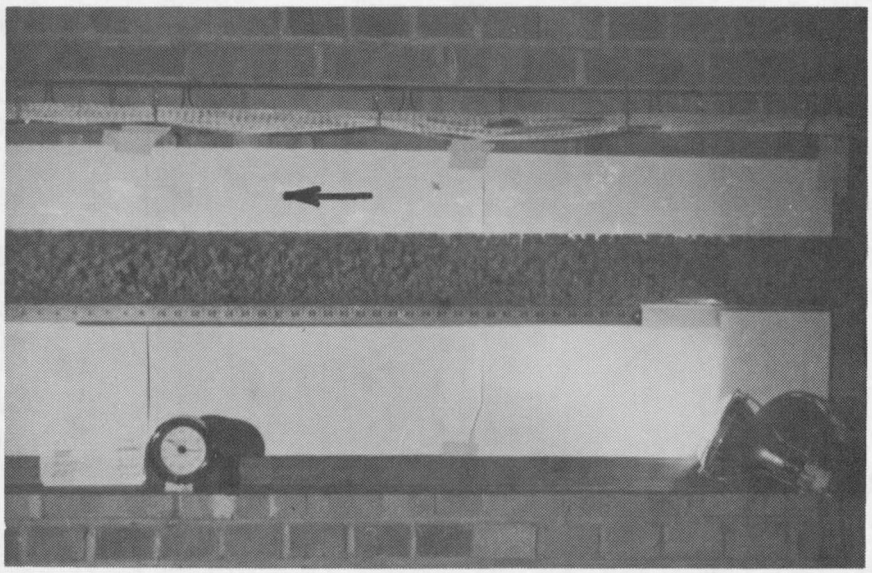

b. V_m = 5.35 fps; C_v = 26.6 per cent

Fig. 5-3. Flows with Heavy Chips

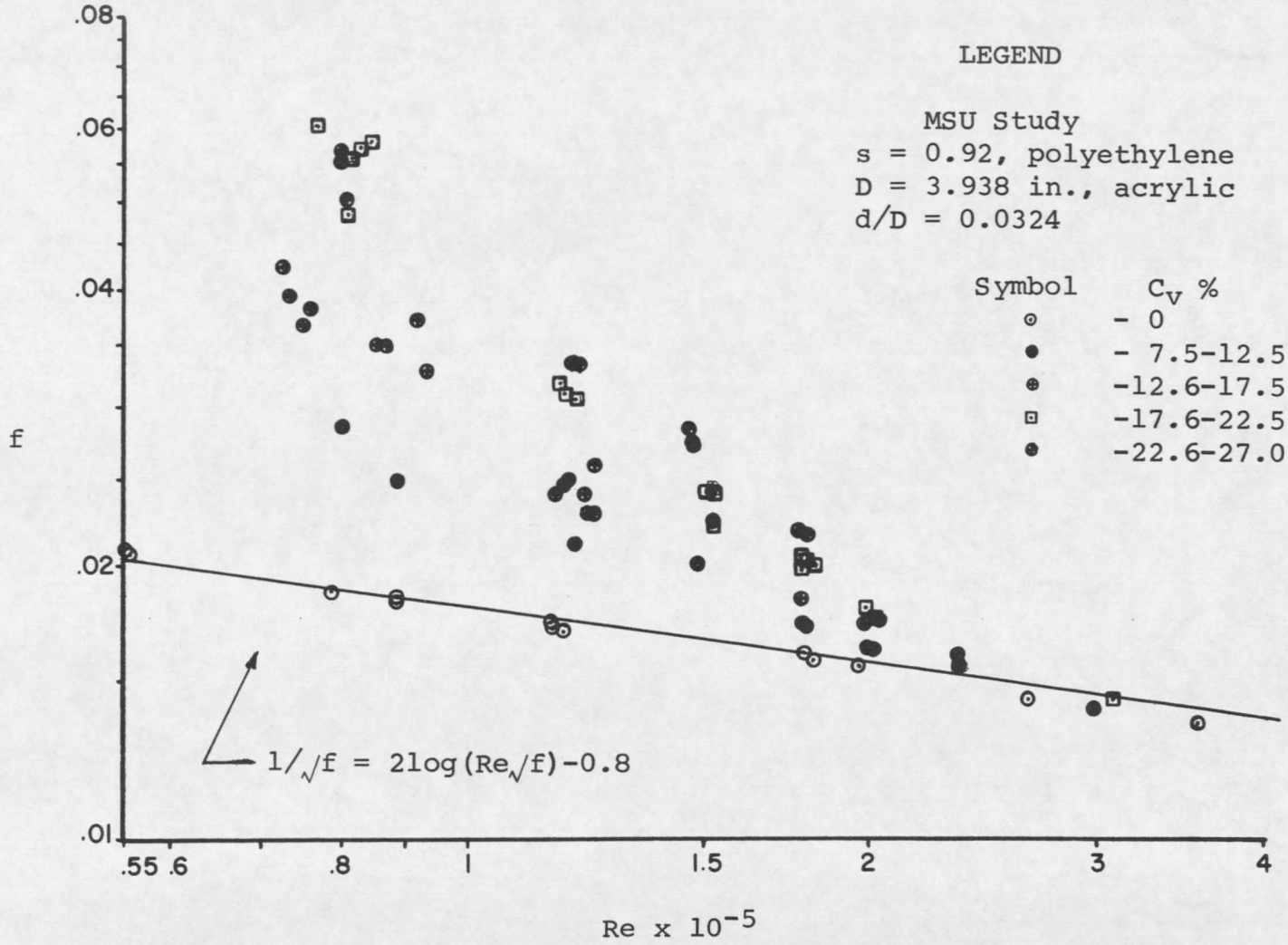

Fig. 5-4. Stanton Diagram for Plastic Chips.

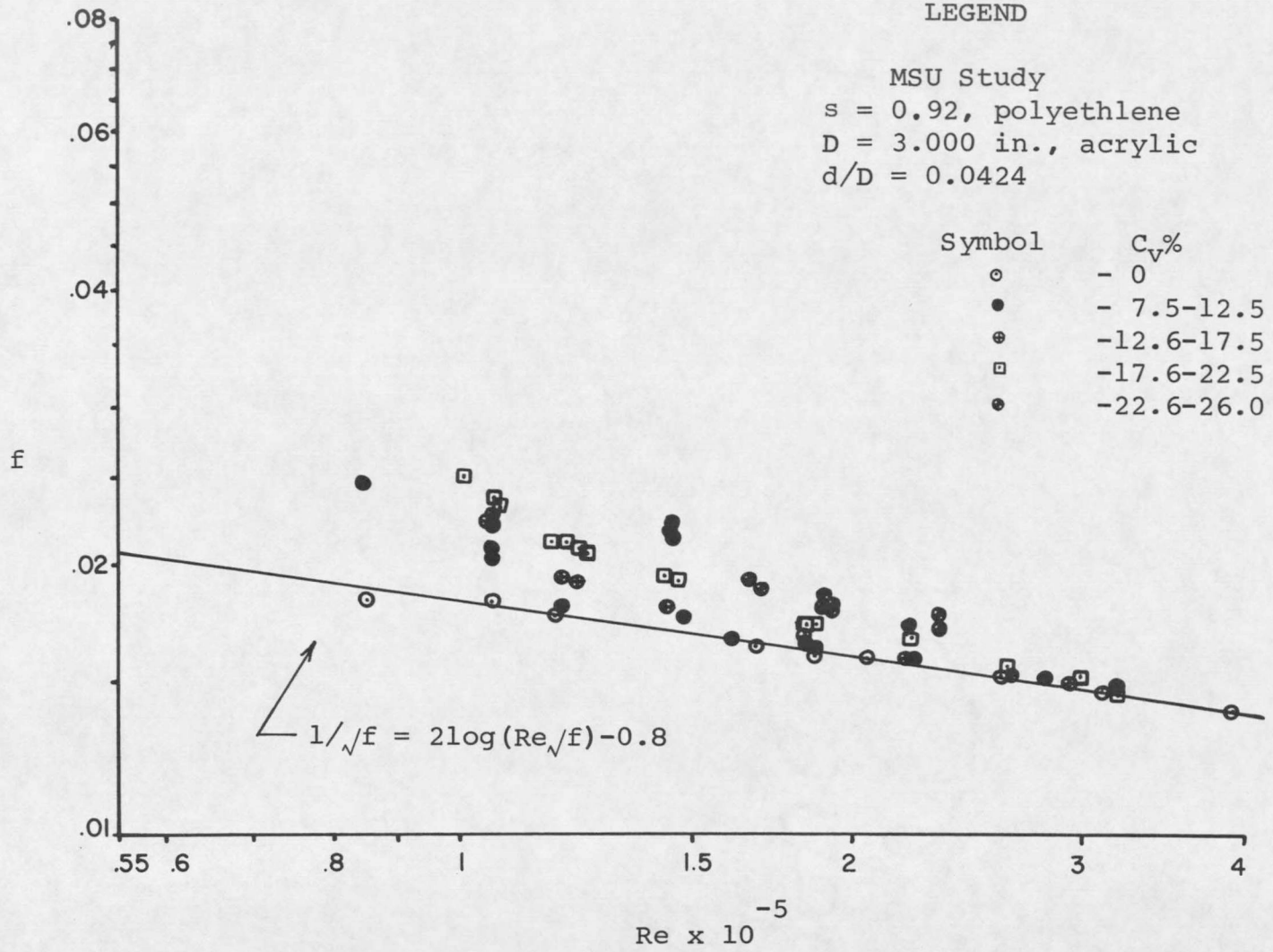

Fig. 5-5. Stanton Diagram for Plastic Chips

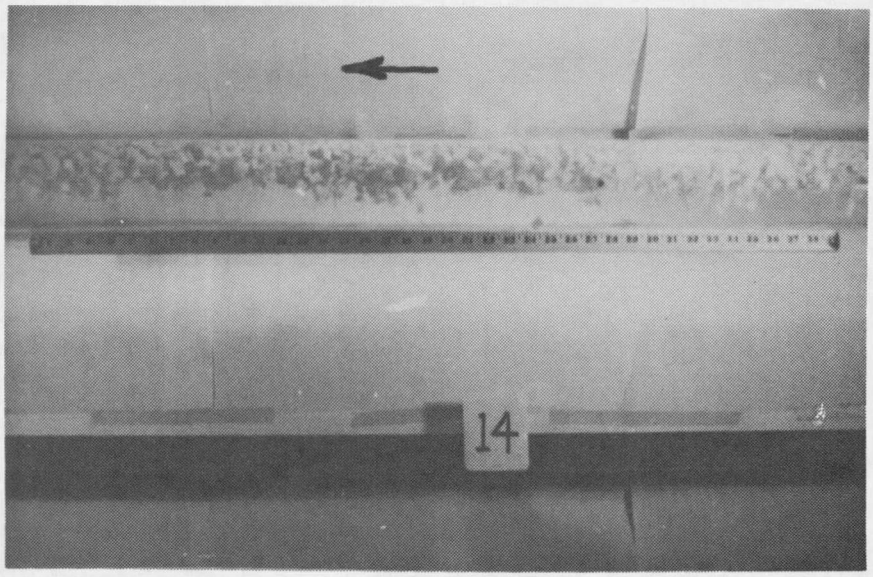

a. V_m = 4.03 fps; C_v = 12.4 per cent

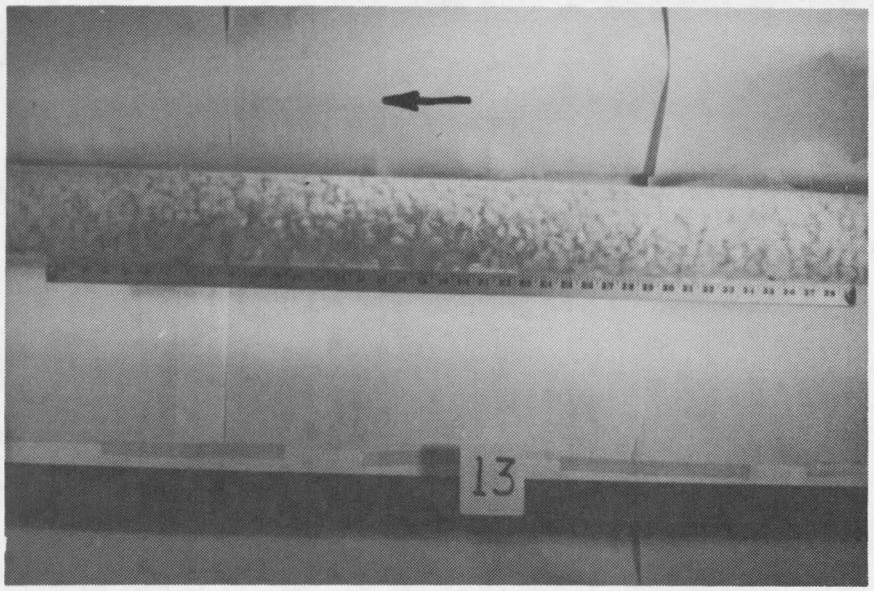

b. V_m = 4.95 fps; C_v = 24.4 per cent

Fig. 5-6. Flows with Light Chips

to discern but was nevertheless complicated by varying degrees of agitation in the sliding bed. Here, the sliding-bed regime was one in which the chips packed themselves in either the upper or lower part of the pipe (depending on s) and moved almost as a solid mass sliding over the pipe wall. Only that part of the bed near the center-line of the pipe underwent noticeable shearing. Table III gives the approximate Reynolds numbers and concentrations at which a pronounced sliding bed developed.

TABLE III. - OCCURRENCE OF SLIDING-BED REGIME

Chip type	Pipe diameter D, inches	Volumetric concentration C_v, per cent	Approximate Reynolds numbers, Re_m
(1)	(2)	(3)	(4)
heavy (s= 1.045)	3.938	10	130,000
		25	200,000
	3,000	10	100,000
		20	120,000
light (s = 0.092)	3.938[a]	-	-
	3.000	10	85,000
		15	100,000
		25	150,000

[a] no observations made

Empirical Correlations of Results

An attempt was made to correlate the five parameters; f_m, Re_m, C_v, d/D and s, with a single mathematical equation. It appeared that the data could be correlated by several forms of equations. A typical data set, in this case a 20 per cent concentration of heavy chips in the 4-in. diameter pipe, was plotted several ways as shown in Fig. 5-7. One method, shown by Fig. 5-7a, taken from Fig. 5-1, indicated that f_m might be approximated by a polynomial in f_m and Re_m. To keep the equation simple, a second-order polynomial of the form:

$$\log f_m = c_1 + c_2 \log Re_m + c_3 (\log Re_m)^2 \quad \ldots\ldots (5.2)$$

was selected where c_1, c_2 and c_3 were functions of C_v, d/D, and s.

Next, the friction factor ratio f_m/f, was chosen as the ordinate versus mixture Reynolds numbers so that for large values of Re_m, the ratio approached unity, an observable fact in most two-phase flow studies. The following equations were selected:

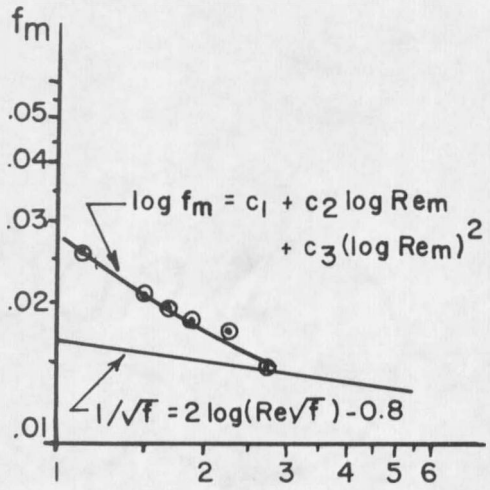

$Re_m \times 10^{-5}$

a) Logarithmic

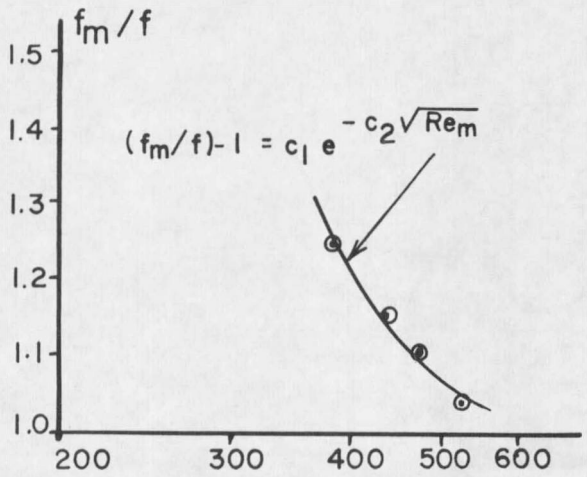

$\sqrt{Re_m}$

b) Exponential

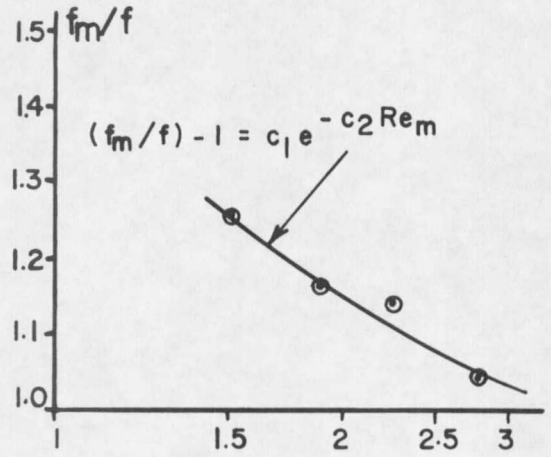

$Re_m \times 10^{-5}$

c) Exponential

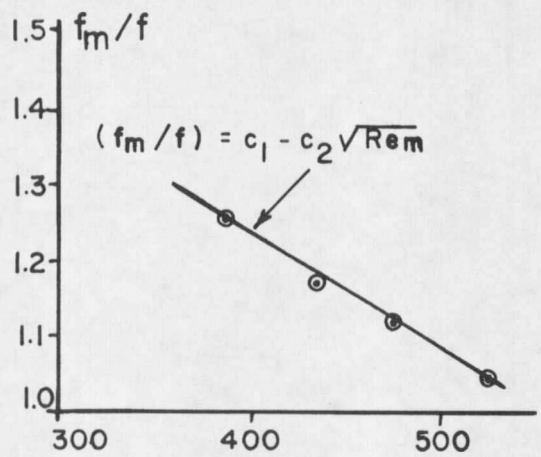

$\sqrt{Re_m}$

d) Rectangular

Fig. 5-7. Plastic Chip Data Plotted in Various Ways for C_v = 20%, s = 1.045, d/D = 0.0324

$$(f_m/f) - 1 = c_1 e^{-c_2\sqrt{Re_m}} \quad \ldots\ldots\ldots\ldots\ldots\ldots \quad (5.3)$$

$$(f_m/f) - 1 = c_1 e^{-c_2 Re_m} \quad \ldots\ldots\ldots\ldots\ldots\ldots \quad (5.4)$$

$$f_m/f = c_1 - c_2 \sqrt{Re_m} \quad \ldots\ldots\ldots\ldots\ldots\ldots \quad (5.5)$$

where c_1 and c_2 were functions of C_v, d/D and s. The equations are shown in Figs. 5-7b,c,d, respectively. The clear-water friction factor for smooth pipes was computed directly from the Nikuradse equation (21):

$$f = 0.0032 + 0.221 / Re^{0.237} \quad \ldots\ldots\ldots\ldots\ldots\ldots \quad (5.6)$$

This equation yielded values of f within 2 per cent of those given by Eq. (5.1) for Reynolds numbers from 100,000 to 600,000. Eq. (5.5) does not permit any asymptotic behavior, that is, the friction factor ratio is unity for some finite value of Re_m and becomes less than unity for larger values of Re_m. This form was chosen because most of the data did not extend into a range of high Reynolds numbers where f_m/f approached unity.

The next step required fitting the data to the selected equations. Powe and Smith (22) have presented a method by

which a correlation equation can be obtained to reproduce data involving several independent variables. The method consists of first assuming a functional relationship between the dependent variable and one of the independent variables. The constants in this equation are then evaluated and plotted against a second independent variable to obtain functional relationships which are substituted into the first equation. The process is repeated until an equation is developed which correlates the dependent variable with all of the independent variables. The correlation can be computed quickly, since generally, only one application of a standard least square analysis is required for each of the independent variables.

This curve fitting technique was applied to the multivariable functional relationship

$$f_m = f_m\ (Re_m,\ C_v,\ d/D,\ s) \quad \ldots\ldots\ldots\ldots\ldots \quad (5.7)$$

defining a system of two-phase flow in smooth pipes. The method described below is for the plastic chips.

To start the process, C_v was fixed at nominal values of 10, 15, 20, 25, 30 per cent with limits of ± 2.5. For

example, concentrations between 22.6 and 27.5 per cent were considered as 25 per cent. The first functional relationship chosen was of the form

$$f_m = f_m\ (Re_m) \qquad \ldots\ldots\ldots\ldots\ldots\ldots\ldots\ (5.8)$$

for constant values of C_v, d/D and s. The plastic chip data were fitted to each of Eqs. (5.2, 3, 4, and 5) by a least-squares method using a computer program which also contained an error analysis subroutine. The program is on file with the Civil Engineering Department of Montana State University. The error analysis, in essence a measure of goodness of fit, compared the deviation or absolute difference between the experimentally-obtained friction factor and the friction factor predicted by the correlation equation. The average per cent deviation Da, and the maximum per cent deviation Dm, of the mixture friction factor were measured. The average per cent deviation was the average of the absolute values of the differences between the experimental values of f_m and those predicted by the correlation equation. The maximum per cent deviation was the maximum value of the absolute difference between the predicted and experimental

values of f_m. The most meaningful output of the error analysis were the percentages of data points E, falling within 5, 10, 15, 20 and 25 per cent of the values predicted by the correlation equation.

Table IV lists the output of the computer program in the form of the coefficients for Eqs. (5.2, 3, 4, and 5), the average and maximum per cent deviation of the experimental mixture friction factors from those predicted by each of the correlation equations, and the percentage of data points falling within 5, 15 and 25 per cent of the values of f_m predicted by the correlation equations. Only the equations for a concentration of 20 per cent are listed. Similar trends were obtained for the other values of C_v; 10, 15, 25 and 30 per cent. These data are on file with the Civil Engineering Department of Montana State University.

The second-order polynomial, Eq. (5.2), which was found to fit the data best at this stage, was extended to include the other parameters: C_v, d/D and s, as follows: each of the coefficients c_1, c_2 and c_3 were plotted against each nominal value of concentration for each of the four chip tests

TABLE IV. - CORRELATIONS FOR PLASTIC CHIP FRICTION FACTORS

Study	s = 1.045 D = 3.938in.	s = 1.045 D = 3.000in.	s = 0.92 D = 3.938in.	s = 0.92 D = 3.000in.
Runs	126	40	71	60
(1)	(2)	(3)	(4)	(5)
(a) Eq. (5.2): $\log f_m = c_1 + c_2 \log Re_m + c_3 (\log Re_m)^2$ for C_v = 20%				
c_1	34.3232	8.07541	34.0811	21.5994
c_2	-13.1402	-3.35251	-12.7131	-8.48389
c_3	1.19541	0.282364	1.12354	0.768407
Da%[a]	3.4	1.1	3.5	1.1
Dm%[b]	8.6	2.8	16.9	2.9
E<5%	72.2	100.0	81.8	100.0
E<15%	100.0	100.0	95.5	100.0
E<25%	100.0	100.0	100.0	100.0
(b) Eq. (5.3): $(f_m/f)-1 = c_1 e^{-c_2/Re_m}$ for C_v = 20%				
c_1	1.72081	0.614208	4.98266	1.922174
c_2	-0.007347	-0.005936	-0.014923	-0.009532
Da%	29.1	6.3	15.1	8.8
Dm%	43.7	13.4	52.3	27.0
E<5%	8.3	41.7	14.3	37.5
E<15%	47.2	100.0	61.9	87.5
E<25%	66.7	100.0	85.7	93.8

Continued

TABLE IV. - FRICTION FACTOR CORRELATIONS - CONTINUED

Study	s = 1.045 D = 3.938in.	s = 1.045 D = 3.000in.	s = 0.92 D = 3.938in.	s = 0.92 D = 3.000in.
Runs	126	40	71	60
(1)	(2)	(3)	(4)	(5)
(c) Eq. (5.4): $(f_m/f)-1 = c_1 e^{-2Re_m}$ for C_v = 20%				
c_1	0.044171	-0.790528	2.385213	-0.064874
c_2	-0.000008	-0.000006	-0.000021	-0.000011
Da%	34.0	7.6	18.7	11.0
Dm%	55.5	19.6	73.5	35.3
E<5%	5.6	41.7	23.8	31.3
E<15%	41.7	91.7	66.7	75.0
E<25%	72.2	100.0	81.0	93.4
(d) Eq. (5.5): $f_m/f = c_1-c_2\sqrt{Re_m}$ for C_v = 20%				
c_1	2.241830	1.506637	5.606219	1.787749
c_2	-0.002193	-0.000762	-0.010009	-0.001500
Da%	6.6	2.8	15.9	4.1
Dm%	26.9	6.1	93.2	7.7
E<5%	44.4	81.3	13.6	81.3
E<15%	94.4	100.0	63.6	100.0
E<25%	97.2	100.0	95.5	100.0

a Da = Σ 100% $(f_m$calc.$-f_m$exp.$)/f_m$exp. /no. of obs.

b Dm = max. 100% $(f_m$calc.$-f_m$exp.$)/f_m$exp.

c E<5% = per cent of data within 5 per cent of equation

that is, against fixed values of d/D and s. See Figs. 5-8a, b, c. All three coefficients increased with concentration and could be represented reasonably by linear functions passing through the origin, i.e.,

$$c_1 = c_4 C_v \quad \ldots\ldots\ldots\ldots\ldots\ldots\ldots \quad (5.9)$$

$$c_3 = c_6 C_v \quad \ldots\ldots\ldots\ldots\ldots\ldots\ldots \quad (5.10)$$

where C_v was expressed as a percentage rather than a decimal fraction. However, the coefficient c_2 was forced to be constant,

$$c_2 = c_5 \quad \ldots\ldots\ldots\ldots\ldots\ldots\ldots \quad (5.11)$$

thereby omitting C_v from the second term in Eq. (5.12) so that in the absence of a solid phase (C_v equal to zero), there existed a finite value of f for the clear liquid phase. Substituting Eqs. (5.9, 10, 11) into Eq. (5.2) gave

$$\log f_m = c_4 C_v + c_5 \log Re_m + c_6 C_v (\log Re_m)^2 \quad \ldots (5.12)$$

which provided a possibility for producing a clear-water friction factor when the solids concentration was zero. The new coefficients, c_4, c_5 and c_6 were then determined by the method of least squares. The program output listing the

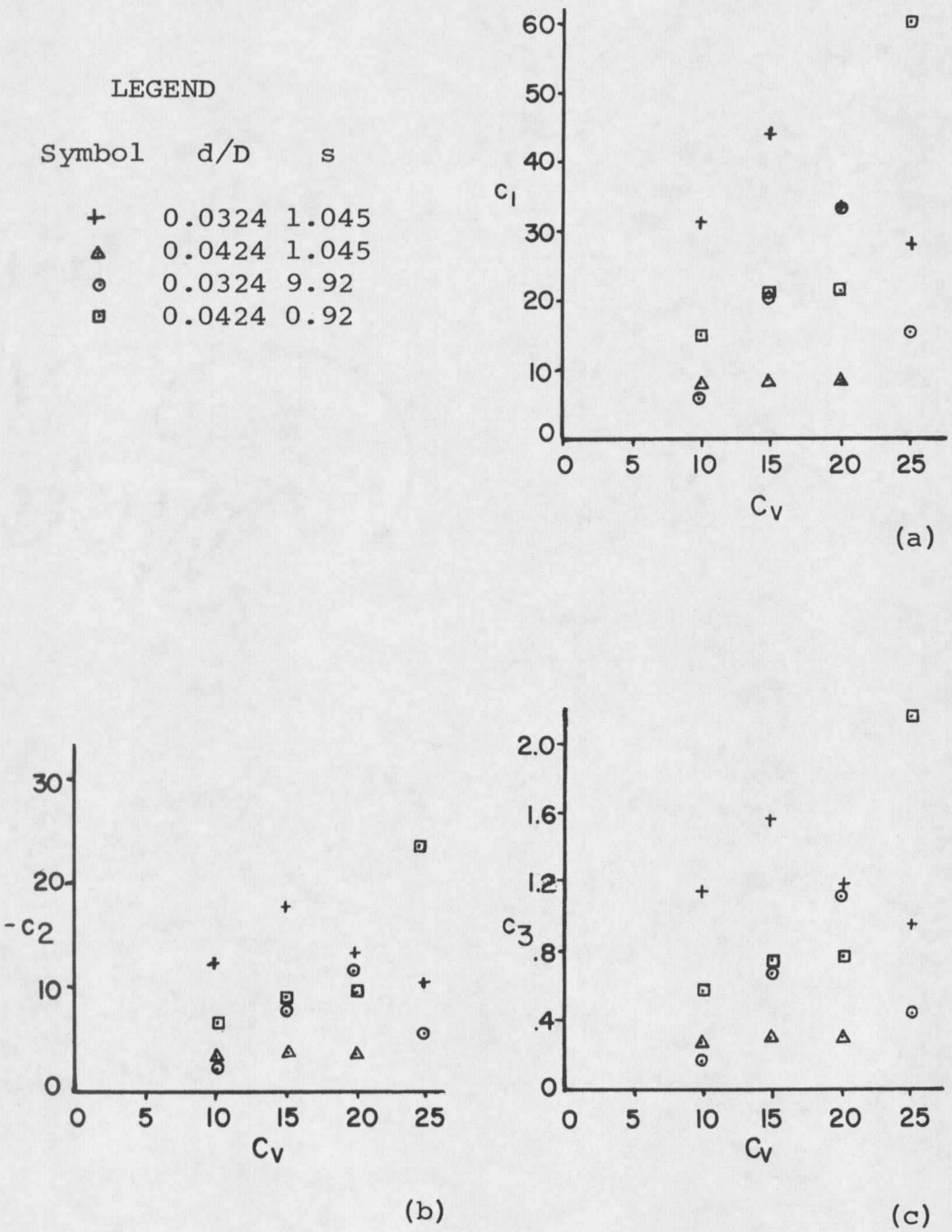

Fig. 5-8. c_1, c_2, c_3 versus C_v for Plastic Chip Tests

coefficients and goodness of fit is tabulated in Table V.

The parameter d/D was then related to the coefficients c_4 and c_6. The coefficient c_5 was changed to c_9 to preserve Eq. (5.12)'s ability to produce a value of f for single-phase flow. Because only two values of d/D were tested for each value of s, a straight-line relationship only between the coefficients and the parameter d/D would normally be justifiable. However, a straight-line relationship in rectangular coordinates involves the addition or subtraction of two separate terms whereas a power-law relationship involves only one term. Therefore, to keep the number of terms to a minimum in the correlation equation, logarithmic forms given by

$$c_4 = c_7 \ (d/D)^{c_8} \qquad \ldots\ldots\ldots\ldots\ldots\ldots\ldots\ldots \quad (5.13)$$

$$c_6 = c_{10} \ (d/D)^{c_{11}} \qquad \ldots\ldots\ldots\ldots\ldots\ldots\ldots\ldots \quad (5.14)$$

were substituted into Eq. (5.12 to give

$$\log f_m = c_7 \ (d/D)^{c_8} \ C_v + c_9 \log Re_m + c_{10} \ (d/D)^{c_{11}} \ C_v \ (\log Re_m)^2 \qquad \ldots\ldots\ldots\ldots \quad (5.15)$$

TABLE V. - CORRELATIONS FOR PLASTIC CHIP FRICTION FACTORS

Study	s = 1.045 D = 3.938in.	s = 1.045 D = 3.000in.	s = 0.92 D = 3.938in.	s = 0.92 D=3.000in.
Runs	126	40	71	60
	(1)	(2)	(3)	(4)	(5)

Eq. (5.12): $\log f_m = c_4 C_v + c_5 \log Re_m + c_6 C_v (\log Re_m)^2$

c_4	0.042040	-0.000090	0.104711	0.011273
c_5	-0.345107	-0.340611	-0.346494	-0.343861
c_6	-0.001280	0.000097	-0.003560	-0.000290
Da%	7.8	2.3	6.7	3.4
Dm%	35.1	6.5	23.3	11.3
E<5%	34.9	95.0	54.9	80.0
E<15%	69.0	100.0	74.6	96.7
E<25%	89.7	100.0	88.7	100.0

Evaluation of c_8 and c_{11} of Eqs. (5.13 and 5.14) from Table V indicated that starting values of

$$c_8 = 0.020 \quad \ldots\ldots\ldots\ldots\ldots\ldots\ldots\ldots \quad (5.16)$$

$$c_{11} = 0.015 \quad \ldots\ldots\ldots\ldots\ldots\ldots\ldots\ldots \quad (5.17)$$

could be inserted into Eq. (5.15) to initiate the least-square process. With the coefficient c_{11} fixed at 0.015 Eq. (5.15) was tested with the above initial value of c_8

incremented by ± 10 per cent until a minimum value of the sum of the squares of the deviations (f_m calculated- f_m experimental) was obtained. The program tested fifty values of c_8 before printing out the value which minimized the deviations. Then c_8 was fixed at this best value while the program repeated the procedure for c_{11}. When the values of c_8 and c_{11} were finalized, the values of the coefficients c_7, c_9, c_{10} and the goodness of the fit of the data to the correlation equation were printed. Table VI lists the computer output for each value of s.

The final step involved replacing the coefficients c_7 and c_{10} by a relationship containing the parameter s. The best values of the coefficients c_8 and c_{11}, obtained by the previous application of the least-square method, were rounded off to four places and coefficient c_9 was changed to c_{14}. Again the logarithmic form:

$$c_7 = c_{12} (s)^{c_{13}} \quad \ldots\ldots\ldots\ldots\ldots\ldots\ldots\ldots \quad (5.18)$$

$$c_{10} = c_{15}(s)^{c_{16}} \quad \ldots\ldots\ldots\ldots\ldots\ldots\ldots\ldots \quad (5.19)$$

was employed for the coefficients c_7 and c_{10} to simplify the correlation. Substitution into Eq. (5.15) gave

TABLE VI. - CORRELATIONS FOR PLASTIC CHIP FRICTION FACTORS

Study	s = 1.045 D = 3.938, 3.000in.	s = 0.92 D = 3.938 3.000in.
Runs	166	131
(1)	(2)	(3)
Eq. (5.15): $\log f_m = c_7(d/D)^{c_8} C_v + c_9 \log Re_m + c_{10}(d/D)^{c_{11}} C_v (\log Re_m)^2$		
c_7	0.034348	0.081291
c_8	0.002128	0.002128
c_9	-0.345881	-0.343623
c_{10}	-0.001001	0.002763
c_{11}	0.001184	0.001184
Da%	7.8	11.9
Dm%	38.8	41.4
E<5%	40.4	31.3
E<15%	91.0	71.0
E<25%	97.6	85.5

$$\log f_m = c_{12}(s)^{c_{13}}(d/D)^{c_8} C_v + c_{14} \log Re_m + c_{15}(s)^{c_{16}}(d/D)^{c_{11}} C_v (\log Re_m)^2 \quad \ldots\ldots \quad (5.20)$$

or

$$\log f_m = c_{12}(s)^{c_{13}}(d/D)^{0.0021} C_v + c_{14} \log Re_m + c_{15}(s)^{c_{16}}(d/D)^{0.0012} C_v (\log Re_m)^2 \quad \ldots \quad (5.21)$$

Preliminary calculations using Eqs. (5.18) and (5.19) gave

the following values for the coefficients c_{13} and c_{16}:

$$c_{13} = -6.80 \quad \text{.....(5.22)}$$

$$c_{16} = -8.03 \quad \text{.....(5.23)}$$

These were rounded off to fixed values of -7.0 and -8.0, respectively and inserted into Eq. (5.21) to give

$$\log f_m = c_{12}(s)^{-7} (d/D)^{0.0021} C_v + c_{14} \log Re_m + c_{15}(s)^{-8} (d/D)^{0.0012} C_v (\log Re_m)^2 \quad \text{.. (5.24)}$$

Varying values of c_{13} and c_{16} were not tested because their computed values had almost the same magnitude and s did not vary over a wide range. All the plastic chip data were then correlated by applying the method of least squares to Eq. (5.24). Table VII gives the computer output in the form of coefficients and goodness of fit. Also included are the deviations (expressed in per cent) of the friction factor values for zero concentration, as given by Eq. (5.24), and those given by the smooth pipe resistance equation, Eq. (5.1) for several values of Reynolds numbers.

TABLE VII. - CORRELATION FOR PLASTIC CHIP FRICTION FACTORS

Study: s = 0.92 to 1.045; D = 3.000 to 3.938in.

Runs: 297

Eq. (5.24): $\log f_m = c_{12} (s)^{-7} (d/D)^{0.0021} C_v +$

$c_{14} \log Re_m + c_{15} (s)^{-8} (d/D)^{0.0012} C_v (\log Re_m)^2$

c_{12} = 0.033371 Da% = 11.6 E<5% = 24.9
c_{14} = -0.340281 Dm% = 49.7 E<15% = 73.1
c_{15} = -0.001004 E<25% = 93.6

Re	Percentage Discrepancy in f^a
100,000	10.6
200,000	5.1
400,000	-9.4
600,000	-15.1

a ((f_m calculated for C_v = 0%) - f) x 100/f

Previous Woodchip Tests

The available woodchip data were reworked into Stanton-type diagrams as Figs. 5- 9, 10, 11 and 12. The data are listed in Tables G-I, II, III, and IV of Appendix G.

In Table I of Chapter II a comparison of three of the woodchip tests was made using Durand's equation in the form

$$\phi = k\ (\psi_1)^m \qquad \ldots\ldots\ldots\ldots\ldots\ldots\ldots\ldots \quad (2.8)$$

Soucy's data (26) in a 6-in. diameter pipe and data taken from the four plastic chip tests were used to check Durand's equation also, this time in the form:

$$\phi = a\psi^b \qquad \ldots\ldots\ldots\ldots\ldots\ldots\ldots\ldots \quad (5.25)$$

where $\phi = (i_m - i)/C_v.i$

$\psi = k_i\ V_m^2/gD$

k_i = constant depending on chip properties, size and settling velocity. These were absorbed in the coefficient a and exponent b.

The plastic chip tests provided an excellent means of checking Durand's equation because the effects of the controlled parameters d/D and s, could be readily determined.

Lines of best fit and their coefficient of correlation R, were obtained by the method of least squares. Wiley (31) has noted that the mathematical equation which best fits the logarithms of data will not necessarily give the best approximation to the data itself. Therefore, the

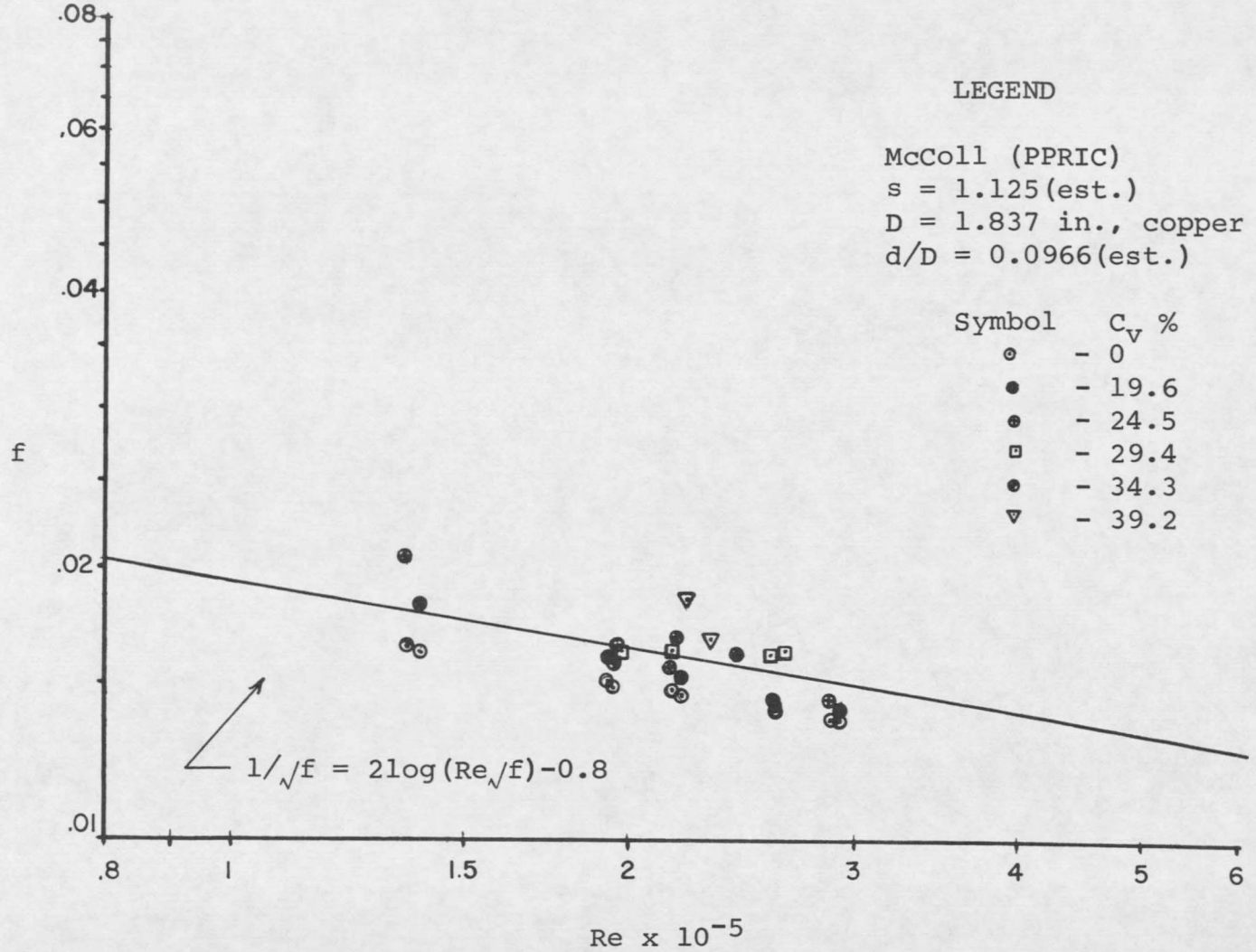

Fig. 5-9. Stanton Diagram for Woodchips.

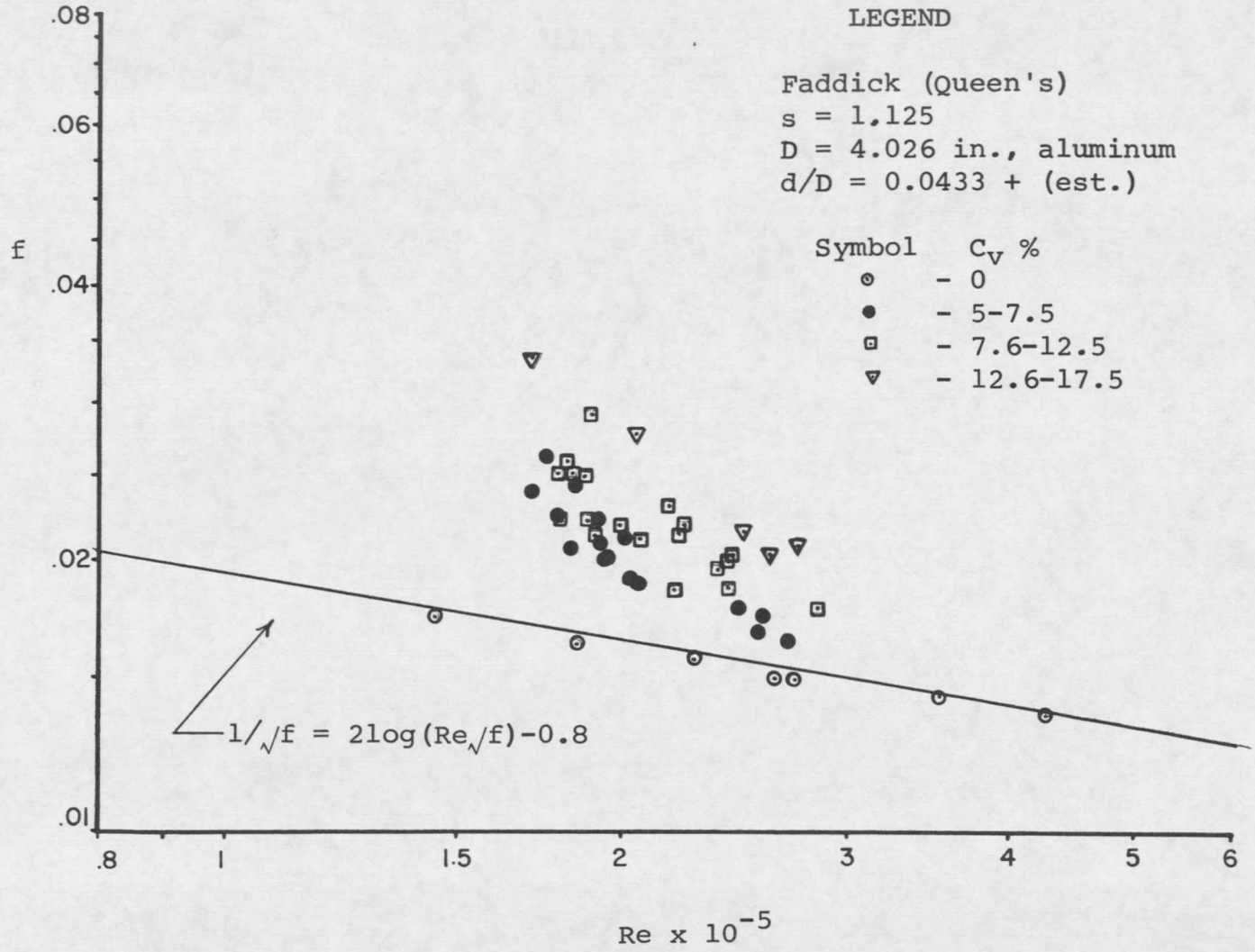

Fig. 5-10. Stanton Diagram for Woodchips.

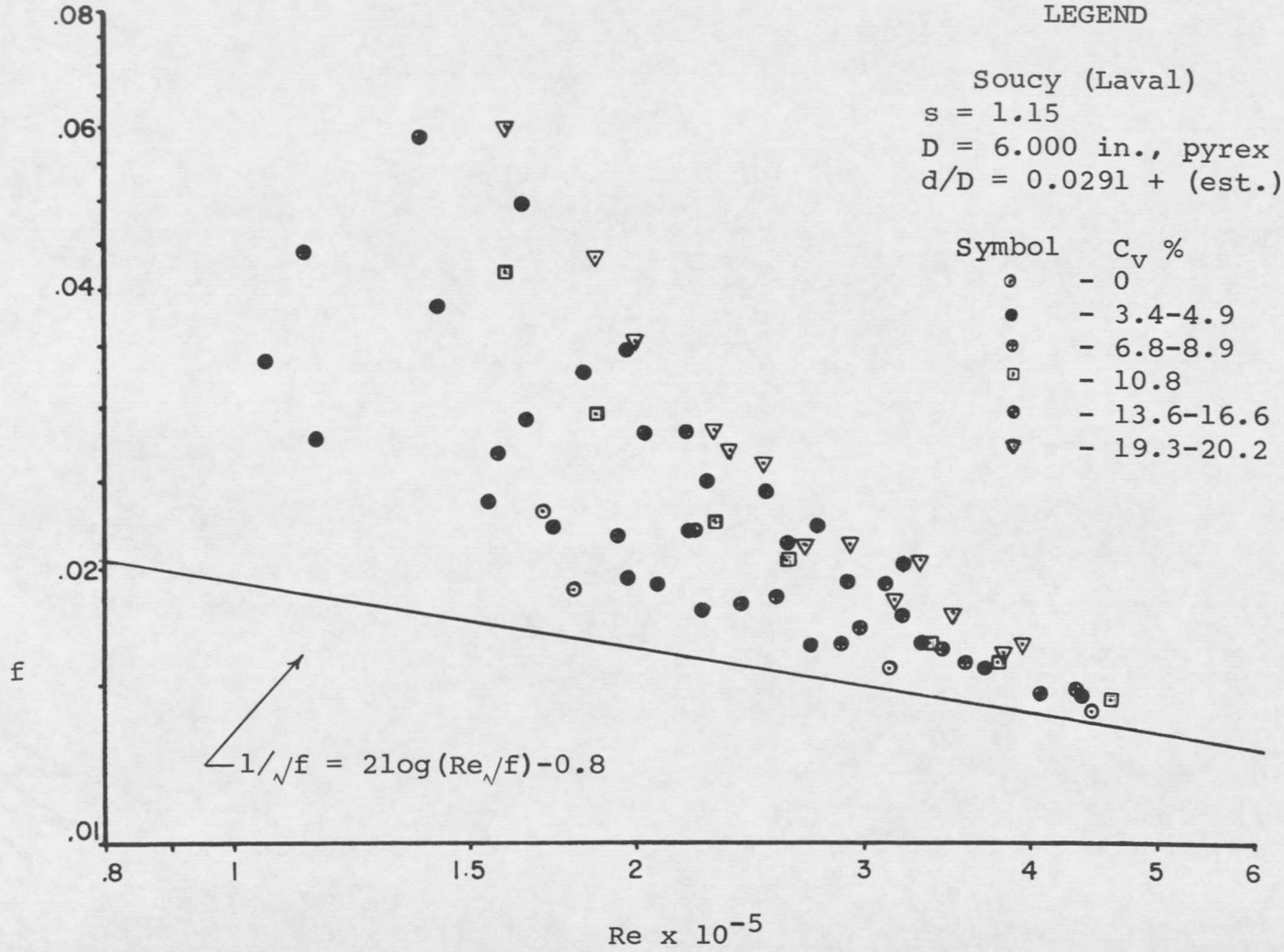

Fig. 5-11. Stanton Diagram for Woodchips.

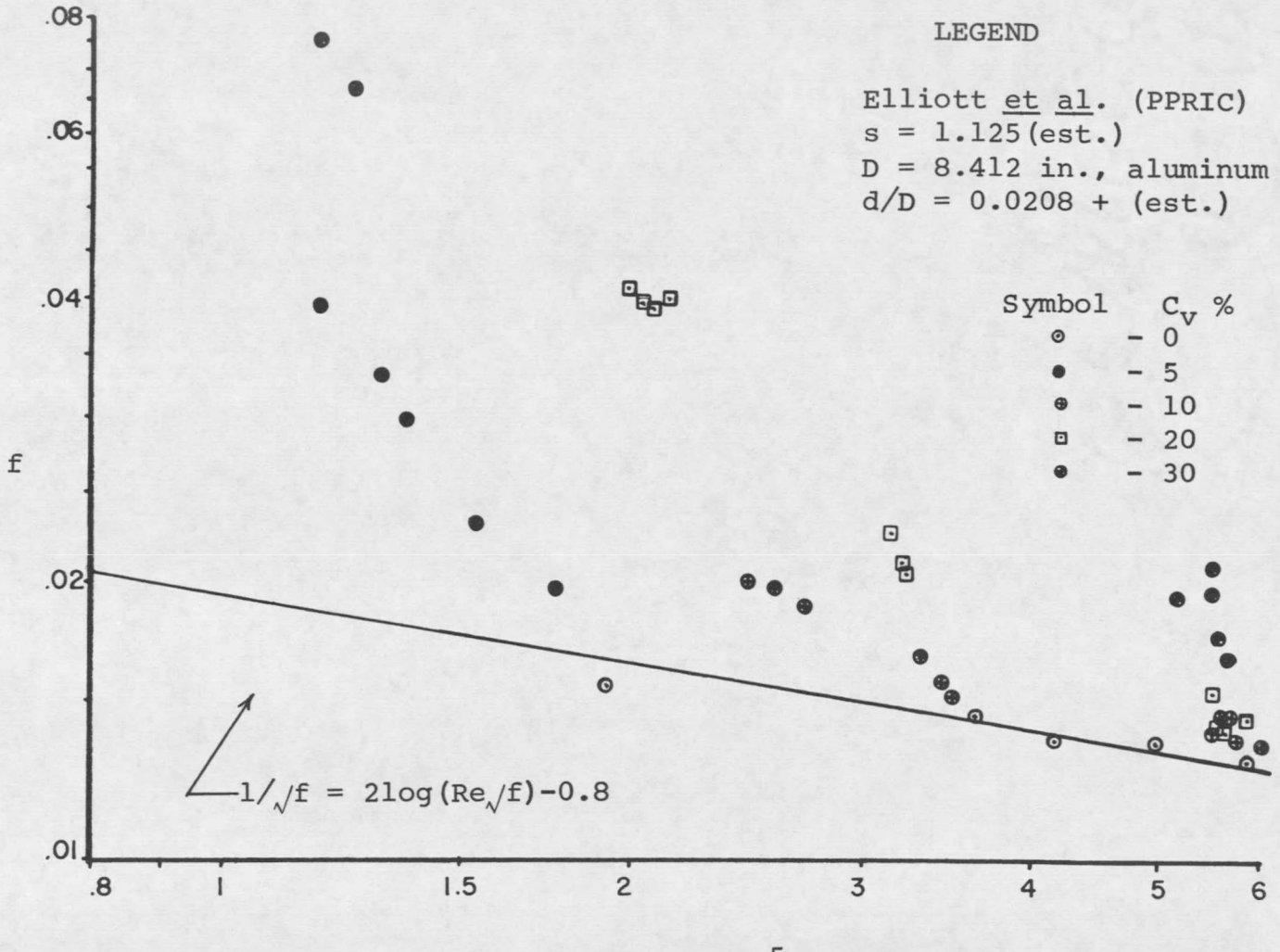

Fig. 5-12. Stanton Diagram for Woodchips.

Newton-Raphson method was employed to give values of a and b for the mathematical equation. The procedure is outlined in Appendix H. The results are given in Table VIII. The values obtained by the method of least squares are also listed because they provided the initial value of b for the Newton-Raphson method.

Curve Fitting the Woodchip Friction Factors

The same procedure used in correlating the plastic chip data was used to correlate the woodchip data. Table IX lists the coefficients, parameters and goodness of fit for the second order polynomial Eq. (5.12), selected to fit the woodchip data. McColl's data were not correlated because he did not consider his headloss data to be reliable.

The estimation required in the parameter d/D for the woodchip tests did not merit separate correlations for the woodchip tests. Therefore, the woodchip and plastic chip tests were combined to include the d/D parameter in the correlation. Eq. (5.15) as used for the plastic chip data

TABLE VIII.- COEFFICIENTS FOR POWER MODEL $\emptyset = a\psi^b$

Study	Pipe, inches	Runs	Least Squares			Newton-Raphson	
			a	b	R[1]	a	b
(1)	(2)	(3)	(4)	(5)	(6)	(7)	(8)
McColl	1.837	18	7.338	-0.930	-0.561	4.972	-0.777
Faddick	4.026	42[2]	21.031	-1.418	-0.836	24.663	-1.527
Soucy	6.000	59	4.527	-1.271	-0.886	4.977	-0.966
PPRIC	8.412	34	4.121	-1.134	-0.938	3.135	-1.493
heavy[3] chips	3.938	126	3.475	-0.693	-0.740	4.678	-0.973
heavy chips	3.000	40	4.731	-0.123	-0.368	5.061	-0.139
light[4] chips	3.938	69	5.238	-1.257	-0.954	5.216	-1.042
light chips	3.000	60	4.663	-0.108	-0.276	5.400	-0.167

1. Coefficient of Correlation
2. Excludes all concentrations less than 5 per cent
3. MSU study, s = 1.045
4. MSU study, s = 0.92

TABLE IX. - CORRELATION FOR WOODCHIP FRICTION FACTORS

Study	Faddick	Soucy	PPRIC
	D = 4.026in.	D = 6.000in	D = 8.412in.
(1)	(2)	(3)	(4)
Runs	42	59	34
	Eq. (5.12): $\log f_m = c_4 C_v + c_5 \log Re_m + c_6 C_v (\log Re_m)^2$		
c_4	0.178613	0.167033	0.114952
c_5	-0.336907	-0.329408	-0.331564
c_6	-0.005780	-0.005334	-0.003370
d/D(est.)	0.0433	0.0291	0.0208
s	1.125	1.150	1.125 (est.)
Da%	4.2	7.3	14.5
Dm%	16.9	21.1	47.1
E<5%	69.0	35.6	20.6
E<15%	95.2	91.5	52.9
E<25%	100.0	100.0	82.3

was also used for the combined data. Table X lists the coefficients, goodness of fit and the percentage discrepancy in f (when C_v = 0%) obtained from the computer output.

Because the specific gravity of saturated woodchips was somewhat variable, 1.10 to 1.15, and because its variation was not determined in all the available woodchip tests, no attempt was made to include s in the combined

TABLE X. - CORRELATION FOR COMBINED TESTS

Eq. (5.15): $\log f_m = c_7 (d/D)^{c_8} C_v + c_9 \log Re_m$

$+c_{10} (d/D)^{c_{11}} C_v (\log Re_m)^2$

Data source: 4 plastic chip tests, 3 woodchip tests

Total observations: 432

Coefficients

$c_7 = 0.025432$	$c_8 = 0.002128$
$c_9 = -0.326723$	$c_{10} = -0.000796$
$c_{11} = 0.001184$	

Range of Parameters

	Re_m	C_v	d/D (est.)	s
Min.	70,000	0	0.0208	0.92
Max.	600,000	33	0.0433	1.15

Error Analysis

Da%	Dm%	E<5%	E<15%	E<25%
16.8	67.3	14.8	47.9	78.2

Re	Percentage Discrepancy in f
100,000	29.2
200,00	18.6
400,000	7.9
600,000	1.7

correlation equation. Instead, Eq. (5.15) as defined in Table X is restricted to plate-shaped particles having near-neutral buoyancy (-8 to +15 per cent from unity) being transported hydraulically in smooth pipes.

CHAPTER VI

DISCUSSION OF RESULTS

The friction factors measured for the flow of clear water in the 3- and 4-in. acrylic pipes did not deviate more than a maximum of 5 per cent from the curve given by Nikuradse's smooth-pipe resistance equation.

Each of the Stanton-type diagrams, Figs. 5-1, 2, 4, 5 shows the effect of the parameters Re_m and C_v, on the mixture friction factor, f_m. Comparison of the diagrams shows the effect of the parameters d/D and s on f_m. The effect of each parameter on f_m is discussed below in qualitative terms mainly, because actual woodchips were not used in the experimental study.

Effect of Reynolds Number

Each Stanton diagram shows an increase in f_m with decreasing Re_m, where the rate of increase of f_m increases with decreasing Re_m.

Visual observations indicated that the amount of deviation of f_m from f, the clear-water friction factor, was proportional to the depth of the sliding bed of chips. Qualitatively speaking, at higher Reynolds numbers the

establishment of a heterogeneous suspension flow regime results in f_m becoming asymptotic with f. As the velocity of flow with a given concentration decreases and the turbulence decreases, f_m becomes increasingly greater than f, particularly as the chips migrate toward the top or bottom of the pipe (depending on s) to form a sliding bed. The increase in f_m is due to a combination of effects: the sliding bed restricts the cross sectional area of the clear-water flow passage thereby increasing the frictional loss. The sliding bed also increases the roughness of the clear-water flow passage and permits more chips to come into physical contact with the walls of the pipe. This latter effect increases the shear stress at the walls.

The deviation of f_m from f is more pronounced in the 4-in. diameter pipe than in the 3-in. diameter pipe because for a given value of Re_m, the mixture velocity in the 4-in. diameter pipe is about 3/4 the mixture velocity in the 3-in. diameter pipe. The smaller velocity supports fewer chips causing the particle distribution to become more asymmetric over the pipe's cross section. The mixture friction factor increases for the same reasons cited above.

Effect of Concentration

For a given Reynolds number the friction factor increases with volumetric concentration. The greater the concentration of the mixture, the greater is the apparent viscosity of the mixture and more energy is required to pump the thicker mixture. Also, the effect of higher concentrations is to increase the value of Re_m at which f_m becomes asymptotic to f.

Effect of d/D

The ratio d/D was changed by varying the pipe diameter D. A comparison of Figs. 5-1 and 5-2 (heavy chips in the 4-in. and 3-in. diameter pipes) shows that the mixture friction factor f_m, for the 4-in. diameter pipe deviates up to 50 per cent more from the clear-water friction factor f, than for the 3-in. diameter pipe over the range of Reynolds numbers tested. In other words, f_m increases as d/D decreases for a given Re_m. See Fig. 6-1. The mixture hydraulic gradient i_m decreases under these conditions however. In terms of the Darcy-Weisbach equation

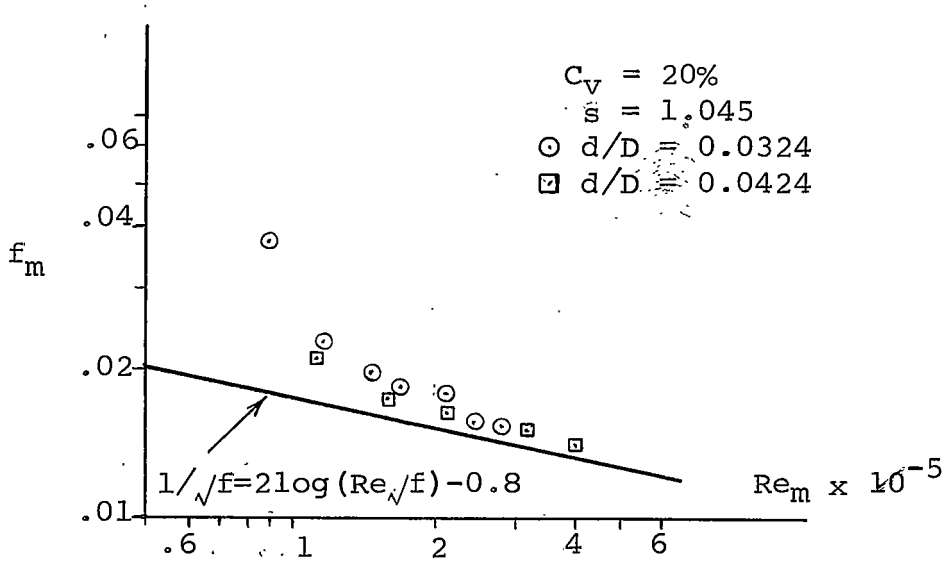

Fig. 6-1 Effect of d/D (from Figs. 5-1,2)

$$i_m = f_m \, V^2/2gD \qquad \ldots\ldots\ldots\ldots\ldots\ldots\ldots \quad (6.1)$$

From the definition of the mixture Reynolds number, Eq. (3.13)

$$V_m = \nu Re_m/D \qquad \ldots\ldots\ldots\ldots\ldots\ldots\ldots \quad (6.2)$$

giving $$i_m = f_m \, (\nu Re_m)^2/2gD^3 \qquad \ldots\ldots\ldots\ldots\ldots\ldots \quad (6.3)$$

The mixture hydraulic gradient in Eq. (6.3) decreases because while a decrease in d/D causes an increase in

f_m this increase is small compared to the decrease in i_m due to the cubic power of D in the denominator of Eq. (6.3). Table III in Chapter V shows that the effect of the increase in the d/D ratio on the flow regime delineations is to shift the occurrence of the sliding-bed regime to a lower Reynolds number.

The same remarks pertain to a comparison of Figs. 5-4 and 5-5 (light chips in the 4-in. and 3-in. diameter pipes).

Effect of Specific Gravity

Excluding surface texture, specific gravity was the only physical difference between the two batches of plastic chips; 0.92 for the light chips and 1.045 for the heavy chips. A comparison of Figs. 5-1 and 5-4 (tests in the 4-in. diameter pipe) shows that for Re_m less than 150,000-200,000, f_m for the light chips exceeded f_m for the heavy chips by as much as 25 per cent at a concentration of 20 per cent. The light chips in water possess a greater density differential ρ (1-0.92), than the heavy chips, ρ (1.045-1), and pack more tightly in a slding-bed regime

than the heavy chips as is seen by comparing Figs. 5-3a and 5-6a. This tighter packing of the light chips increases the shear stress at the wall. In addition, the tighter packing of the light chips produces a well-defined phase separation in the bedload regime which also apparently increases the boundary roughness for the water phase. The end result is an increased friction factor in the bedload regime for the light chips over that for the heavy chips.

For Re_m greater than 200,000, f_m for the light chips is 5 per cent less than f_m for the heavy chips at a concentration of 25 per cent. At higher flows there is sufficient turbulence to suspend the chips and to overcome the effects of gravity. The density differential between the chips and water is no longer significant but the density of the chips is still important. Light particles possess a smaller mass than heavy particles and are accelerated easier by the turbulent fluctuations of the flow than heavier particles of the same size and shape.

Figs. 5-2 and 5-5 display little difference in the friction factors for the heavy and light chips in the

3-in. diameter pipe. The flow regimes were observed to be mainly heterogeneous suspension and heterogeneous saltation flows.

Plastic Chip Friction Factor Correlation

Table IV shows that of the four proposed mathematical equations for the f_m-Re_m relationship, the equation

$$\log f_m = c_1 + c_2 \log Re_m + c_3 (\log Re_m)^2 \quad \ldots\ldots\ldots \quad (5.2)$$

was best in that it had the greatest percentage of data points falling within defined limits (5, 15, 25 per cent) of the mixture friction factor values predicted by the equation. For each of the four chip tests, all of the data points (experimental mixture friction factors) were within 25 per cent of the calculated mixture friction factors given by Eq. (5.2). Eq. (5.2) also produced the best fit for the other values of concentration in each of the four chip tests.

When C_v was incorporated into the correlation equation, Eq. (5.12), the goodness of fit reduced slightly because of the $\pm$ 2.5 per cent tolerance placed on the

nominal values of concentration. Table V shows that at least 89 per cent of the data from the four tests were within 25 per cent of the values predicted by Eq. (5.12).

Table VI indicates that inclusion of the parameter d/D in the correlation equation, Eq. (5.15), reduced the goodness of fit only slightly such that 85.5 per cent of the data fell within 25 per cent of Eq. (5.15).

Adding the last parameter s, a correlation equation, Eq. (5.24) as given in Table VII, was obtained in which 93.6 per cent of all the data were within 25 per cent of the values predicted by the equation. The increased goodness of fit was due to the larger number of data points being fitted to the equation. Based on this type of error analysis, Eq. (5.24) represented a good correlation of the data despite the fact that only two values each of d/D and s were tested. A further test of the acceptability of the correlation equation was that Eq. (5.24) gives a clear-water friction factor (for C_v = 0%) which is only 10.6 per cent higher than f given by the smooth pipe resistance equation, Eq. (5.1), for a Reynolds number

of 100,000. At a Reynolds number of 600,000 the percentage discrepancy in f is -15.1 per cent.

Previous Woodchip Tests

Figs. 5-9, 10, 11, and 12 show that the woodchip mixtures behave in a manner similar to plastic chip mixtures. Qualitatively, the mixture friction factor increases with decreasing Reynolds number, increases with concentration, and increases as d/D decreases for a given Reynolds number. All the woodchips were saturated in these tests so that their specific gravity was constant at about 1.125 to 1.150.

The Durand correlation given in Table VIII shows the coefficient a, and the exponent b, to vary at least fivefold among the woodchip tests. Although the woodchips did not have identical properties, the plastic chips did; yet the heavy chips also produced different values of a and b for the 3-in. and 4-in. diameter pipes as did the light chips. Nevertheless, each equation obtained by the Newton-Raphson method as listed in Table VIII is valid for the particular study from which it was formulated.

It is not recommended however, to use any one equation to calculate headlosses for woodchip mixtures in pipe sizes other than the one used in the study from which the equation was formulated. It appears therefore, that this form of the Durand equation does not suffice for correlating data for the hydraulic transportation of large plate-shaped particles in smooth pipes.

Woodchip Friction Factor Correlation

The choice of Eq. (5.12) to represent the woodchip data is substantiated in Table IX. At least 82.3 per cent of the experimental mixture friction factors were within 25 per cent of the mixture friction factors predicted by Eq. (5.12). This is less than the figure of 89 per cent obtained for the plastic chip data using the same correlation but this is to be expected when comparing independent experimental studies.

Because the parameter d/D required estimation in each of the woodchip studies but could be determined accurately for the plastic chip studies, Eq. (5.15) containing f_m,

Re_m, C_v and d/D, was used to correlate the pooled woodchip and plastic chip data.

Table X shows that 78 per cent of the experimental mixture friction factors were within 25 per cent of the mixture friction factors predicted by the empirical equation, Eq. (5.15). The same equation as applied to the plastic chip data only, gave a comparable figure of 85.5 and 97.6 per cent (Table VI) for the light and heavy chips, respectively. These higher values are to be expected because the d/D ratio was estimated for non-uniform woodchip sizes but was accurately known for the plastic chips.

As mentioned earlier it was not considered meaningful to include the chip specific gravity, s, in the combined correlation equation, because of its limited range, doubtful accuracy for woodchips, and because the correlation already contained a parameter (d/D) of doubtful accuracy. Therefore,

$$\log f_m = c_7 (d/D)^{c_8} C_v + c_9 \log Re_m + c_{10} (d/D)^{c_{11}} C_v (\log Re_m)^2 \quad \ldots\ldots\ldots (5.15)$$

is considered to be the final form of an empirical equation designed to correlate the friction factor data of four plastic chip tests performed in this study along with three available woodchip tests. The fact that 78 per cent of all the data points fall within 25 per cent of the mixture friction factors predicted by Eq. (5.15), is not a poor fit considering that Zandi and Govatos (33) have shown the limits of Durand's equation to be $\pm$ 40 per cent. Furthermore, Eq. (5.15) gives a clear-water friction factor (for C_v = 0%) which is 29 per cent higher than f given by the smooth pipe resistance equation, Eq. (5.1), for a Reynolds number of 100,000. This Reynolds number is too small for solids transport. At Reynolds numbers of 200,000 and 600,000, the percentage discrepancy in f reduces from 18.6 to 1.7 per cent respectively, which are acceptable limits.

CHAPTER VII

CONCLUSIONS AND RECOMMENDATIONS

1. The Durand equation

$$(i_m - i) / C_v . i = k_1 (V_m^2 / gD)^m \quad \ldots\ldots\ldots\ldots \quad (7.1)$$

when applied to plate-shaped particles of near-neutral buoyancy was found to be inadequate to completely define a two-phase flow system such as woodchips and water. The equation does not appear to account for the ratio of particle size and shape to the pipe diameter (d/D), nor does it appear to reflect the role of the mixture Reynolds number Re_m, that is, the ratio of inertial to viscous forces. The effect of the pipe wall roughness (k/D) is also not apparent in Eq. (7.1).

2. An analysis of a heterogeneous two-phase flow system yielded the following variables:

$$h_{f_m},\ L,\ C_v,\ d,\ D,\ \rho_s,\ \rho,\ k,\ V_m,\ g,\ \mu$$

From dimensional analysis the following functional relationship

$$f_m = f_m\ (Re_m,\ C_v,\ d/D,\ s,\ k/D) \quad \ldots\ldots\ldots\ldots\ldots \quad (3.15)$$

was obtained which reduced to

$$f_m = f_m\ (Re_m,\ C_v,\ d/D,\ s) \quad \ldots\ldots\ldots\ldots\ldots \quad (7.2)$$

for heterogeneous two-phase flow systems in smooth pipes.

Data from the limited experimental program and the available woodchip data were plotted as Stanton diagrams for each value of d/D and s. In all cases, the mixture friction factor f_m, increased with decreasing Reynolds number, increased with concentration, increased as d/D decreased at a given Reynolds number, increased with increasing s in the heterogeneous suspension regime and increased with increasing absolute values of particle-fluid specific gravity differential ((s-1) or (1-s)), in the sliding-bed regime.

3. Four plastic chip tests and three woodchip tests were combined for a correlation by a standard least squares technique. A second order polynomial

$$\log f_m = c_7 (d/D)^{c_8} C_v + c_9 \log Re_m + c_{10} (d/D)^{c_{11}} C_v (\log Re_m)^2 \quad \ldots\ldots\ldots\ldots \quad (5.15)$$

whose coefficients are given in Table X, was formulated.

An analysis of the goodness of fit of Eq. (5.15) to the combined data indicated that 78 per cent of the experimental mixture friction factors were within 25 per cent of the mixture friction factors predicted by the empirical equation. Eq. (5.15) yielded clear-water friction factors (for C_v = 0%) which were 18.6 and 1.7 per cent higher than f predicted by the smooth pipe roughness equation, Eq. (5.1), for Reynolds numbers of 200,000 and 600,000, respectively. The available woodchip data and the experimental program did not test a sufficient variation in s to permit its inclusion in the correlation equation. Therefore, Eq. (5.15) is applicable to heterogeneous mixtures of plate-shaped solids of near-neutral buoyancy (s = 0.92 to 1.15) being transported hydraulically in smooth pipes.

The study produced two subsidiary conclusions:

1. By noting the effect of particle specific gravities slightly less than and slightly greater than unity, on the mixture friction factor, it was concluded that a mixture of neutrally-buoyant particles would produce a headloss, not equal to that of clear water as indicated by the

Durand equation, but greater than that of clear water.

2. The particle shape is as important as the particle size, particularly for plate-shaped particles.

Recommendations

Further work is recommended:

1. The range of d/D and s should be extended as much as possible to expand the range of the correlation equation. In the case of the parameter d/D, either the particle geometry, pipe diameter, or both, can be varied.

2. The effect of particle surface texture should be tested.

3. Any correlation equation, to be truly universal for heterogeneous solids, must be formulated from experimental work in rough pipes as well as smooth pipes.

4. The proposed parameters should be investigated with heterogeneous mixtures of other types of solids, e.g., sands, mineral slurries, and artificial solids.

APPENDICES

APPENDIX A

NOMENCLATURE

A = intercept of pressure transducer equation, $Y = A + BX$

a = largest dimension of particle, ft

B = slope of pressure transducer equation, $Y = A + BX$

b = shortest width dimension of particle, ft

C_d = weighted mean drag coefficient of the solids

C_v = volumetric concentratration of solids (fraction)

c = particle thickness, ft

c_1 = coefficient in friction factor correlation equations

D = internal pipe diameter, ft

d = representative particle dimension, ft

d_a = diameter of a sphere having the same surface area as the particle, ft

d_n = weighted mean nominal particle diameter, ft, or diameter of a sphere of the same volume as the particle

f = clear-water friction factor

f_m = mixture friction factor

g = gravitational acceleration, ft/sec^2

h_{f_m} = mixture headloss, ft of water

i = clear-water hydraulic gradient, ft of water/ft of pipe length

i_m = mixture hydraulic gradient, ft of water/ft of pipe length

K = constant, dependent on particle properties

k = Nikuradse equivalent sand-grain roughness, ft

k_1 = constant, depending on woodchip properties

L = pipe length over which headloss is measured, ft

m = constant, dependent on particle properties

N = number of observations

P = pressure, psf

p_n = n number of size fractions

Q = fluid discharge, cfs

Q_m = mixture discharge, cfs

Q_w = water discharge, cfs

R = coefficient of correlation

R_e = clear-water Reynolds number = VD/ν

R_{e_m} = mixture Reynolds number = V_mD/ν

r = radial coordinate, ft

SF = shape factor

s = specific gravity of the solids

s_m = mixture specific gravity

t = time, sec

u = axial turbulent velocity fluctuation, fps

V = mean fluid (water) velocity, fps

V_m = mean mixture velocity, fps

V_s = weighted mean settling velocity of the solids, fps

v = radial turbulent velocity fluctuation, fps

w = tangential turbulent velocity fluctuation, fps

X = ratio of transducer output voltage to excitation (input) voltage

Y = piezometer head, ft

z = axial coordinate, ft

θ = tangential coordinate, radians

μ = dynamic viscosity of fluid (water), lb-sec/ft^2

ν = kinematic viscosity of fluid (water), ft^2/sec

ρ = fluid density (water), slugs/ft^3

ρ_m = mixture density, slugs/ft^3

ρ_s = solids density, slugs/ft^3

τ_o = shear stress at wall for fluid, psf

τ_{om} = shear stress at wall for mixture, psf

$\varphi = (i_m - i)/C_v \cdot i$

$\Psi = V_m^2 \sqrt{gd_n/V_s^2}/gD$

$\Psi_1 = 4gD/V_m^2$

APPENDIX B

DIMENSIONAL ANALYSIS

The functional expression

$$i_m = i_m\ (C_v,\ d,\ D,\ \rho s,\ \rho,\ k,\ V_m,\ g,\ \mu) \ \ldots\ldots\ (3.14)$$

states that the dependent variable i_m, is a function of nine independent variables. For purposes of dimensional analysis i_m is replaced by the fundamental variables h_{f_m} and L, where h_{f_m} is the mixture headloss measured in feet of water over the test section length, L. Thus, there are eleven physical quantities and three primary dimensions; force (F), length (L), and time (T), which means that eight dimensionless groups or parameters are required to correlate the data. Using the Buckingham π-method (21), the parameters can be expressed as

$$\varphi(\pi_1,\ \pi_2,\ \pi_3,\ \pi_4,\ \pi_5,\ \pi_6,\ \pi_7,\ \pi_8) = C_1 \ \ldots\ldots\ (B.1)$$

By choosing ρ, V_m and D as repeating primary variables, and assigning a positive unit exponent for each non-repeating variable so that each π-term appears in its familiar form, the eight π-terms are formed as follows:

$$\pi_1 = \rho^{a1} V_m^{b1} D^{c1} h_{f_m}^{1}$$

$$\pi_2 = \rho^{a2} V_m^{b2} D^{c2} C_v^{1}$$

$$\pi_3 = \rho^{a3} V_m^{b3} D^{c3} d^{1}$$

$$\pi_4 = \rho^{a4} V_m^{b4} D^{c4} \rho_s^{1}$$

$$\pi_5 = \rho^{a5} V_m^{b5} D^{c5} k^{1}$$

$$\pi_6 = \rho^{a6} V_m^{b6} D^{c6} g^{1}$$

$$\pi_7 = \rho^{a7} V_m^{b7} D^{c7} \mu^{1},$$

$$\pi_8 = \rho^{a8} V_m^{b8} D^{c8} L^{1}$$

Using FLT as fundamental dimensions

$$\pi_1 = F^{\circ}L^{\circ}T^{\circ} = (FT^2L^{-4})^{a1} (LT^{-1})^{b1} (L)^{c1} (L)^{1}$$

F: $0 = a1$

L: $0 = -4a1 + b1 + c1 + 1$

T: $0 = 2a1 - b1$

$a1 = 0;\ b1 = 0;\ c1 = -1$

Hence $\pi_1 = h_{f_m}/D$

A similar procedure is followed to solve for the other π-terms:

$$\pi_2 = C_v$$

$$\pi_3 = d/D$$

$$\pi_4 = \rho_s/\rho$$

$$\pi_5 = k/D$$

$$\pi_6 = gD/V_m^2$$

$$\pi_7 = \mu/\rho V_m D = \nu/V_m D$$

$$\pi_8 = L/D$$

When these results are substituted into the π-equation:

$$\varphi(h_{f_m}/D,\ C_v,\ d/D,\ \rho_s/\rho,\ k/D,\ gD/V_m^2,$$

$$\nu/V_m D,\ L/D) = C_1 \qquad \ldots\ldots\ldots\ldots\ldots\ldots\ldots \quad (B.2)$$

The mixture friction factor is given by

$$f_m = 2gD\ i_m/V_m^2 = 2\pi_6\pi_1/\pi_8 \qquad \ldots\ldots\ldots\ldots\ldots\ldots \quad (B.3)$$

Therefore, the following functional relationship is obtained:

$$f_m = f_m\ (V_m D/\nu,\ C_v,\ k/D,\ d/D,\ s) \ldots\ldots\ldots\ldots\ldots \quad (3.15)$$

APPENDIX C

ANALOG-TO-DIGITAL DATA RECORDING SYSTEM

Electronic sensors measured voltage outputs of the five pressure transducers and the input excitation voltage to drive the sensors. A Sorenson Q. Nobatron D.C. power supply provided 15 volts to drive the sensors. Amplification or attenuation of some signals was required to provide a full scale output of one volt. For example, the pressure transducers were excited by the same 15-volt source but it was reduced to supply slightly less than one volt.

Output voltages from the various electronic sensors were fed into a 30-channel EECO 765 multiplexer unit manufactured by Electronic Engineering Corporation of California. However, as previously stated, only 20 channels were employed for monitoring pipeline data. An EECO 761 analog-to-digital converter (A-to-D) transformed the selected data (in voltages) to binary digits for processing on an IBM 1620 II digital computer.

Interfacing circuitry and a timing control system were developed by the Electronic Research Laboratory of

Montana State University for the multiplexer. This permitted an automatic or manual sequential scan of any or all of the channels in use. Scanning time was variable up to a rate of 10,000 readings per second which permitted a complete 30-channel scan in 3 milliseconds, giving essentially a simultaneous reading of all channels. The A-to-D converter transformed analog signals to three-significant-figure digital form at a conversion rate equal to the multiplexer scan rate. Cycle time between complete scans could be varied from continuous scanning to intermittent scanning thus enabling computer operations, if desired, between complete scans.

A Fortran II program commanded readout of the data on an "on line" printer and on punched cards. The program contained a multiplexer sub-routine which called for a single scan of the 20 channels of data at a rate pre-selected by the operator. The data on each of the channels were averaged by the computer before being printed and punched.

The speed of data recording varied as follows: one line of computer output (21 pieces of data) could be

printed and punched every 2.4 seconds if the data (voltages) in the twenty channels were read five times each and averaged before being recorded. Increasing to ten the number of readings to be averaged gave a line of computer output every 4 seconds. Averaging twenty readings per data channel required 7.5 seconds for a one line print-out. It was found convenient to average ten readings to give one line of computer output every 4 seconds. At this rate data accumulation was not too copious yet any flow unsteadiness exhibited by the transducer output voltages could be spotted quickly. Data recording was limited to slightly more than one minute unless reduced by either flow or electronic unsteadiness.

APPENDIX D

CALIBRATION OF APPARATUS

Flowmeters

Both flowmeters were calibrated with clear water before and after each test program. The pipeline was re-routed into a weir box from where the flow was discharged into a calibrated tank. A sight gauge and vertical scale on the side of the tank provided a means for measuring the flow volumetrically over a known period of time. Diversion times ranged from 30 sec. to 2 min. The flow measurements were corrected for temperature changes. Each discharge setting was remeasured until repeatability of less than 1/2 per cent was attained. Then the pens of both flowcharts were adjusted to coincide with the measured flow. The flow meters were calibrated in this manner in 50 gpm increments up to the maximum flow of 400 gpm.

Initial pen adjustments reduced "chart painting" to about 2 gpm at all clear-water flows. However, when plastic chips were being pumped, the mixture flowchart pen painted a line which fluctuated about 5 gpm for all flow

settings. Therefore, readings of the mixture flow were subject to an error of ± 2.5 per cent for a flow of 100 gpm and ± 5/8 per cent for a flow of 400 gpm.

The flowmeter manufacturer claimed a calibration accuracy of ± 1 per cent of full scale (400 gpm) throughout the entire scale for the complete system of transmitter, connecting cables and receiver; and ± 0.5 per cent of full scale for repeatability. The manufacturer also claimed that the average velocity measured by the meter was not affected by variations in density, viscosity, line pressure, conductivity and temperature. These claims were never disproven during the test program.

Combining the chart painting error with the flowmeter error of ± 1 per cent and the mix tank error of ± 1 per cent, the maximum error in the flow and volumetric concentration measurements was less than ± 5 per cent.

Pressure Transducer Calibration

Six multiplexer channels were used to measure pipeline pressure. One channel monitored the input excitation

voltage to all the transducers while the other five channels monitored the output voltages of each of the transducers. The output voltage of the transducers was a function of input voltage and pipeline pressure. Therefore, the ratio of transducer output voltage (in millivolts) was proportional to the mixture pressure acting on the transducer element.

The transducer calibration consisted of computing the ratio of transducer output voltage to excitation voltage as measured by the analog computer and recorded by the digital computer, and relating this to observed manometer readings of pipeline pressure.

For the transducer calibration all the data channels were scanned sequentially ten consecutive times. The data (in millivolts) was averaged, printed and punched within four seconds. The pertinent data consisted of the transducer output voltages (in millivolts) and the excitation voltages (in millivolts) supplied for each transducer. Therefore, each reading of manometer pressure corresponded to an average of ten readings of transducer output voltage.

The transducers were calibrated statically five times during the testing program. The 221-ft long test section was isolated and completely filled with water. Compressed air was injected into the test section until the pressure transducers were subjected to the pressure ranges given in Table D-I. Static heads were measured on a 60-in. water-mercury manometer connected to transducer #2 by a tee-connection.

Since the manufacturer claimed a linear relationship between the ratio of output voltage to input voltage and the allowable pressure range of each transducer, a simple linear regression analysis was performed on the calibration curve for each transducer. The mathematical relationship was

$$Y = A + B X \quad \ldots\ldots\ldots\ldots\ldots\ldots\ldots \quad (D.1)$$

where Y = piezometer head, ft;

A = intercept of Eq. (D.1);

B = slope of Eq. (D.1); and

X = ratio of transducer output voltage to excitation (input) voltage.

Table D-I gives the equation coefficients A, B, the number of observations N, and the coefficient of correlation R, for each transducer. The prime data and computer programs are on file with the Civil Engineering Department of Montana State University.

TABLE D-I. -PRESSURE TRANSDUCER DATA

Transducer Number	1	2	3	4	5
Pressure Range, psig	0-15	0-15	0-20	0-20	0-30
Pipe Elev., ft	100.00	100.00[a]	100.01	97.97	100.03
Transducer, Elev., ft	97.95	97.93	97.91	97.88	97.92
Intercept, A	-7.312	-7.663	-4.506	-4.292	-9.305
Slope, B	33.883	36.532	49.901	49.617	72.823
Observations, N	31	37	64	70	94
Correlation Coefficient, R	0.999	0.999	0.999	0.999	0.999

a datum

APPENDIX E

COMPILATION OF PLASTIC CHIP DATA

Due to the voluminous data collected in this study only the more important measurements are presented. All the data and computer programs are on file with the Civil Engineering Department of Montana State University.

Table E-I lists the data obtained for the heavy chips in the 4-in. pipe of the 700-ft. loop system. Table E-II lists the data for the heavy chips in the 4-in. pipe of the 200-ft. loop system. This extra test was performed to extend the lower range of the Reynolds numbers obtained in the 700-ft. system. Data taken from the valve tests by Johnson (19) using the same 4-in. pipe in the short loop system are compiled in Table E-III.

Table E-IV pertains to the heavy chips in the 3-in. pipe of the short loop system.

Table E-V is for the light chips in the 4-in. pipe of the long loop system.

Data for the light chips in the 3-in. pipe of the short loop system are given in Table E-VI.

TABLE E-I. PLASTIC CHIP TEST DATA

ETHOCELL/CYCOLAC CHIPS
SPECIFIC GRAVITY - 1.05/1.04
SIZE - 1/2 X 3/8 X 1/10 IN.
FALL VELOCITY - 0.125 FPS

PIPE MATERIAL - ACRYLIC
PIPE INT. DIAM. - 3.938 IN.
WATER TEMPERATURE - 61-70 F
KINEMATIC VISC - 0.0000116

(1) VOLUME CONCENTRATION (PERCENT) CV	(2) MIXTURE VELOCITY (FT/SEC) VM	(3) MIXTURE GRADIENT (FT/FT) IM	(4) (IM-IW)/(CV*IW) PHI	(5) (VM*VM)/G*D PSI	(6) FRICTION FACTOR F	(7) REYNOLDS NUMBER RE
10.3	10.01	0.068505	0.30605	9.49005	0.014437	283,185
9.9	9.86	0.073749	1.41952	9.20777	0.016019	278,942
8.9	8.85	0.056156	0.57693	7.41800	0.015141	250,368
10.3	7.91	0.050153	1.40981	5.92589	0.016927	223,776
10.5	7.88	0.045782	0.49951	5.88102	0.015569	222,927
10.0	6.85	0.036033	0.61180	4.44408	0.016216	193,788
10.7	6.01	0.031519	1.58715	3.42097	0.018427	170,024
8.8	6.01	0.028416	0.62150	3.42097	0.016613	170,024
12.0	5.06	0.021628	0.73525	2.42494	0.017838	143,149
10.5	4.00	0.015945	2.05529	1.51538	0.021044	113,161
10.1	3.93	0.017930	4.06456	1.46280	0.024515	111,181
13.9	9.85	0.071314	0.75438	9.18910	0.015521	278,659
15.1	7.85	0.048249	0.77264	5.83633	0.016534	222,078
15.8	6.14	0.032330	0.98354	3.57057	0.018109	173,702
16.4	5.33	0.025287	0.97918	2.69063	0.018796	150,787
19.2	9.88	0.070076	0.41591	9.24516	0.015160	279,507
20.1	9.86	0.076232	0.89021	9.20777	0.016558	278,942
20.0	8.96	0.059988	0.49411	7.60355	0.015779	253,480
19.7	8.92	0.059260	0.47770	7.53581	0.015728	252,349
18.8	8.83	0.058504	0.53039	7.38451	0.015845	249,803
20.8	7.99	0.052745	0.88055	6.04636	0.017447	226,039
20.4	7.99	0.052546	0.87593	6.04636	0.017381	226,039
20.2	7.96	0.051516	0.80841	6.00104	0.017169	225,190
20.2	7.96	0.051004	0.75117	6.00104	0.016998	225,190
19.7	7.90	0.050833	0.82913	5.91091	0.017200	223,493
19.4	7.88	0.050227	0.79707	5.88102	0.017081	222,927
19.1	7.85	0.053112	1.20009	5.83633	0.018201	220,078
19.1	6.75	0.039788	1.06093	4.31527	0.018441	190,959
21.0	6.14	0.035409	1.26398	3.57057	0.019834	173,702

CONTINUED

TABLE E-I. PLASTIC CHIP TEST DATA-CONTINUED

CV	VM	IM	PHI	PSI	F	RE
20.2	6.11	0.034955	1.28752	3.53576	0.019772	172,853
19.6	6.06	0.035225	1.47141	3.47813	0.020255	171,439
19.7	5.91	0.032049	1.14394	3.30807	0.019376	167,195
22.0	5.37	0.028272	1.27518	2.73117	0.020703	151,918
24.8	9.86	0.075902	0.70093	9.20777	0.016487	278,942
25.1	8.93	0.066290	0.88239	7.55272	0.017554	252,632
25.9	8.04	0.056347	0.96558	6.12227	0.018407	227,453
26.3	8.01	0.055764	0.93292	6.07667	0.018354	226,605
25.4	7.99	0.056014	1.00978	6.04636	0.018528	226,039
25.5	7.96	0.055115	0.95909	6.00104	0.018369	225,190
24.8	7.85	0.055526	1.14955	5.83633	0.019028	222,078
24.8	6.80	0.045726	1.46855	4.37943	0.020882	192,373
27.2	6.12	0.035894	1.06689	3.54734	0.020237	173,136
26.8	6.09	0.037220	1.30422	3.51265	0.021192	172,287
22.9	6.09	0.033972	1.01207	3.51265	0.019343	172,287
26.6	6.06	0.036409	1.24700	3.47813	0.020936	171,439
24.9	6.03	0.039007	1.76428	3.44378	0.022654	170,590
23.9	5.95	0.038500	1.90189	3.35301	0.022965	168,327
23.9	5.95	0.037929	1.81162	3.35301	0.022624	168,327
23.6	5.93	0.039069	2.05450	3.33050	0.023461	167,761
24.6	5.90	0.034055	1.24374	3.29689	0.020659	166,912
26.3	5.36	0.031536	1.64675	2.72101	0.023180	151,636
26.6	5.35	0.032041	1.73256	2.71086	0.023639	151,353
24.9	5.30	0.030348	1.63389	2.66043	0.022814	149,938
24.1	5.24	0.029637	1.66731	2.60054	0.022793	148,241
23.8	5.22	0.029372	1.67528	2.58072	0.022763	147,675
29.4	9.85	0.083421	0.99466	9.18910	0.018157	278,659
28.7	9.75	0.082549	1.05298	9.00347	0.018337	275,830
28.5	9.07	0.076000	1.27158	7.79139	0.019509	256,592
31.9	8.44	0.074488	1.61937	6.74661	0.022082	238,769
32.2	8.01	0.077315	2.25667	6.07667	0.025447	226,605
30.0	7.99	0.066489	1.63818	6.04636	0.021993	226,039
32.8	7.96	0.077271	2.27097	6.00104	0.025753	225,190
29.1	7.77	0.060047	1.42654	5.71798	0.021003	219,815
30.8	7.01	0.061243	2.37488	4.65411	0.026318	198,314
29.5	6.62	0.050271	1.94124	4.15065	0.024223	187,281
30.9	6.06	0.048130	2.46088	3.47813	0.027676	171,439
30.0	5.98	0.047246	2.56392	3.38690	0.027899	169,175
30.4	5.90	0.048484	2.82662	3.29689	0.029412	166,912

CONTINUED

TABLE E-I. PLASTIC CHIP TEST DATA-CONTINUED

CV	VM	IM	PHI	PSI	F	RE
31.2	5.37	0.041351	2.79787	2.73117	0.030281	151,918
30.3	5.22	0.039987	2.98419	2.58072	0.030989	147,675
28.4	5.19	0.036498	2.66150	2.55114	0.028613	146,826
30.9	5.03	0.037485	2.93211	2.39627	0.031286	142,300
28.8	4.66	0.034240	3.44755	2.05670	0.033296	131,832
31.0	4.66	0.034219	3.19894	2.05670	0.033276	131,832
31.0	4.66	0.034145	3.18505	2.05670	0.033204	131,832

TABLE E-II. PLASTIC CHIP TEST DATA

ETHOCELL/CYCOLAC CHIPS
SPECIFIC GRAVITY = 1.05/1.04
SIZE - 1/2 X 3/8 X 1/10 IN.
200 FT LOOP SYSTEM

PIPE MATERIAL - ACRYLIC
PIPE INT. DIAM. = 3.938 IN.
FALL VELOCITY - 0.125 FPS

(1) VOLUME CONCENTRATION (PERCENT) CV	(2) MIXTURE VELOCITY (FT/SEC) VM	(3) MIXTURE GRADIENT (FT/FT) IM	(4) TEMPERATURE F T	(5) FRICTION FACTOR F	(6) REYNOLDS NUMBER RE
0.	6.58	0.031760	66.0	0.015457	196,308
0.	6.01	0.027473	66.2	0.016075	179,302
0.	3.95	0.012704	66.5	0.017194	117,844
0.	2.64	0.006193	66.5	0.018763	78,762
10.4	6.09	0.028580	66.2	0.016292	181,689
10.0	5.01	0.020962	66.2	0.017662	149,468
10.6	3.98	0.015880	66.8	0.021185	118,739
12.4	3.08	0.010481	67.0	0.023288	91,889
11.3	3.03	0.014133	66.5	0.032507	90,397
10.0	2.61	0.011434	67.0	0.035487	77,867
10.0	2.64	0.011592	66.5	0.035120	78,762
15.6	6.09	0.030172	66.2	0.017199	181,689
14.4	4.95	0.022232	66.2	0.019133	147,678
15.7	5.03	0.022232	66.2	0.018537	150,065
15.9	3.98	0.017786	66.8	0.023728	118,739
16.0	3.06	0.013339	67.0	0.030152	91,292
17.2	2.69	0.012386	66.5	0.036146	80,253
16.7	2.53	0.015880	68.0	0.052315	69,248
19.6	6.03	0.032078	66.2	0.018606	179,899
20.6	5.05	0.025091	66.8	0.020812	150,662
19.5	3.93	0.018421	66.8	0.025238	117,248
18.5	3.85	0.018738	67.0	0.026738	114,861
20.6	3.06	0.017150	67.0	0.038766	91,292
25.0	6.01	0.040971	68.5	0.023953	166,021
24.8	4.98	0.031125	69.2	0.026503	138,595
26.2	5.03	0.032395	69.4	0.027038	140,248
26.3	4.00	0.024138	69.4	0.031699	111,529

TABLE E-III. PLASTIC CHIP TEST DATA

EXPERIMENTER - JOHNSON(1968)
SPECIFIC GRAVITY - 1.045
SIZE - 1/2 X 3/8 X 1/10 IN.
FALL VELOCITY - 0.125 FPS

PIPE MATERIAL - ACRYLIC
PIPE INT. DIAM. - 3.938 IN.
WATER TEMPERATURE- UNMEASURED
KINEMATIC VISC-0.0000100(EST)

(1) VOLUME CONCEN-TRATION (PERCENT) CV	(2) MIXTURE VELOCITY (FT/SEC) VM	(3) MIXTURE GRADIENT (FT/FT) IM	(4) (IM-IW)/ (CV*IW) PHI	(5) (VM*VM)/ G*D PSI	(6) FRICTION FACTOR F	(7) REYNOLDS NUMBER RE
9.5	10.06	0.07393	1.31995	9.58509	0.015426	330,136
10.1	10.00	0.07270	1.17367	9.47110	0.015352	328,167
9.6	9.96	0.07327	1.41040	9.39548	0.015597	326,854
10.4	8.01	0.05040	1.46071	6.07667	0.016588	262,861
9.9	7.98	0.04980	1.47317	6.03123	0.016514	261,877
10.1	7.98	0.04840	1.12506	6.03123	0.016050	261,877
9.9	7.97	0.04883	1.27315	6.01613	0.016233	261,549
11.0	6.07	0.03060	1.33536	3.48962	0.017538	199,197
11.1	6.04	0.03114	1.59900	3.45521	0.018025	198,213
10.6	6.03	0.02860	0.79854	3.44378	0.016610	197,884
10.5	6.00	0.03020	1.48149	3.40960	0.017715	196,900
9.9	5.97	0.02880	1.13018	3.37558	0.017064	195,915
11.2	4.01	0.01553	1.95731	1.52296	0.020395	131,915
10.2	3.99	0.01479	1.68160	1.50781	0.019618	130,938
9.1	3.94	0.01473	2.12428	1.47025	0.020037	129,298
20.6	10.03	0.07800	0.94025	9.52801	0.016373	329,151
19.7	9.97	0.07673	0.94866	9.41436	0.016301	327,182
19.8	9.94	0.07610	0.92670	9.35779	0.016265	326,198
20.3	8.04	0.05351	1.05846	6.12227	0.017480	263,846
20.3	8.01	0.05247	0.98140	6.07667	0.017269	262,861
19.4	7.94	0.05173	1.03591	5.97092	0.017327	260,564
19.2	7.91	0.05233	1.16211	5.92589	0.017662	259,580
19.7	6.00	0.03413	1.55295	3.40960	0.020020	196,900
19.9	5.99	0.03331	1.39877	3.39824	0.019604	196,572
20.1	5.96	0.03280	1.34382	3.36428	0.019499	195,587
20.6	4.02	0.01827	2.07752	1.53057	0.023874	3 T
18.8	3.93	0.01847	2.67602	1.46280	0.025253	128,969
19.3	3.93	0.01752	2.20611	1.46280	0.023954	128,969

TABLE E-IV. PLASTIC CHIP TEST DATA

ETHOCELL/CYCOLAC CHIPS
SPECIFIC GRAVITY - 1.05/1.04
SIZE - 1/2 X 3/8 X 1/10 IN.

PIPE MATERIAL - ACRYLIC
PIPE INT. DIAM. - 3.000 IN.
FALL VELOCITY - 0.125 FPS

(1) VOLUME CONCENTRATION (PERCENT) CV	(2) MIXTURE VELOCITY (FT/SEC) VM	(3) MIXTURE GRADIENT (FT/FT) IM	(4) TEMPERATURE F T	(5) FRICTION FACTOR F	(6) REYNOLDS NUMBER RE
0.	18.10	0.273740	68.3	0.013446	415,076
0.	17.15	0.251211	68.7	0.013744	395,110
0.	13.59	0.166424	68.8	0.014495	313,728
0.	11.51	0.124273	69.0	0.015100	266,847
0.	8.86	0.076550	69.0	0.015704	205,364
0.	6.99	0.050145	69.0	0.016511	162,102
0.	5.08	0.028343	69.5	0.017644	118,885
0.	4.58	0.023619	69.0	0.018106	106,240
10.4	17.02	0.250046	69.0	0.013886	393,998
9.4	14.89	0.196503	69.7	0.014258	349,470
9.2	12.80	0.151985	70.1	0.014923	302,447
11.1	11.07	0.116644	70.3	0.015313	262,436
10.7	11.03	0.116616	70.3	0.015420	261,360
10.5	9.08	0.082122	70.4	0.016032	215,725
10.0	9.03	0.082122	70.4	0.016193	214,646
10.3	7.94	0.064923	70.4	0.016554	188,759
10.5	6.94	0.051599	69.0	0.017212	161,049
12.1	5.99	0.039971	69.5	0.017914	140,114
10.0	4.99	0.031977	69.5	0.020636	116,762
14.5	16.93	0.250238	69.4	0.014045	395,559
15.7	15.02	0.200638	70.0	0.014307	354,665
15.5	14.98	0.200700	70.0	0.014388	353,593
15.1	12.94	0.156397	70.1	0.015026	305,665
14.8	12.89	0.155171	70.1	0.015024	304,592
14.7	10.80	0.114102	70.3	0.015737	255,983
14.1	8.99	0.082849	70.4	0.016502	213,568
15.3	7.99	0.066618	70.4	0.016794	189,838
14.9	7.94	0.066134	70.4	0.016863	188,759
16.0	7.08	0.055717	69.0	0.017878	164,207
14.2	5.76	0.038760	69.5	0.018765	134,807

CONTINUED

TABLE E-IV. PLASTIC CHIP TEST DATA-CONTINUED

CV	VM	IM	T	F	RE
13.9	4.90	0.031008	69.5	0.020759	114,639
12.9	4.22	0.025194	70.0	0.022746	99,649
19.3	16.93	0.254122	69.7	0.014263	397,416
20.9	15.11	0.206454	70.0	0.014547	356,808
21.2	15.07	0.207181	70.0	0.014676	355,736
20.0	14.98	0.203058	70.0	0.014557	353,593
20.0	12.94	0.160269	70.3	0.015398	306,534
22.1	11.07	0.124147	70.3	0.016298	262,436
20.9	9.12	0.086725	70.4	0.016762	216,804
20.1	9.03	0.086483	70.4	0.017053	214,646
20.4	7.99	0.068799	70.4	0.017344	190,019
20.9	7.13	0.057413	69.0	0.018188	165,260
21.4	5.08	0.034642	69.5	0.021565	118,885
21.8	5.04	0.034642	69.5	0.021955	117,823
24.2	8.99	0.091570	70.2	0.018239	212,557
24.2	8.99	0.092781	70.2	0.018480	212,557
26.6	8.03	0.078246	70.2	0.019503	190,013
22.7	5.99	0.044089	69.5	0.019759	140,114

TABLE E-V. PLASTIC CHIP TEST DATA

POLYETHYLENE CHIPS
SPECIFIC GRAVITY - 0.92
SIZE - 1/2 X 3/8 X 1/10 IN.
RISE VELOCITY - 0.15' FPS

PIPE MATERIAL - ACRYLIC
PIPE INT. DIAM. - 3.000 IN.
WATER TEMPERATURE - 64-70 F
KINEMATIC VISC - 0.000011

(1) VOLUME CONCEN-TRATION (PERCENT) CV	(2) MIXTURE VELOCITY (FT/SEC) VM	(3) MIXTURE GRADIENT (FT/FT) IM	(4) (IM-IW)/ (CV*IW) PHI	(5) (VM*VM)/ G*D PSI	(6) FRICTION FACTOR F	(7) REYNOLDS NUMBER RE
10.0	9.99	0.065901	-0.04172	9.45217	0.013944	298,035
9.7	9.95	0.065346	-0.05701	9.37663	0.013938	296,842
10.6	7.93	0.046064	0.44484	5.95589	0.015468	236,578
9.7	7.85	0.045341	0.50894	5.83633	0.015538	234,192
9.3	6.80	0.035456	0.62154	4.37943	0.016192	202,867
9.3	6.77	0.035613	0.76157	4.34088	0.016408	201,972
8.9	6.77	0.035425	0.73229	4.34088	0.016322	201,972
9.0	6.75	0.035094	0.67507	4.31527	0.016265	201,375
11.5	6.67	0.034395	0.53722	4.21359	0.016326	198,988
7.5	6.67	0.034155	0.72495	4.21359	0.016212	198,988
10.0	6.03	0.029331	0.82274	3.44378	0.017034	179,895
11.1	5.93	0.028990	0.91709	3.33050	0.017409	176,912
10.4	4.97	0.023398	2.06972	2.33944	0.020003	148,272
12.4	4.03	0.016210	1.77250	1.53819	0.021077	120,228
10.7	3.95	0.018154	3.88205	1.47773	0.024570	117,842
9.6	2.94	0.010132	3.45476	0.81864	0.024753	87,710
10.8	2.69	0.009687	4.53550	0.68534	0.028269	80,252
15.0	7.84	0.046297	0.49274	5.82147	0.015906	233,893
14.5	6.81	0.037906	0.88249	4.39233	0.017260	203,165
12.6	6.67	0.036043	0.89408	4.21359	0.017108	198,988
13.7	5.98	0.031299	1.25565	3.38690	0.018482	178,403
17.1	5.09	0.027412	2.13399	2.45378	0.022343	151,852
17.1	5.09	0.027150	2.05770	2.45378	0.022129	151,852
14.6	4.14	0.020708	3.32734	1.62331	0.025513	123,510
14.6	4.14	0.018389	2.18770	1.62331	0.022656	123,510
14.1	4.11	0.018251	2.31527	1.59987	0.022816	122,615
13.5	4.08	0.018800	2.84572	1.57660	0.023849	121,720
15.8	4.00	0.018757	2.72291	1.51538	0.024756	119,333
12.9	3.87	0.016946	2.86728	1.41848	0.023893	115,455
16.6	3.10	0.014953	4.75592	0.91017	0.032858	92,483

CONTINUED

TABLE E-V. PLASTIC CHIP TEST DATA-CONTINUED

CV	VM	IM	PHI	PSI	F	RE
15.5	3.06	0.016352	6.46692	0.88684	0.036877	91,290
14.5	2.90	0.013853	5.96799	0.79652	0.034784	86,517
13.0	2.85	0.013470	6.69567	0.76929	0.035019	85,025
15.5	2.71	0.017549	10.73460	0.69557	0.050460	80,848
12.6	2.52	0.011382	7.65665	0.60145	0.037848	75,180
16.9	2.50	0.010791	5.26126	0.59194	0.036460	74,583
15.1	2.45	0.011215	6.85295	0.56850	0.039455	73,092
14.1	2.42	0.011808	8.43670	0.55467	0.042577	72,197
21.7	10.26	0.071071	0.11281	9.97000	0.014257	306,090
19.7	6.78	0.038283	0.75182	4.35371	0.017586	202,270
20.6	6.67	0.037700	0.79517	4.21359	0.017895	198,988
20.7	6.11	0.035523	1.35533	3.53576	0.020094	182,282
20.1	6.03	0.035066	1.46213	3.44378	0.020365	179,895
18.9	5.98	0.034679	1.57985	3.38690	0.020478	178,403
20.8	5.95	0.033136	1.21104	3.35301	0.019765	177,508
21.8	5.09	0.030070	2.28101	2.45378	0.024509	151,852
21.8	5.09	0.029729	2.20313	2.45378	0.024231	151,852
21.8	5.09	0.029642	2.18325	2.45378	0.024160	151,852
21.8	5.09	0.029479	2.14602	2.45378	0.024027	151,852
17.6	5.09	0.027288	2.03828	2.45378	0.022242	151,852
21.4	5.06	0.029155	2.18204	2.42494	0.024046	150,957
21.6	4.03	0.023480	3.55024	1.53819	0.030529	120,228
20.6	3.95	0.022775	3.76532	1.47773	0.030824	117,842
19.6	3.90	0.022869	4.20209	1.44055	0.031750	116,350
22.4	2.82	0.021866	9.34666	0.75318	0.058063	84,130
21.7	2.79	0.021320	9.55760	0.73724	0.057837	83,235
20.2	2.74	0.020026	9.80821	0.71105	0.056328	81,743
20.2	2.74	0.019831	9.66450	0.71105	0.055779	81,743
18.0	2.70	0.016722	8.63877	0.69044	0.048438	80,550
19.4	2.58	0.019074	11.12540	0.63043	0.060511	76,970
27.0	5.99	0.036778	1.38195	3.39824	0.021645	178,702
25.6	5.88	0.035988	1.51718	3.27458	0.021980	175,420
24.4	4.95	0.031655	2.68799	2.32065	0.027281	147,675
24.0	4.93	0.031634	2.77774	2.30194	0.027485	147,078
23.6	4.90	0.031974	2.97821	2.27401	0.028121	146,183
24.7	4.04	0.025966	3.82743	1.54583	0.033595	120,527
24.2	4.03	0.025668	3.84916	1.53819	0.033374	120,228
23.9	4.02	0.025811	3.97828	1.53057	0.033727	119,930

CONTINUED

TABLE E-V. PLASTIC CHIP TEST DATA-CONTINUED

CV	VM	IM	PHI	PSI	F	RE
23.2	3.98	0.025147	4.02816	1.50026	0.033524	118,737
22.6	2.69	0.019710	8.98825	0.68534	0.057519	80,252
22.6	2.69	0.018925	8.45405	0.68534	0.055228	80,252

TEMP. F

0.	1.88	0.003468	67	0.020723	55,085
0.	1.89	0.003468	67	0.020502	55,378
0.	3.00	0.007847	67	0.018413	87,902
0.	3.01	0.007847	67	0.018290	88,195
0.	3.92	0.012592	67	0.017305	114,858
0.	3.93	0.012592	67	0.017216	115,151
0.	6.19	0.028470	67	0.015691	181,371
0.	8.00	0.043313	75	0.014291	262,533
0.	10.82	0.074270	75	0.013397	355,076

TABLE E-VI. PLASTIC CHIP TEST DATA

POLYETHYLENE CHIPS
SPECIFIC GRAVITY - 0.92
SIZE - 1/2 X 3/8 X 1/10 IN.

PIPE MATERIAL - ACRYLIC
PIPE INT. DIAM. - 3.000 IN.
RISE VELOCITY - 0.15 FPS

(1) VOLUME CONCENTRATION (PERCENT) CV	(2) MIXTURE VELOCITY (FT/SEC) VM	(3) MIXTURE GRADIENT (FT/FT) IM	(4) TEMPERATURE F T	(5) FRICTION FACTOR F	(6) REYNOLDS NUMBER RE
0.0	12.98	0.156250	58.9	0.014917	261,927
0.0	9.08	0.080669	60.0	0.015748	186,477
0.0	8.12	0.065892	60.9	0.016059	168,980
0.0	4.04	0.018411	61.8	0.018150	85,080
10.9	17.11	0.263808	54.2	0.014490	321,886
10.6	17.07	0.263808	54.2	0.014571	321,032
10.0	14.98	0.208576	54.5	0.014956	283,035
10.2	12.94	0.156492	60.0	0.015045	265,730
9.9	12.89	0.155766	60.0	0.015081	264,797
10.8	10.94	0.116279	60.0	0.015633	224,705
10.4	10.94	0.115310	60.0	0.015503	224,705
11.0	9.12	0.083818	60.0	0.016201	187,409
10.5	9.08	0.083333	60.0	0.016268	186,477
10.6	9.03	0.082364	60.0	0.016241	185,545
9.8	7.85	0.064438	60.3	0.016813	161,968
8.3	7.81	0.062985	60.3	0.016625	161,032
12.2	7.13	0.055233	60.9	0.017498	148,211
7.2	5.76	0.037306	61.1	0.018062	120,291
12.5	5.08	0.033309	61.2	0.020735	106,172
11.6	5.08	0.032534	61.2	0.020253	106,172
7.9	3.99	0.024467	61.8	0.024672	84,124
13.2	14.64	0.196948	58.5	0.014787	293,693
14.8	12.89	0.156734	60.0	0.015174	264,797
14.1	12.85	0.156977	60.0	0.015305	263,865
15.8	10.94	0.117248	60.0	0.015764	224,705
14.6	10.80	0.114099	60.0	0.015729	221,908
14.6	10.80	0.114341	60.0	0.015763	221,908
14.6	9.03	0.084787	60.0	0.016719	185,545
14.1	8.99	0.083576	60.0	0.016647	184,612

CONTINUED

TABLE E-VI. PLASTIC CHIP TEST DATA-CONTINUED

CV	VM	IM	T	F	RE
13.8	6.94	0.053779	61.0	0.017940	144,676
15.4	5.90	0.041424	61.1	0.019141	123,132
14.7	5.86	0.041182	61.1	0.019325	122,185
14.0	5.81	0.040455	61.1	0.019282	121,238
16.2	5.04	0.034884	61.8	0.022109	106,110
16.2	5.04	0.035611	61.8	0.022569	106,110
15.4	4.99	0.034642	61.8	0.022356	105,155
19.8	14.89	0.206880	58.7	0.015016	299,425
19.1	12.80	0.157946	60.0	0.015509	262,933
19.6	10.85	0.120155	60.0	0.016426	222,840
20.5	9.08	0.087209	60.1	0.017025	186,784
20.1	9.03	0.086240	60.1	0.017005	185,850
19.2	8.94	0.085271	60.1	0.017158	183,982
20.6	7.04	0.058624	61.1	0.019054	146,812
19.1	6.90	0.056928	61.1	0.019241	143,970
22.0	5.99	0.045785	61.2	0.020519	125,131
20.7	5.90	0.045300	61.2	0.020931	123,235
21.6	5.76	0.043362	61.2	0.020994	120,391
21.6	5.63	0.041667	61.2	0.021161	117,548
22.3	5.08	0.037549	61.8	0.023374	107,066
21.6	5.04	0.037064	61.8	0.023490	106,110
21.6	5.04	0.037549	61.8	0.023797	106,110
17.9	4.81	0.035853	61.8	0.024917	101,331
25.8	11.07	0.128391	61.8	0.016840	233,252
25.8	11.07	0.133479	61.8	0.017507	233,252
23.1	10.58	0.119671	61.8	0.017213	222,736
25.9	9.12	0.091570	62.1	0.017699	192,959
25.9	9.12	0.093992	62.1	0.018167	192,959
24.7	8.99	0.090116	62.1	0.017950	190,079
24.7	8.99	0.093508	62.1	0.018625	190,079
26.0	8.03	0.076066	62.1	0.018960	169,919
24.3	7.85	0.073886	62.1	0.019278	166,079
24.3	6.90	0.062985	60.9	0.021288	145,919
24.3	6.90	0.065407	60.9	0.022107	145,919
24.3	6.90	0.064438	60.9	0.021779	145,919

APPENDIX F

SAMPLE CALCULATIONS AND ESTIMATES OF ERRORS

The following data were selected from Table E-I to show the calculations for the mixture friction factor and Reynolds number for a typical test run:

Q_m = 233 gpm or 0.519 cfs

D = 3.938 in. or 0.328 ft.

i_m = 0.035409 ft/ft

ν = 0.0000116 $ft^2/sec.$

$$f_m = 2gDi_m/V_m^2 = g\pi^2 i_m D^5/8Qm^2 \quad \text{..... (F-1)}$$

$$= 32.2 \times 3.14^2 \times 0.035409 \times 0.328^5/8 \times 0.519^2$$

giving f_m = 0.019834 ft/ft

$$Re_m = V_m D/\nu = 4Qm/\pi D\nu \quad \text{..... (F-2)}$$

$$= 4 \times 0.519/3.14 \times 0.328 \times 0.0000116$$

giving Re_m = 173,702.

Using the logarithmic error procedure the relative error in fm and Re_m is obtained as follows:

$$df_m = \frac{\partial f_m}{\partial D} dD + \frac{\partial f_m}{\partial i_m} di_m + \frac{\partial f_m}{\partial Q_m} dQ_m \quad \ldots\ldots\ldots\ldots \quad (F-3)$$

Differentiating Eq. (F-1) with resepct to each of the independent variables D, i_m and Q_m gives

$$df_m = \frac{C_1 i_m 5D^4}{Qm^2} dD + \frac{C_1 D^5}{Qm^2} di_m - \frac{C_1 D^5 i_m{}^2}{Qm^3} dQ_m \quad \ldots\ldots \quad (F-4)$$

Changing the total differentials to Δ's and dividing by f_m gives

$$\frac{\Delta f_m}{f_m} = \frac{5\Delta D}{D} + \frac{\Delta i_m}{i_m} - \frac{2\Delta Q_m}{Q_m} \quad \ldots\ldots\ldots\ldots\ldots\ldots\ldots \quad (F-5)$$

Similarly, $dRe_m = \frac{\partial Re_m}{\partial Q_m} dQ_m + \frac{\partial Re_m}{\partial D} dD + \frac{\partial Re_m}{\partial \nu} d\nu \quad \ldots\ldots \quad (F-6)$

$$= \frac{C_2}{D\nu} dQ_m - \frac{C_2 Q_m}{D^2 \nu} dD - \frac{C_2 Q_m}{D\nu^2} d\nu \quad \ldots\ldots \quad (F-7)$$

from differentiating Eq. (F-2) and hence,

$$\frac{\Delta Re_m}{Re_m} = \frac{\Delta Q_m}{Q_m} + \frac{\Delta D}{D} - \frac{\Delta \nu}{\nu} \quad \ldots\ldots\ldots\ldots\ldots\ldots \quad (F-8)$$

The errors were estimated to be:

$\Delta D = \pm 1/32$ in.

$\Delta i_m = \pm$ 0.000455 ft/ft (standard deviation obtained from data file)

$\Delta Q_m = \pm$ 8.3 gpm; From the section on "Flowmeter Calibration," in Appendix D, the error in Q_m was 2.5 gpm + (2.5% x 233 gpm)

$\Delta \nu = \pm$ 0.0000001 ft^2/sec

Substituting in Eqs. F-5 and F-8, respectively, the relative errors are

$$\frac{\Delta f_m}{f_m} = \frac{5(\pm 1)}{32x3.938} + \frac{(\pm 0.000455)}{0.035409} - 2\frac{(\pm 8.3)}{233}$$

$= \pm$ 0.01876 or 1.9 per cent in the mixture friction factor and

$$\frac{\Delta Re_m}{Re_m} = \frac{(\pm 8.3)}{233} - \frac{(\pm 1)}{32x3.938} - \frac{(\pm 0.0000001}{0.0000116}$$

$= \pm$ 0.01902 or 1.9 per cent in the mixture Reynolds number.

The maximum possible errors are 12.4 per cent in f_m and 5.2 per cent in Re_m.

APPENDIX G

COMPILATION OF WOODCHIP DATA

Table G-I lists the data by McColl (19) of PPRIC. The water temperature, which was not given originally, was estimated to be 85 F. The chip size and specific gravity were also estimated.

Table G-II lists Faddick's (13) data. Only volumetric concentrations exceeding 5 per cent are tabulated. The water temperature was 66 F for the clear-water runs and averaged 75 F for the mixture tests. An estimate of the chip size was made.

Table C-III is a compilation of Soucy's (26) data, for which the author used the relationship

$$C_v = 0.45\ C_{av} \quad \ldots\ldots\ldots\ldots\ldots\ldots\ldots\ldots \quad (C.1)$$

where the volumetric concentration was assumed to be about 45 per cent of the apparent volumetric concentration. The factor 0.45, obtained from reference 13, accounts for the void content in a 6-in. diameter pipe containing loosely-packed saturated woodchips. The water temperature ranged from 64 to 70 F. Only the chip size required estimation.

The data measured by Elliott and de Montmorency (12) of PPRIC is given in Table G-IV. The water temperature was estimated to be 55 F. Chip size and specific gravity also required estimation.

TABLE G-I. WOODCHIP HEADLOSS DATA

EXPERIMENTER - PPRIC (1957)
SPECIFIC GRAVITY - 1+(EST)
SIZE - 1-1/2 X 1/2 X 1/8 IN.
FALL VELOCITY - UNMEASURED
PIPE MATERIAL - COPPER
PIPE INT. DIAM. - 1.837 IN.
WATER TEMPERATURE - UNMEASURED
KINEMATIC VISC - .0000825(EST)

(1) VOLUME CONCEN-TRATION (PERCENT) CV	(2) MIXTURE VELOCITY (FT/SEC) VM	(3) MIXTURE GRADIENT (FT/FT) IM	(4) (IM-IW)/ (CV*IW) PHI	(5) (VM*VM)/ G*D PSI	(6) FRICTION FACTOR F	(7) REYNOLDS NUMBER RE
0.	15.80	0.3430			0.013535	293,178
0.	15.50	0.3300			0.013531	287,611
0.	14.05	0.2780			0.013873	260,706
0.	14.00	0.2770			0.013922	259,778
0.	11.90	0.2080			0.014469	220,811
0.	11.75	0.2040			0.014555	218,028
0.	10.55	0.1680			0.014869	195,761
0.	10.45	0.1650			0.014884	193,905
0.	7.50	0.0925			0.016199	139,167
0.	7.30	0.0884			0.016341	135,456
19.6	15.80	0.3511	0.120485	50.6852	0.013854	293,178
19.6	14.05	0.2812	0.058729	40.0793	0.014032	260,706
19.6	11.90	0.2177	0.237932	28.7515	0.015145	220,811
19.6	10.45	0.1759	0.337045	22.1717	0.015867	193,905
19.6	7.50	0.1036	0.612245	11.4206	0.018143	139,167
24.5	15.50	0.3470	0.210265	48.7787	0.014228	287,611
24.5	14.00	0.2852	0.120829	39.7945	0.014334	259,778
24.5	11.75	0.2167	0.254101	28.0313	0.015461	218,028
24.5	10.55	0.1777	0.235666	22.5981	0.015727	195,761
24.5	7.30	0.1097	0.983472	10.8196	0.020278	135,456
29.4	14.35	0.3387	0.598781	41.8091	0.016202	266,272
29.4	13.90	0.3140	0.510827	39.2280	0.016009	257,922
29.4	11.75	0.2247	0.345138	28.0313	0.016032	218,028
29.4	10.75	0.1890	0.436592	23.4630	0.016104	199,472
34.3	11.80	0.2362	0.427411	28.2703	0.016710	218,955
34.3	13.10	0.2817	0.436723	34.8425	0.016170	243,078
39.2	12.05	0.2712	0.697039	29.4809	0.018398	223,594
39.2	12.60	0.2685	0.427019	32.2335	0.016660	233,800

TABLE G-II. WOODCHIP HEADLOSS DATA

EXPERIMENTER - FADDICK(1962)
SPECIFIC GRAVITY - 1.125
SIZE - 1 X 3/4 X 1/8 IN.
FALL VELOCITY - 0.212 FPS
PIPE MATERIAL - ALUMINUM
PIPE INT. DIAM. - 4.026 IN.
WATER TEMPERATURE - 62-81 F
KINEMATIC VISC - 0.00001(AVE.)

(1) VOLUME CONCEN-TRATION (PERCENT) CV	(2) MIXTURE VELOCITY (FT/SEC) VM	(3) MIXTURE GRADIENT (FT/FT) IM	(4) (IM-IW)/ (CV*IW) PHI	(5) (VM*VM)/ G*D PSI	(6) FRICTION FACTOR F	(7) REYNOLDS NUMBER RE
6.7	8.08	0.0491	0.90261	6.04819	0.016236	271,084
6.4	7.70	0.0475	1.83824	5.49267	0.017296	258,335
5.3	7.62	0.0447	1.07052	5.37914	0.016620	255,651
5.9	7.41	0.0452	2.25139	5.08673	0.017772	248,605
4.9	6.23	0.0339	2.96470	3.59566	0.018856	209,016
5.7	6.22	0.0340	2.60787	3.58412	0.018973	208,681
5.3	6.14	0.0328	2.77081	3.49252	0.018783	205,997
5.0	6.07	0.0326	3.12057	3.41334	0.019102	203,648
6.7	6.04	0.0356	4.05117	3.37969	0.021067	202,642
7.0	5.91	0.0330	3.04622	3.23577	0.020397	198,280
6.5	5.86	0.0319	3.06536	3.18125	0.020055	196,603
7.3	5.81	0.0347	4.30677	3.12719	0.022192	194,925
5.8	5.80	0.0323	4.17772	3.11644	0.020729	194,590
6.7	5.53	0.0340	6.13117	2.83304	0.024003	185,531
6.0	5.48	0.0285	3.46045	2.78204	0.020489	183,854
6.5	5.35	0.0296	4.76515	2.65161	0.022326	179,492
6.2	5.25	0.0331	8.24864	2.55341	0.025926	176,137
5.3	5.14	0.0293	7.20897	2.44753	0.023943	172,447
11.5	8.50	0.0596	1.64888	6.69330	0.017809	285,175
11.4	7.30	0.0499	2.45164	4.93683	0.020215	244,915
9.9	7.25	0.0490	2.78830	4.86944	0.020126	243,237
7.5	7.23	0.0454	2.55468	4.84260	0.018750	242,566
8.8	7.10	0.0460	2.84091	4.67002	0.019700	238,205
9.2	6.70	0.0455	3.89358	4.15865	0.021882	224,785
8.7	6.66	0.0437	3.77319	4.10914	0.021270	223,443
8.6	6.59	0.0376	1.95002	4.02321	0.018692	221,094
10.3	6.52	0.0452	4.17844	3.93820	0.022955	218,746
11.7	6.18	0.0374	2.78839	3.53817	0.021141	207,339
9.9	5.99	0.0364	3.17252	3.32396	0.021902	200,964
7.5	5.74	0.0326	3.64583	3.05229	0.021361	192,577

CONTINUED

TABLE G-II. WOODCHIP HEADLOSS DATA-CONTINUED

CV	VM	IM	PHI	PSI	F	RE
9.2	5.70	0.0435	7.67263	3.00990	0.028905	191,235
10.7	5.65	0.0366	4.39139	2.95733	0.024752	189,557
7.9	5.65	0.0326	3.98122	2.95733	0.022047	189,557
9.2	5.50	0.0351	5.09369	2.80239	0.025050	184,525
9.4	5.46	0.0353	5.34178	2.76177	0.025563	183,183
7.5	5.41	0.0300	3.76068	2.71142	0.022129	181,505
8.3	5.36	0.0332	5.57296	2.66153	0.024948	179,828
17.4	8.20	0.0650	2.10084	6.22917	0.020870	275,110
14.8	7.78	0.0573	2.22612	5.60740	0.020437	261,019
17.5	7.47	0.0557	2.20327	5.16944	0.021550	250,618
13.3	6.14	0.0484	5.11696	3.49254	0.027716	205,997
14.7	5.13	0.0410	6.41584	2.43802	0.033634	172,111
* 0.	14.83	0.1360			0.013350	428,919
0.	12.22	0.0975			0.014096	353,432
0.	9.41	0.0606			0.014775	272,160
0.	9.09	0.0563			0.014710	262,905
0.	7.94	0.0454			0.015547	229,644
0.	6.40	0.0306			0.016128	185,103
0.	4.99	0.0200			0.017340	144,323

*WATER TEST TEMP. 66 F

TABLE G-III. WOODCHIP HEADLOSS DATA

EXPERIMENTER - SOUCY(1968)
SPECIFIC GRAVITY - 1.15
SIZE - 1 X 3/4 X 1/8 +
FALL VELOCITY - UNMEASURED

PIPE MATERIAL - PYREX
PIPE INT. DIAM. - 6.000 IN.
WATER TEMPERATURE - 64-70 F
KINEMATIC VISC = 0.00001106

(1) VOLUME CONCEN-TRATION (PERCENT) CV	(2) MIXTURE VELOCITY (FT/SEC) VM	(3) MIXTURE GRADIENT (FT/FT) IM	(4) (IM-IW)/ (CV*IW) PHI	(5) (VM*VM)/ G*D PSI	(6) FRICTION FACTOR F	(7) REYNOLDS NUMBER RE
3.4	7.35	0.0277	1.33186	3.35814	0.016497	332,278
3.4	4.64	0.0128	2.49252	1.33832	0.019128	209,765
3.4	4.39	0.0116	2.47389	1.19799	0.019366	198,463
3.4	3.47	0.0088	6.04353	0.74849	0.023514	156,872
3.4	2.55	0.0056	8.02138	0.40421	0.027709	115,280
4.9	9.80	0.0430	0.73764	5.97004	0.014405	443,038
4.9	8.22	0.0325	0.98749	4.20018	0.015476	371,609
4.9	6.07	0.0189	0.32917	2.29035	0.016504	274,412
4.9	5.00	0.0140	0.75586	1.55405	0.018017	226,040
4.9	3.88	0.0103	3.47866	0.93581	0.022013	175,407
4.9	2.34	0.0057	10.20410	0.34037	0.033493	105,787
6.8	9.70	0.0426	0.76253	5.84882	0.014567	438,517
6.8	7.95	0.0310	0.80032	3.92879	0.015781	359,403
6.8	6.43	0.0213	0.57389	2.57008	0.016575	290,687
6.8	5.40	0.0166	1.04364	1.81264	0.018316	244,123
6.8	4.33	0.0126	2.77470	1.16547	0.021622	195,750
6.8	3.52	0.0102	5.03096	0.77021	0.026486	159,132
6.8	2.50	0.0085	14.36390	0.38851	0.043757	113,020
8.9	7.70	0.0302	0.88283	3.68558	0.016388	348,101
8.9	6.63	0.0234	0.82466	2.73245	0.017128	299,729
8.9	5.72	0.0189	1.25578	2.03384	0.018586	258,589
8.9	4.95	0.0166	2.78787	1.52312	0.021797	223,779
8.9	3.72	0.0124	5.55029	0.86022	0.028830	168,174
8.9	3.16	0.0119	9.98751	0.62073	0.038342	142,857
10.8	10.35	0.0477	0.55556	6.65895	0.014327	467,902
10.8	8.47	0.0350	0.56117	4.45956	0.015697	382,911
10.8	7.50	0.0290	0.79762	3.49661	0.016588	339,060

CONTINUED

TABLE G-III. WOODCHIP HEADLOSS DATA-CONTINUED

CV	VM	IM	PHI	PSI	F	RE
10.8	5.82	0.0215	1.80041	2.10557	0.020422	263,110
10.8	5.15	0.0185	2.80386	1.64869	0.022442	232,821
10.8	4.18	0.0160	5.55556	1.08612	0.029463	188,969
10.8	3.57	0.0165	10.58200	0.79225	0.041654	161,392
13.6	9.03	0.0366	0.12255	5.06874	0.014414	408,228
13.6	7.10	0.0276	0.99855	3.13358	0.017616	320,976
13.6	6.48	0.0251	1.31179	2.61021	0.019232	292,948
13.6	5.82	0.0223	2.01681	2.10557	0.021182	263,110
13.6	5.05	0.0196	3.16660	1.58529	0.024727	228,300
13.6	4.54	0.0178	4.02814	1.28126	0.027785	205,244
13.6	4.08	0.0167	5.57276	1.03477	0.032278	184,448
13.6	3.06	0.0169	13.35790	0.58206	0.058070	138,336
16.6	7.20	0.0322	1.79751	3.22248	0.019985	325,497
16.6	6.95	0.0286	1.30736	3.00258	0.019050	314,195
16.6	6.12	0.0259	2.18770	2.32824	0.022249	276,673
16.6	5.62	0.0236	2.59219	1.96335	0.024041	254,069
16.6	4.90	0.0209	3.66080	1.49251	0.028007	221,519
16.6	4.39	0.0206	5.46632	1.19799	0.034391	198,463
16.6	3.68	0.0208	9.63856	0.84182	0.049417	166,365
19.3	8.57	0.0366	0.56524	4.56548	0.016033	387,432
19.3	7.85	0.0341	0.97489	3.83058	0.017804	354,882
19.3	7.04	0.0283	0.85290	3.08085	0.018372	318,264
19.3	6.02	0.0238	1.41309	2.25277	0.021130	272,152
19.3	5.15	0.0232	3.28395	1.64869	0.028144	232,821
19.3	4.50	0.0221	4.95209	1.25878	0.035113	203,436
20.2	8.84	0.0401	0.68913	4.85768	0.016510	399,638
20.2	7.35	0.0342	1.68899	3.35814	0.020368	332,278
20.2	6.53	0.0281	1.67374	2.65064	0.021202	295,208
20.2	5.61	0.0254	2.67027	1.95637	0.025967	253,617
20.2	5.30	0.0235	2.80528	1.74613	0.026917	239,602
20.2	4.18	0.0236	6.73267	1.08612	0.043458	188,969
20.2	3.57	0.0239	10.41530	0.79225	0.060335	161,392

TABLE G-IV. WOODCHIP HEADLOSS DATA

EXPERIMENTER - PPRIC(1960-3)
SPECIFIC GRAVITY - 1+
SIZE - 1 X 3/4 X 1/8 +
FALL VELOCITY - UNMEASURED

PIPE MATERIAL - ALUMINUM
PIPE INT. DIAM. - 8.412 IN.
WATER TEMPERATURE - UNMEASURED
KINEMATIC VISC - 0.0000132

(1) VOLUME CONCEN-TRATION (PERCENT) CV	(2) MIXTURE VELOCITY (FT/SEC) VM	(3) MIXTURE GRADIENT (FT/FT) IM	(4) (IM-IW)/ (CV*IW) PHI	(5) (VM*VM)/ G*D PSI	(6) FRICTION FACTOR F	(7) REYNOLDS NUMBER RE
5.0	2.23	0.00436	26.6310	0.220490	0.039549	118,426
5.0	2.47	0.00446	20.0000	0.27050	0.032976	131,172
5.0	2.58	0.00436	15.7377	0.29513	0.029546	137,014
5.0	2.92	0.00436	8.6842	0.37804	0.023066	155,070
5.0	3.35	0.00488	4.8280	0.49758	0.019615	177,905
10.0	2.23	0.00830	34.3850	0.22049	0.075287	118,426
10.0	2.37	0.00825	29.8550	0.24904	0.066254	125,861
10.0	4.68	0.00965	3.4214	0.97111	0.019874	248,536
10.0	4.86	0.01025	3.2088	1.04725	0.019575	258,095
10.0	5.15	0.01100	2.7907	1.17596	0.018708	273,496
10.0	6.28	0.01450	1.7886	1.74862	0.016585	333,506
10.0	6.49	0.01455	1.0227	1.86752	0.015582	344,658
10.0	6.60	0.01447	0.6397	1.93137	0.014984	350,500
10.0	10.41	0.03310	0.6090	4.80484	0.013778	552,834
10.0	10.55	0.03510	0.9688	4.93494	0.014225	560,269
10.0	10.72	0.03620	0.9697	5.09526	0.014209	569,297
10.0	10.80	0.03480	0.2959	5.17160	0.013458	573,545
10.0	11.28	0.03740	0.3889	5.64151	0.013259	599,036
20.0	3.78	0.01290	8.2444	0.63352	0.040725	200,741
20.0	3.89	0.01315	7.7670	0.67093	0.039199	206,583
20.0	3.94	0.01340	7.6415	0.68829	0.038937	209,238
20.0	4.06	0.01450	8.0867	0.73085	0.039680	215,611
20.0	5.97	0.01770	2.9018	1.58025	0.022402	317,043
20.0	6.06	0.01695	2.3696	1.62825	0.020820	321,823
20.0	6.11	0.01692	2.2308	1.65523	0.020444	324,478
20.0	10.35	0.03582	0.7961	4.74961	0.015083	549,648
20.0	10.48	0.03400	0.3797	4.86967	0.013964	556,551
20.0	10.64	0.03440	0.3416	5.01950	0.013707	565,048
20.0	11.00	0.03840	0.5331	5.36491	0.014315	584,167

CONTINUED

TABLE G-IV. WOODCHIP HEADLOSS DATA-CONTINUED

CV	VM	IM	PHI	PSI	F	RE
30.0	10.50	0.04230	1.1287	4.88828	0.017307	557,614
30.0	10.65	0.04130	0.9688	5.02894	0.016425	565,580
30.0	9.79	0.04060	1.5173	4.24955	0.019108	519,908
30.0	10.38	0.04900	1.9355	4.77718	0.020514	551,241
30.0	10.35	0.04580	1.6558	4.74961	0.019286	549,648
* 0.0	3.66	0.00453			0.015254	194,368
0.0	6.91	0.01510			0.014265	366,963
0.0	7.90	0.01860			0.013444	419,538
0.0	9.39	0.02630			0.013455	498,666
0.0	11.07	0.03450			0.012699	587,884

*ESTIMATED WATER TEMP. 55 F

APPENDIX H

CURVE FITTING BY THE NEWTON-RAPHSON METHOD

The mathematical relationship assumed is $y = ax^b$ where $Y = \varphi$ and $x = \psi$. The sample points are (x_i, y_i) where i goes from 1 to n.

$$\text{Let } S = \sum_{i=1}^{n} (y_1 - y_i')^2 = \sum_{i=1}^{n} (y_i - ax_i^b)^2 \quad \ldots\ldots\ldots\ldots\ldots \text{(H.1)}$$

Minimizing S with respect to a and b gives

$$\frac{\partial S}{\partial a} = 2 \sum_{i=1}^{n} (y_1 - ax_i^b)\, x_1^b \quad \ldots\ldots\ldots\ldots\ldots\ldots \text{(H.2)}$$

$$\sum_{i=1}^{n} y_i\, x_i^b - a \sum_{i=1}^{n} x_i^{2b} = 0 \quad \ldots\ldots\ldots\ldots\ldots\ldots \text{(H.3)}$$

$$\frac{\partial S}{\partial b} = 2 \sum_{i=1}^{n} (y_i - ax_i^b)\, ax_i^b \ln x_i \quad \ldots\ldots\ldots\ldots\ldots \text{(H.4)}$$

$$\sum_{i=1}^{n} y_1 x_i^b \ln x_i - \sum_{i=1}^{n} x_i^{2b} \ln x_i = 0 \quad \ldots\ldots\ldots\ldots \text{(H.5)}$$

In Eq. (D.5), the trivial and inconsistent solution, a = 0 has been ignored. From Eq. (D.3),

$$a = \sum_{i=1}^{n} y_1 x_i^b \Big/ \sum_{i=1}^{n} x_i^{2b} \quad \ldots\ldots\ldots\ldots\ldots \text{(H.6)}$$

is obtained. If b is known, a can be computed. Substituting the value of a into Eq. (D.5) gives

$$\sum_{i=1}^{n} y_i x_i^b \ln x_i - \frac{\sum_{i=1}^{n} y_1 x_1^b}{\sum_{i=1}^{n} x_1^{2b}} \sum_{i=1}^{n} x_i^{2b} \ln x_i = 0 \quad \ldots\ldots \text{(H.7)}$$

Let the above expression be denoted by f(b). The problem has now been reduced to one of finding the solution to the equation

$$f(b) = 0 \quad \ldots\ldots \text{(H.8)}$$

A numerical technique called the Newton-Raphson method can be used to find the roots of the equation.

The basic iteration is

$$b_{n+1} = b_n - \frac{f(b_n)}{f'(b_n)} \quad \ldots\ldots \text{(H.9)}$$

which is continued until $|b_{n+1} - b_n| < \epsilon$. The permissible error used was 0.01.

$$f(b) = \sum_{i=1}^{n} y_i x_i^b \ln x_i - \frac{\sum_{i=1}^{n} y_i x_i^b}{\sum_{i=1}^{n} x_i^{2b}} \sum_{i=1}^{n} x_i^{2b} \ln x_i \quad \ldots \text{(H.10)}$$

$$f'(b) = \sum_{i=1}^{n} y_i x_i^b (\ln x_i)^2 - \frac{\sum_{i=1}^{n} y_i x_i^b \ln x_i}{\sum_{i=1}^{n} x_i^{2b}} \sum_{i=1}^{n} x_i^{2b} \ln x_i$$

$$\frac{-2 \sum_{i=1}^{n} y_i x_i^b}{\sum_{i=1}^{n} x_i^{2b}} \left[\sum_{i=1}^{n} x_i^{2b} (\ln x_i)^2 - \frac{\left(\sum_{i=1}^{n} x_i^{2b} \ln x_i \right)^2}{\sum_{i=1}^{n} x_i^{2b}} \right] \quad \text{(H.11)}$$

The value of b_n is obtained from the method of least squares.

LITERATURE CITED

1. Alberta Research Council, Fuels Branch, Forty-eighth Annual Report, 1967.

2. Alger, G. R., D. B. Simons, "Fall Velocity of Irregular Shaped Particles," ASCE JOURNAL OF THE HYDRAULICS DIV., Vol. 94, No. HY3, May, 1968, pp. 721-37.

3. Babcock, H. A., "Heterogeneous Flow of Heterogeneous Solids," paper presented to the International Symposium on Solid-Liquid Flow in Pipes and its Application to Solid-Waste Collection and Removal, University of Pennsylvania, Philadelphia, Pa., March 4-6, 1968.

4. Barr, D. I. H., Discussion of "Heterogeneous Flow of Solids in Pipelines," by I. Zandi, G. Govatos, ASCE JOURNAL OF THE HYDRAULICS DIV., Vol. 94, No. HY1, Jan., 1968, pp. 333-336.

5. Barr, D. I. H., Discriminating Formulation of n term Nondimensional Functional Equations from (n+1) term Dimensionally Homogeneous equations with Particular Reference to Incompressible Viscous Flow," PROC. INST. OF CIVIL ENGINEERS, London, Vol. 39, Feb., 1968, pp. 305-309.

6. Colorado School of Mines, THE TRANSPORTATION OF SOLIDS IN PIPELINES, Colorado School of Mines Research Foundation, Inc., Golden, Colorado, 1963, p. 3.

7. Condolios, E., E. E. Chapus, J. A. Constans, "Designing Solids Handling Pipelines," CHEMICAL ENGINEERING, July 8, 1963, p. 131.

8. Condolios, E., E. E. Chapus, J. A. Constans, "New Trends in Solids Pipelines," CHEMICAL ENGINEERING, May 8, 1967, pp. 131-138.

9. Daily, J.W., R.L. Hardison, "Rigid Particle Suspensions in Turbulent Shear Flow," Report No. 67, Hydrodynamics Laboratory, MIT, April, 1964.

10. Durand, R., E. Condolios, "The Hydraulic Transport of Coal and Solid Materials in Pipes," Proc. of a Colloquium on the Hydraulic Transport of Coal, Scientific Dept., National Coal Board of Great Britain, Nov., 1952.

11. Durand, R., untitled internal report from Le Laboratoire Dauphinois d'Hydraulique, Grenoble, to Le Service Maritime des Ponts et Chaussées de la Loire Inferieure (in French), France, 1954.

12. Elliott, D.R., W.H. de Montmorency, "The Transportation of Pulpwood Chips in Pipelines," Pulp and Paper Research Institute of Canada, Technical Reports, 334 series, August, 1963.

13. Faddick, R.R., "The Aqueous Transportation of Pulpwood Chips in a Four-Inch Aluminum Pipeline," M.Sc. Thesis, Queen's University at Kingston, Ontario, Jan., 1963.

14. Gibert, R., "Transport Hydraulique et Refoulement des Mixtures en Conduites," ANNALES DES PONTS ET CHAUSSÉES, May-June, 1960, pp. 507-563.

15. Govier, G.W., M.E. Charles, "The Hydraulics of the Pipeline Flow of Solid-Liquid Mixtures," THE ENGINEERING JOURNAL, August, 1961, pp. 50-57.

16. Hunt, W.A., "Economic Analysis of a Woodchip Pipeline," FOREST PRODUCTS JOURNAL, Vol. 17, No. 9, Sept. 1967, pp. 68-74.

17. Johnson, D.A., "The Effect of Chip-Shaped Solids on Valve Headloss Characteristics," M.S. Thesis, Civil Engineering Dept., Montana State University, Bozeman, Montana, Sept., 1968.

18. Laufer, J., "The Structure of Turbulence in Fully Developed Flow," Report 1174, NACA, National Bureau of Standards, Oct. 24, 1952, pp. 417-434.

19. McColl, B.J., Data supplied to author by Pulp and Paper Research Institute of Canada, 1962.

20. Newitt, O.M., J.F. Richardson, M. Abbott and R.B. Turtle, "Hydraulic Conveying of Solids in Horizontal Pipes," TRANS. INST. OF CHEMICAL ENGINEERING, London, 1955, Vol. 33, pp. 93-113.

21. Pao, R.H.F., FLUID MECHANICS, John Wiley & Sons, Inc., New York, 1968, pp. 221-2.

22. Powe, E.J., G.V. Smith, "Curve Fitting with Several Independent Variables," JOURNAL OF THE MISSISSIPPI ACADEMY OF SCIENCES, State College, Mississippi, C.M. Crawford, ed., 1968.

23. Richardson, E.V., R.S., McQuivey, "Measurement of Turbulence in Water," ASCE JOURNAL OF THE HYDRAULICS DIV., Vol. 94, No. HY2, Proc. Paper 5855, March, 1968, pp. 411-430.

24. Schmidt, R.E., "Design and Construction of Test Facilities for Woodchip Pipeline Research," Report of the Intermountain Forest and Range Experiment Station, Bozeman, Montana, April, 1966.

25. Soo, S.J., FLUID DYNAMICS OF MULTIPHASE SYSTEMS, Blaisdell Publishing Co., Waltham, Mass., 1967.

26. Soucy, A., Data supplied to author by Laval University, Quebec City, Quebec, Dec., 1968.

27. Spells, K.E., "Correlations for Use in Transport of Aqueous Suspensions of Fine Solids Through Pipes," TRANS. INST. OF CHEMICAL ENGINEERING, London, Vol. 33, 1955, pp. 79-84.

28. Stepanoff, A.J., PUMPS AND BLOWERS, TWO-PHASE FLOW, J. Wiley & Sons, Inc., New York, 1965, pp. 277.

29. Wasp, E.J., T.J. Regan, J.W. Withers, P.A.C. Cook, J.W. Clancy, "Cross Country Coal Pipeline Hydraulics," PIPELINE NEWS, July, 1963, pp. 20-28.

30. Wasp, E.J., T.C. Aude, T.L. Thompson, C.D. Bailey, "Economics of Chip Pipelining," paper presented to TAPPI, 21st Engineering Conference, Boston, Oct., 1966.

31. Wiley, C.R., ADVANCED ENGINEERING MATHEMATICS, 3rd ed., McGraw-Hill Book Co., New York, 1966, pp. 138-141.

32. Worster, R.C., "The Hydraulic Transport of Solids," Proc. of a Colloquium on the Hydraulic Transport of Coal held by the National Coal Board Scientific Dept., in London, Nov. 5-6, 1952.

33. Zandi, I., G. Govatos, "Heterogeneous Flow of Solids in Pipelines," ASCE JOURNAL OF THE HYDRAULICS DIV., Paper No. 5244, Vol. 93, No. HY3, May, 1967, pp. 145-159.

MONTANA STATE UNIVERSITY LIBRARIES
3 1762 10005446 7

D378
F12
cop.2

Faddick, R. R.

The hydraulic transportation of solids in pipelines

NAME AND ADDRESS

MAY 5
5-12-71
1977
APR - 0
R